BIODEGRADABLE POLYMER MICRO- AND NANOPARTICLES AS PROTEIN DELIVERY SYSTEMS: INFLUENCE OF MICROPARTICLE MORPHOLOGY AND IMPROVEMENT OF PROTEIN LOADING CAPACITY OF NANOPARTICLES

Dissertation

Zur
Erlangung des Doktorgrades
der Naturwissenschaften
(Dr. rer. nat.)

dem
Fachbereich Pharmazie
der Philipps-Universität Marburg

vorgelegt von
Cuifang Cai
aus Shandong/China

Marburg/Lahn 2007

Vom Fachbereich Pharmazie der Philipps-Universität Marburg als Dissertation am 08.08.2007 angenommen.

Erstgutachter: Prof. Dr. Thomas Kissel
Zweitgutachter: Prof. Dr. Udo Bakowsky

Tag der mündlichen Prüfung am 12.9.2007

Die vorliegende Arbeit entstand auf Anregung und unter der Leitung von

Herrn Prof. Dr. Thomas Kissel

am Institut für Pharmazeutische Technologie und Biopharmazie

der Philipps-Universität Marburg

Acknowledgements

First of all, I would like to express my deep gratitude to my supervisor, Professor Dr. Thomas Kissel, for discussions critical to the progress of the research, for the help he gives to tackle all scientific challenges, for support and encouragement during my studies here in Marburg. I really appreciate his care and efforts to ensure my professional development and my successful integration here. All these were extremely essential for the completion of this dissertation. I consider myself very fortunate that he taught me critical scientific thinking and that he was willing to share with me his scientific visions of the pharmaceutical research. I have learned a lot from him, how to become a wise scientist, to be an excellent professor.

I would like to acknowledge the German Academic Exchange Service (DAAD, Der Deutsche Akademische Austauschdienst) for the financial support during my doctoral study. Thanks to Professor Dawei Chen for his support during my studies.

Special thanks goes to Dr. Erik Rytting and Dr. Terry Steele for the discussion and suggestions during the work and for language correction the thesis. I would like to give thanks to Dr. Shirui Mao for her chitosan derivatives synthesis and discussions during my work. Thanks also should go to Dr. Xiaoying Wang for synthesis of negatively charged polymer.

I am particularly grateful to Professor Dr. Udo Bakowsky and Johannes Sitterberg for the AFM images. Thanks to Dr. Andreas K. Schaper for the very helpful discussions about technical problems regarding TEM sample procedures. Special thanks to Michael Hellwig and Dr. Larissa Parchina for great help with sample preparation and SEM, TEM images, and thanks also go to Oliver Germershaus for the CLSM images.

My deep gratitude goes to Julia Michaelis, Kerstin Weber, Klaus Keim and Lothar-Walter Kempf for their day-to-day support in the laboratory work and for managing the ordering of reagents.

The kind help of my other colleagues, namely: Claudia Packhäuser, Sascha

Maretschek, Nina Seidel, Tobias Lebhardt, Jens Schäfer, Olivia Merkel, Frank Morell, Juliane Nguyen, Regina Reul, Farhad Pazan, Christoph Schweiger，Dr. Yu Liu, Nan Zhao, Nadja Bege, and Eva Mohr are highly appreciated. I am also grateful to all of my colleagues for giving me a helping hand during this whole process.

Last, but not least, I would like to thank my parents and my family for encouragement, unconditional love, and support throughout the years.

Table of Contents

Chapter 1 Introduction 1

1. Biodegradable microspheres and nanoparticles delivery systems for proteins 2

1.1 Biodegradable microspheres as protein delivery system 3

1.2 Biodegradable polymeric nanoparticles as protein carrier 5

2. PLGA microspheres and release of drug substance 6

2.1 Biodegradable poly(lactide-co-glycolide) (PLGA) microspheres 6

2.2 Release mechanism 8

2.3 Water/oil/water double-emulsion (w/o/w) method 9

3. Nanoparticles preparation 10

3.1 Solvent displacement 11

3.2 Adsorption processs 12

3.3 Surface adsorption on preformed particles with ionic surface charge 13

4. Chitosan coated nanoparticles 14

5. Objectives of this work 15

6. Reference 17

Chapter 2 Influence of morphology and drug distribution on the release process of FITC-dextran loaded microspheres prepared with different types of PLGA 27

Abstract 28

1. Introduction 29

2. Materials and Methods: 30

2.1 Materials: 30

2.2 Standard preparation method (w/o/w) 31

2.3 Characterization of microspheres 31

2.4 External and internal morphology of microspheres 32

2.5 Drug distribution 33

2.6 Differential scanning calorimetry (DSC) 33
2.7 Water uptake and size evolution 33
2.8 Calculations and Statistics 34
3. Results and discussion 34
3.1 The Effect of polymer molecular weight and end group 34
3.2 Influence of porosity 39
3.3 The influence of pore size 46
3.4 Influence of drug loading on microsphere properties 50
3.5 Influence of PEG addition 53
4. Conclusions 55
References 55
Chapter 3 Charged nanoparticles as protein delivery systems: A feasibility study using lysozyme as model protein. 60
Abstract 61
1. Introduction 62
2. Materials and Methods 64
2.1 Materials 64
2.2 Preparation of PLGA-PSS nanoparticles 64
2.3. Physicochemical and morphological characterization of negatively charged nanoparticles 65
2.4. Loading capacity of PLGA–PSS nanoparticles for lysozyme 66
2.5. In vitro release of lysozyme from nanoparticles 67
2.6. In vitro bioactivity of Lysozyme 67
2.7. Statistical analysis 68
3. Results and Discussion 68
3.1 Solubility of PSS and compatibility of PSS and PLGA 68
3.2. Characterization of PLGA–PSS blend nanoparticles 70
3.3. Lysozyme loading capacity of the polymer blend nanoparticles 72
3.4. Adsorption of BSA and Cytochrome c 83

3.5. Release and bioactivity 85

4. Conclusions 88

Acknowledgments 88

References 89

Chapter 4 Layer-by-layer nanostructured protein loaded nanoparticles: A feasibility study using lysozyme as model protein and chitosan as coating material 94

Abstract 95

1. Introduction 96

2. Materials and methods 98

2.1.Materials 98

2.2. PLGA/PSS Nanoparticles preparation 99

2.3. Preparation of protein-loaded PLGA/PSS nanoparticles 100

2.4. Preparation of polymer coated proteins 100

2.5. Particle size and Zeta potential measurements 101

2.6. Transmission electron microscopy (TEM) 101

2.7. Scanning electron microscopy (SEM) 102

2.8. In vitro release of lysozyme from nanoparticles 102

2.9. Statistical analysis 102

3. Results and Discussion 103

3.1. Preparation and characterization of chitosan (CS) coated lysoyzme loaded nanoparticles 103

3.2. Effect of chitosan molecular weight 108

3.3. Effect of polymer structure of chitosan 110

3.4. Influence of initial protein loading of lysozyme 113

3.5. Release profiles and stability of chitosan coated lysozyme loaded PLGA/PSS nanoparticles 115

4. Conclusions 117

Acknowledgement **118**

References **118**

Chapter 5 Preliminary study of nanoparticles preparation and loading capacity of model protein lysozyme using new class negatively charged polymer SB-PVA-PLGA and P(VS-VA)-PLGA **122**

Abstract **123**

1. Introduction **124**

2. Materials and methods **127**

2.1. Chemicals 127

2.1.1. SB-PVAL-g-PLGA 127

2.1.2. P(VS-VA)-g- PLGA 129

2.2. Nanoparticles preparation 130

2.3. Loading of model protein lysozyme 131

2.4. Particle size and size distribution 131

2.5. Zeta potential measurements 132

3. Results and discussion **132**

3.1. Characteristics of nanoparticles (NPs) prepared with negatively charged polymer SB-PVA-PLGA and P(VS-VA)-PLGA 132

3.2. Evaluation of loading capacity of nanoparticles prepared with negatively charged polymer 135

4. Conclusions **139**

References **140**

Chapter 6 Summary and outlook **143**

Appendices **148**

ABBREVIATIONS **149**

PUBLICATIONS **150**

CURRICULUM VITAE **152**

Chapter 1

Introduction

This dissertation deals with the micro- and nano- polymer particles as protein carrier system. This work attempted to achieve desired release profiles of PLGA protein loaded microparticles especially in the pore diffusion process through morphology modification of microparticles. Separately, negatively charged nanoparticles were conceived to improve loading capacity of the oppositely charged proteins with full preserved bioactivity. Finally, to further improve stability of protein and release profiles, layer-by-layer nanostructure was designed using chitosan and its derivatives as coating materials for protein loaded nanoparticles.

In this introduction chapter, the particulate polymer delivery system for proteins and peptides will be presented. The release profiles of PLGA microspheres will be summarized. Preparation of protein loaded nanoparticles with regard to the loading efficiency and preservation of bioactivity of protein will be discussed. Finally, chitosan coated nanoparticles as a drug delivery carrier will be addressed.

1. Biodegradable microspheres and nanoparticles delivery systems for proteins

Therapeutic and antigenic proteins are specifically effective at a comparably low dose, gaining increased interest as drug molecules. These very potent and specific peptides and proteins can now be produced in large quantities due to increased knowledge and advancements in biotechnological and pharmaceutical applications [1]. Although these new pharmaceuticals showed high therapeutic promise, the systemic application of proteins to the body quickly became a large hurdle due to the sensitivity of these molecules.

Major research issues in protein delivery include the stabilization of proteins in delivery devices and the design of appropriate protein carriers. Among them, polymeric nanoparticles and microspheres have shown a certain degree of success for the delivery of proteins to the systemic circulation and to the immune system [2]. However, protein stability still remains one of the most important barriers for their successful incorporation in biodegradable drug delivery formulations, such as nano- or microparticulate carriers.

1.1 Biodegradable microspheres as protein delivery system

Biodegradable microspheres as protein carrier are of great interest, due to their versatile administration route, protection of protein from degradation and physiological clearance, as well as a well-defined controlled release profile [3]. Since this technology provides unique advantages over traditional delivery approaches (e.g. improved drug efficacy and patient compliance), several formulations of proteins based on biodegradable microspheres have already been marketed, as shown in Table 1 [4]. Extensive studies are ongoing for sustained protein delivery, *e.g.* prolonged effect of rhVEGF in promoting local angiogenesis has been reported when rhVEGF was encapsulated in poly(lactic-*co*-glycolic acid) (PLGA) microspheres and administered as implants [5].

Owing to their excellent biocompatibility, the biodegradable polyesters poly(lactic acid) (PLA) and poly(lactic-*co*-glycolic acid) (PLGA) are the most frequently used biomaterials and already commercializd for the delivery of protein and peptide drugs. Proteins, as labile and bioactive macromolecules, are subject to denaturation, and it has been difficult to prepare controlled release dosage forms without loss of biological activity. For most preparation techniques of microspheres, exposure of protein to the organic solvent, high shear force, as well as high temperature lead to the denaturation of bioactive compounds [6].

Generally, zero-order release kinetics are desirable for long-term releasing formulations, so that the plasma drug level reflecting pharmacological effects can be maintained. However, most protein loaded biodegradable microspheres show a triphasic release kinetic with a considerable burst effect at the onset, followed by a lag phase and then the final release phase is controlled by polymer erosion [7]. Especially, incomplete release profiles of protein was demonstrated despite significant polymer degradation [8-10]. Furthermore, due to the degradation of polymer during release process, e.g. PLGA, generating the acidic breakdown products, lactic and glycolic acids, which a low pH (as low as pH 3) microenvironment that might affect the stability of the encapsulated protein [10,11].

Drug	Trade name	Company	Route	Application
Leuprolide acetate	Lupron Depot®	Takeda-Abott	3 months depot suspention	Prostate cancer
Recombinant human growth hormone	Nutropine Depot®	Genentech-Alkermes	Monthly S/C injection	Growth hormone deficiency
Goserelin acetate	Zoladex®	I.C.I.	S/C implant	Prostate cancer
Octreotide acetate	Sandostatin LAR® depot	Novartis	Injectable S/C suspension	GH suppression, anticancer
Triptorelin	Decapeptyl® Decapeptyl LP® Trelstar Depot®	Ferring Debiopharm Pfizer	Injectable depot	LHRH agonist
Lanreotide	Somatuline® LA	Ipsen	Injectable depot	Acromegaly
Recombinant bovine somatropin	Posilac®	Monsanto	Injectable depot, oil based injection	To increase milk production in cattle
Buserelin acetate	Suprecur® MP	Novartis	S/C implant	Prostate cancer

Table 1 Marketed formulations of proteins based on biodegradable microspheres

Therefore, the stability of protein during preparation and release process, as well as a desired release profile has been the main research effort in the microsphere protein delivery formulations.

1.2 Biodegradable polymeric nanoparticles as protein carrier

Nanoparticles, first developed around 1970, are polymeric particles ranging in size from 10 to 1000 nm. They were initially devised as carriers for vaccines and anticancer drugs [12]. Polymeric nanoparticles with biodegradable and biocompatible polymers are good candidates as particulate carrier for peptide drug delivery [13], and there has been considerable interest in the use of nanoparticles (NP) as potential protein delivery systems.

Numerous investigations have shown that nanoparticles can not only improve the stability of therapeutic agents against enzymatic degradation, but by modulating polymer characteristics, they can also achieve desired therapeutic levels in target tissues for the required duration for optimal therapeutic efficacy [14]. Furthermore, polymeric nanoparticles could reduce the multi-drug resistance that characterizes many anticancer drugs, by a mechanism of internalization of the drug, reducing its efflux from cells mediated by the P-glycoprotein [15].

Depending on their composition and intended use, they can be administered orally, parenterally, or locally [16]. Different NP manufacturing methods were described allowing modification of physicochemical characteristics such as size, structure, morphology, surface texture, and composition to meet different requirements. For example, targeted nanoparticles for drug delivery through the blood-brain barrier was investigated with poly(butyl cyanoacrylate) (PBCA) nanoparticles coated with polysorbate 80 and showed positive results; bioadhesive polysaccharide chitosan nanoparticles increased the intestinal absorption of protein/peptide [13]. Various polymers are used for the preparation of nanoparticles. A list of polymers using different methods of manufacturing is given in the Table 2 [13].

Methods of Manufacturing	Polymers Used	Biodegradability	Nature of Origin	Reference
Emulsion polymerization	Poly(methylmethacrylate) Poly(alkyl cyanoacrylate)	Non-biodegradable Biodegradable	Synthetic	[17] [18]
Interfacial polymerization	Poly (alkyl cyanoacrylate)	Biodegradable	Synthetic	[19]
Desolvation	Albumin Gelatin	Biodegradable Biodegradable	Natural Natural	[20] [21]
Solvent evaporation	Poly lactic acid Poly lactic acid co-polymer	Biodegradable Biodegradable	Synthetic Synthetic	[22]
Solvent deposition	Poly lactic acid co-polymer	Biodegradable	Synthetic	[23]

Table 2. Polymers Used in Different Methods of Manufacturing

The main issues in this field are the loading efficiency, stability of bioactive agent during preparation and release, release profiles and surface modification. Particles size and surface property (surface charge and hydrophobic or hydrophilic property) are primary factors for the in-vivo fate of NPs. Surface modification of NPs has been achieved mainly by two methods: (i) surface coating with hydrophilic polymers/surfactants; and (ii) development of biodegradable copolymers with charged functional group or hydrophilic segments [24].

2. PLGA microspheres and release of drug substance

2.1 Biodegradable poly(lactide-co-glycolide) (PLGA) microspheres

Among the various biodegradable polymers, PLGA was particularly suitable to be used for the drug delivery application. Due to the biodegradability and biocompatibility, several products such as implantable or injectable drug loaded particles or implant with these polymers as host device are already approved by the US

Food and Drug Administration (FDA). PLGA is synthesized by means of random ring-opening co-polymerization of two different monomers, the cyclic dimers (1, 4-dioxane-2, 5-diones) of glycolic acid and lactic acid. During polymerization, successive monomeric units (of glycolic or lactic acid) are linked together in PLGA by ester linkages, thus yielding a linear, aliphatic polyester as a product [25,26].

Depending on the ratio of lactide to glycolide, different forms of PLGA can be obtained. All PLGAs are amorphous and show a glass transition temperature in the range of 40-60 °C. PLGA degrades by hydrolysis of its ester linkages in the presence of water. It has been shown that the time required for degradation of PLGA is related to the lactide to glycolide ratio, end group (ester or free carboxyl group) and molecular weight.

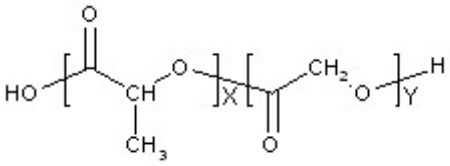

X- Number of units of Lactic Acid
Y- Number of units of Glycolic Acid

Figure 1. Structure of biodegradable poly(lactic-co-glycolic acid)

As the most frequently used biodegradable polymer for microsphere drug delivery system, the effect of different PLGA properties such as molecular weight, lactide/glycolide ratio, and terminal functional groups on drug release have been extensively investigated. PLGA with a lower molecular weight generally leads to a faster polymer degradation and a more rapid drug release [27,28]. An increase in the lactide content decreases the polymer degradation rate and results in a slower drug release [29,30]. The end group of PLGA is a factor that affects the hydrophilicity of the polymer. In general, PLGA carrying free carboxylic end groups caused a high initial burst and release rates compared to the end-capped polymer [31]. Uncapped PLGA with free carboxyl termini is more hydrophilic and has higher hydrolysis rate than its end-capped species with esterified carboxyl termini [32].

Since the release kinetics of protein from microspheres depends on polymer nature, morphology and drug distribution, fundamental understanding of the relationship

among these key characteristics and release mechanisms is essential to yield useful products [33,34].

2.2 Release mechanism

Injectable PLGA microspheres control the release of drugs over a period of several weeks to several months. In many release studies using microspheres, protein release kinetics are often unpredictable; the devices exhibit an initial burst release followed by a very slow release over an extended period, and then culminate with incomplete release despite significant polymer degradation [35].

The release mechanism of protein from biodegradable microspheres is thought to occur in two phases, characterized by pore diffusion in the initial phase and erosion or degradation controlled release at later stages [36]. During degradation, the by-products of the degraded polymer can destabilize the incorporated bioactive molecules [37]. Therefore, diffusion controlled release phase is highlighted and tend to be designed to meet required release rate. Thus, pore diffusion release process will be the focus of study in this work.

For a typical triphasic release curve, pore diffusion phase include the initial burst phase and slow release phase shown in Fig.2. Rapid release occurs within 24 hours and can range from 10 to 80% of the total drug content. This so-called “initial burst” phenomenon poses a serious toxicity threat and is a major hurdle for the development of microsphere products. Secondly, microspheres tend to have a very slow (close to zero) release period after the initial burst period. This period usually lasts for days to weeks and is often referred to as the “lag-time” (or induction) period. During this lag time, the patient may not be effectively treated due to the lack of sufficient drug release.

The initial burst is widely believed to be the result of rapid release of drug from the microsphere surface, whereas the depletion of drug at the surface causes the cessation of initial burst. The lag period then starts and lasts until extensive degradation of the polymer occurs. Efforts have been made to modify the morphology

and drug distribution to achieve desired release profiles. Generally, porous microspheres have a large surface area and hence have a high initial burst. The drug distribution has a great effect on the release property of microspheres. However, drug release from the microspheres remains a complicated process, involving physical and chemical interactions of polymer and drug substance. Hence, how the morphology and drug distribution of microparticles influences drug release still is a question to be answered especially for the pore diffusion process. Few studies have focused on the mechanism of the initial burst and lag time. It is necessary to study further in this direction based on different polymer properties, such as relatively hydrophobic or hydrophilic. This work is of prime importance for the designing of protein loaded microparticles with desired release profiles.

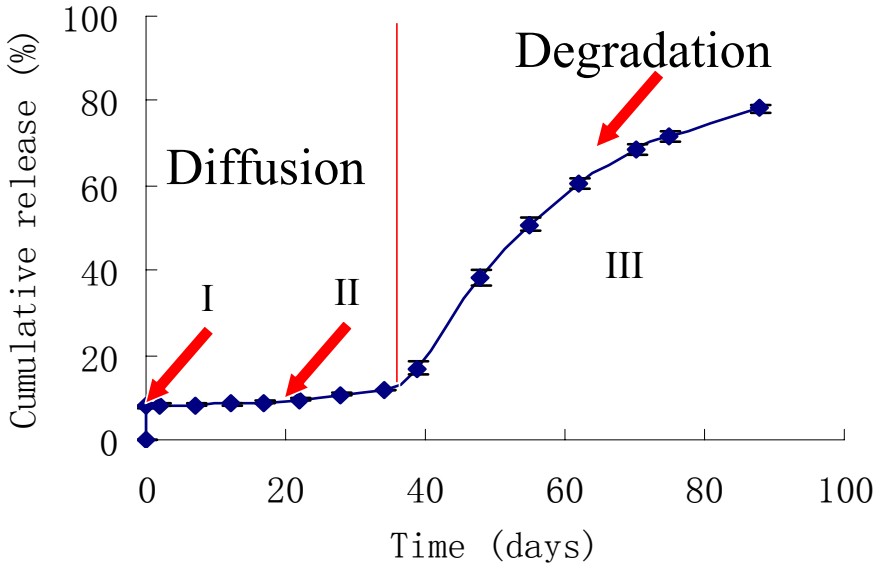

Figure 2.Three-phasic release profile under in vitro conditions (phase I: initial burst; phase II: slow release; phase III: polymer degradation)

2.3 Water/oil/water double-emulsion (w/o/w) method

A wide range of methods have been developed to prepare microspheres with desired release characteristics. These include double emulsion-solvent evaporation, solvent extraction and phase separation. Described firstly by Ogawa et al. in 1988 for

the encapsulation of leuprorelide acetate into PLGA microspheres [38], the w/o/w double-emulsion (w/o/w) method is particularly popular for protein and peptide encapsulation.

To prepare microspheres by the w/o/w double emulsion technique, an aqueous solution of the hydrophilic drug is emulsified into an organic solution of the polymer. Usually, DCM is selected as organic solvent, but other solvents like ethylacetate or methylethyl ketone have also been investigated. This primary w/o emulsion is then injected into a second water phase containing stabilizers, such as polyvinylalcohol, PVA. Subsequently, the solvent is removed by extraction or evaporation and the microspheres are collected by filtration or centrifugation.

Morphology and drug distribution of microspheres are dominantly determined by the process conditions. Influence of process parameters on the morphology and release profiles of PLGA microspheres has been extensively studied, e.g. shear force in the primary emulsion step, polymer concentration in the organic phase The stirring rate in the second emulsion step, Stability of primary emulsion, PVA concentration in the external water phase, volume of the inner water phase, temperature, drug loading, varying the amount of water in the second emulsion of continuous phase, additives in the internal water phase and external water phase (NaCl) [33,39-46].

The morphology of microspheres is characterized by size distribution, external and internal morphology. The size measurements were usually carried out by dynamic light scattering technique. Surface and internal morphology were investigated using scanning electron microscopy (SEM). Internal pore size and porosity can be determined by random sectioning of the porous sample [34] and porosity was also expressed as BET total surface area [47,48]. Confocal laser scanning microscopy (CLSM) provides a good approach to exploring the internal structure of the microspheres and drug distribution.

3. Nanoparticles preparation

Several methods exist for the preparation of nanoparticles from biodegradable

polymers. These include: emulsification solvent evaporation [49], monomer emulsion polymerization [50], salting out [51], and nanoprecipitation [52]. Depending on the preparation method drugs or antigens can either be entrapped in the polymer matrix, encapsulated in a liquid core, surrounded by a shell-like polymer membrane, or bound to the particle surface by adsorption [53]. For drug loading of nanoparticles, three major strategies can be employed: (1) covalent attachment of the drug to the particle surface or to the polymer prior to preparation, (2) adsorption of the drug to a preformed carrier system, and (3) incorporation of the drug into the particle matrix during particle preparation [54]. The release rates of nanoparticles depend upon: (i) desorption of the surface-bound/adsorbed drug; (ii) diffusion through the nanoparticle matrix; (iii) diffusion (in case of nanocapsules) through the polymer wall; (iv) nanoparticle matrix erosion; and (v) a combined erosion/diffusion process [24]. During these preparation and release processes, the bioactivity of therapeutic agent must remain intact. Therefore, the ideal goal would be to achieve satisfactory protein stabilization and appropriate release through a reasonable preparation strategy.

3.1 Solvent displacement

Solvent displacement or nanoprecipitation, also known as the Marangoni effect [55,56], has become a popular technique to prepare nanoparticles due to narrow size distribution，absence of shear stress, and absence of surfactants for amphiphilic polymers [53]. This method differs from the emulsification diffusion and salting-out methods in that formally no precursor emulsion is formed during nanoparticle preparation. Basically, nanoparticle formation can be explained in terms of the interfacial turbulence and the “diffusion-stranding” processes between two unequilibrated liquid phases shown in Figure 3. When both phases are in contact, it is assumed that solvent diffuses from the organic phase into the water and carries with it some polymer chains which are still in solution. During the solvent diffuses further into the water, the associated polymer chains aggregate and form nanoparticle shown in Figure 4. The mechanism of nanoparticle formation can be described based on the water-solvent, water-polymer and solvent-polymer interactions.

With this technique, PLGA [57-59], PCL [60], SB-PVA-g-PLGA [53] and

Methacrylic acid copolymer [61,62] nanoparticles loaded with therapeutic drugs, e.g. TRH and elcatonin, cyclosporin A were extensively studied. However, the exposure to organic solvent for labile proteins during the preparation process and low encapsulation efficiency for water soluble drugs [57] limit the application of this method.

Figure 3. Schematic diagram of the mechanism of Marangoni effect [63]

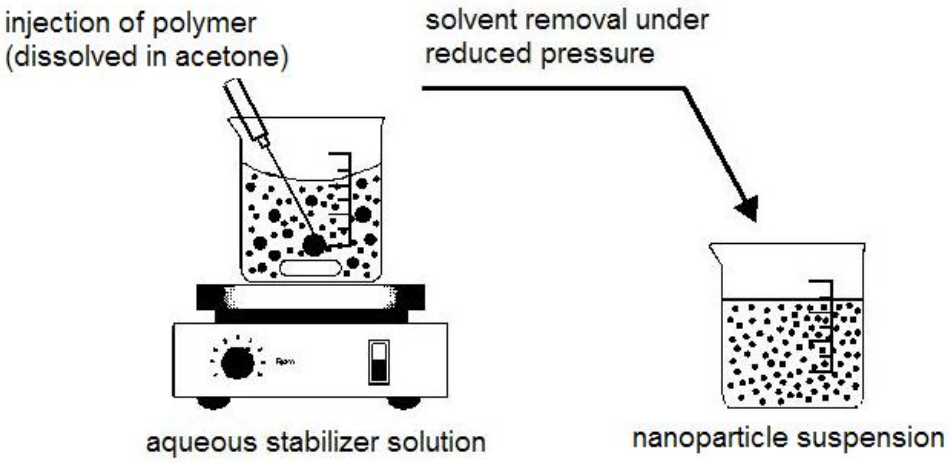

Figure 4. Schematic diagram of nanoparticles preparation using solvent displacement

3.2 Adsorption processs

Stabilization of proteins in delivery devices and design of appropriate protein carriers are major research issues. Preservation of bioactive protein and improvement

of drug loading during nanoparticles preparation based on defined colloidal characteristics are a great challenge. Denaturation of protein during preparation primarily is due to high shear forces and solvent exposure; furthermore, high acidity in the nanoparticles matrix due to the polymer degradation also leads to the loss of bioactivity of protein [64].

Compared to other loading methods, this adsorption technique can be performed in an aqueous solution and at a low temperature, improving the prospects for preserved activity of sensitive drug molecules. Moreover, polymer degradation has no detrimental effect on the protein absorbed on the surface of nanoparticles. However, it is reported that a large amount of drug can be entrapped by the incorporation method when compared to the adsorption [24]. For a successful NP system, a high loading capacity is desirable to reduce the quantity of the carrier required for administration. Many efforts have been made to develop a method to associate the protein to the nanoparticle surface by adsorption [65-70]. Additionally, Fresta et al reported a higher burst release up to 60-70% for the NPs loaded with drug by adsorption [24]. Further efforts related to adsorption process need to be made to investigate the interaction between the protein molecules and surface of NPs, to improve the loading efficiency and to achieve the desired release profile.

3.3 Surface adsorption on preformed particles with ionic surface charge

An elegant and efficient method for protein loading was done by surface adsorption of bioactive materials onto unloaded PLGA particles carrying a surface charge [4,66,71-75]. One may take advantage of the protein's surface charge, which depends on its pI and the pH of the medium in which it is dispersed. PLGA or any other type of particles can be readily decorated with positive or negative surface charges by simply preparing the particles by a $W_1/O/W_2$ solvent evaporation/extraction process where the W_2 phase contains a cationic emulsion stabilizer [hexadecyltrimethylammonium bromide; poly(ethyleneimine); stearlyamine] or an anionic emulsifier (sodium dioctyl-sulfosuccintate; sodium dodecylsulfate). Such

compounds attach tightly to PLGA surfaces during preparation and provide the necessary surface charge for ionic adsorption of counter-ions. In these systems, however, the use of chlorinated solvents and high amounts of surfactants, detergents during particle preparation may affect their biocompatibility, in particular for the development of injectable formulations [76].

A recent approach has been employed using biodegradable polymers carrying cationic or anionic groups, such as sulfobutylated copolymers [53,66]. Particles made from such polyelectrolytes exposed surface charges, which were used to adsorb oppositely charged protein antigens. Provided that the ionic interaction between the particle surface and the adsorbate does not hamper the activity and availability of the bioactive material, such systems should hold great promise for antigen and DNA delivery [75]. The use of particles with ionic surface charge offers several advantages over classical micro- or nano-encapsulation, amongst which the mild conditions for loading is probably the most attractive. PLGA particles with surface adsorbed protein antigens and DNA have been highly efficient in inducing strong immune responses, as recently reviewed by Singh et al [77].

4. Chitosan coated nanoparticles

Surface property of NPs is an important key factor for the destiny of NPs in vivo. Surface modified nanoparticles present several characteristics that make them suitable candidates to develop efficient mucosal administration forms, achieve long circulation time after parental administration, modify the body distribution, and offer drug protection against *in vivo* acid and enzymatic degradation [78]. Some of the widely used surface-coating materials are: polyethylene glycol (PEG), polyethylene oxide (PEO), poloxamer, poloxamine, polysorbate (Tween-80) and lauryl ethers (Brij-35) [24].

Cationic polymer chitosan has a well-known bioadhesive nature, by the establishment of electrostatic interactions with sialic groups of mucins in the mucus layer. It was also demonstrated that chitosan can enhance the absorption of hydrophilic

molecules by promoting a structural reorganization of the tight junction-associated proteins [79]. The interesting features of chitosan regarding its application in nanoparticulate delivery system include its biocompatibility, mucoadhesiviness and ability to enhance transiently the permeability of mucosal barrier [80]. Therefore, chitosan and its derivatives coated or prepared nanoparticles has been the subject of many studies in recent years [78-96].

Chitosan has been coated onto nanoparticles made of different materials, as for example, poly(alkyl cynaoacylate)(PACA) [78,83], poly(methyl methacrylate)(PMMA) [85], poly-ε-caprolactone(PECL)[97,98], DL-lactide/glycolide copolymer [91], and lipid[92]. Chitosan coated nanoparticles for mucosal (oral, nasal, pulmonary and ocular) delivery were investigated and showed enhanced and prolonged systemic absorption of the model protein.

5. Objectives of this work

The objectives of this research were to investigate protein loaded micro- and nano-biodegradable polymer particulate system. The goals were to achieve desired release profiles for microparticles during pore diffusion process, and to improve the protein loading and release profiles with full preserved bioactivity of protein during nanoparticles preparation.

The specific hypotheses of this dissertation are:

1) Due to the problems of protein release from biodegradable microparticles, we attached our research emphasis on the release profile of protein during pore diffusion stage. Considering the diverse properties of polymers, we would like to find the elemental relationship of microparticle morphology, drug distribution and release profiles. It was postulated that for relatively hydrophobic polymer, influence of morphology and drug distribution on release profiles during pore diffusion process is much pronounced on burst release; by contrast, for hydrophilic polymer this influence is significant at the slow release stage. Hence, to achieve desired release profiles different strategies of morphology and drug distribution

modification are required (Chapter 2).

2) To further improve the loading capacity and release profiles of protein loaded polymeric nanoparticles, we assumed that taking advantage of the nanoparticle surface charge, oppositely charged protein can be absorbed onto nanoparticle effectively through electrostatic interaction by adsorption process with full preserved bioactivity. Furthermore, with this variation of electrostatic interaction forces between protein and particles higher loading capacity of protein can be achieved on the nanoparticles with higher surface charge density. Also it is expected with this increase of electrostatic forces desired release profiles are possible to be achieved. For this purpose negatively charged nanoparticles consisting of PLGA and PSS were prepared with variable negative charge density, and loading capacity of positively charged model protein lysozyme was evaluated to test the influence of charge density (Chapter 3).
3) To further improve the release profiles or the stability of protein adsorbed on the surface of nanoparticles, we postulated that it is possible to deposit another polymer layer like chitosan and its derivatives utilizing the surface negative charge surplus as the outmost layer of this nanoparticles. It is hoped that with this new layer-by-layer nanostructure protein is sandwiched within multilayer of polymers, which can improve the stability of protein and release profiles (Chapter 4).
4) New class of negatively charged polymer SB-PVA-PLGA and P(VS-VA)-PLGA have been recently prepared. For SB-PVA-PLGA, grafting of sulfonic groups occurred on the side chain of PVA backbone. By contrast, sulfonic group was grafted directly to the PVA backbone. We postulated that surface charge density of nanoparticles and loading capacity of oppositely charge protein are dependent on the structure of P(VS-VA)-PLGA, like substitution degree of sulfonic group and PLGA chain length (Chapter 5).

6. Reference

[1] V.R. Sinha, A. Trehan, Biodegradable microspheres for protein delivery. J. Control. Release 90 (2003) 261-280.

[2] A. Vila, A. Sanchez, M. Tobio, P. Calvo, M.J. Alonso, Design of biodegradable particles for protein delivery. J. Control. Release 78 (2002) 15-24.

[3] S. Freiberg, X.X. Zhu, Polymer microspheres for controlled drug release. Int. J. Pharm. 282 (2004) 1-18.

[4] V.R. Sinha, A. Trehan, Biodegradable microspheres for protein delivery. J. Control. Release 90 (2003) 261-280.

[5] J.L. Cleland, E.T. Duenas, A. Park, A. Daugherty, J. Kahn, J. Kowalski, A. Cuthbertson, Development of poly-(D,L-lactide--coglycolide) microsphere formulations containing recombinant human vascular endothelial growth factor to promote local angiogenesis. J. Control. Release 72 (2001) 13-24.

[6] U. Bilati, E. Allemann, E. Doelker, Strategic approaches for overcoming peptide and protein instability within biodegradable nano- and microparticles. Eur. J. Pharm. Biopharm. 59 (2005) 375-388.

[7] L.A. Dailey, M. Wittmar, T. Kissel, The role of branched polyesters and their modifications in the development of modern drug delivery vehicles. J. Control. Release 101 (2005) 137-149.

[8] B. Bittner, M. Morlock, H. Koll, G. Winter, T. Kissel, Recombinant human erythropoietin (rhEPO) loaded poly(lactide-co-glycolide) microspheres: influence of the encapsulation technique and polymer purity on microsphere characteristics. Eur. J. Pharm. Biopharm. 45 (1998) 295-305.

[9] J. Rojas, H. Pinto-Alphandary, E. Leo, S. Pecquet, P. Couvreur, E. Fattal, Optimization of the encapsulation and release of beta-lactoglobulin entrapped poly(DL-lactide-co-glycolide) microspheres. Int. J. Pharm. 183 (1999) 67-71.

[10] P.G. Shao, L.C. Bailey, Stabilization of pH-induced degradation of porcine insulin in biodegradable polyester microspheres. Pharm. Dev. Technol. 4 (1999) 633-642.

[11] W. Lu, T.G. Park, Protein release from poly(lactic-co-glycolic acid) microspheres: protein stability problems. PDA J. Pharm. Sci. Technol. 49 (1995)

13-19.

[12] P. Couvreur, B. Kante, L. Grislain, M. Roland, P. Speiser, Toxicity of polyalkylcyanoacrylate nanoparticles II: Doxorubicin-loaded nanoparticles. J. Pharm. Sci. 71 (1982) 790-792.

[13] D.K. Malik, S. Baboota, A. Ahuja, S. Hasan, J. Ali, Recent advances in protein and peptide drug delivery systems. Curr. Drug Deliv. 4 (2007) 141-151.

[14] A. Brunner, K. Maeder, A. Goepferich, pH and osmotic pressure inside biodegradable microspheres during erosion. Pharm. Res. 16 (1999) 847-853.

[15] T. Musumeci, C.A. Ventura, I. Giannone, B. Ruozi, L. Montenegro, R. Pignatello, G. Puglisi, PLA/PLGA nanoparticles for sustained release of docetaxel. Int. J. Pharm. 325 (2006) 172-179.

[16] M.M. Jimenez, J. Pelletier, M.F. Bobin, M.C. Martini, H. Fessi, Poly-epsilon-caprolactone nanocapsules containing octyl methoxycinnamate: preparation and characterization. Pharm. Dev. Technol. 9 (2004) 329-339.

[17] R. Voltan, A. Castaldello, E. Brocca-Cofano, G. Altavilla, A. Caputo, M. Laus, K. Sparnacci, B. Ensoli, S. Spaccasassi, M. Ballestri, L. Tondelli, Preparation and Characterization of Innovative Protein-coated Poly(Methylmethacrylate) Core-shell Nanoparticles for Vaccine Purposes. Pharm. Res. (2007).

[18] C. Chauvierre, D. Labarre, P. Couvreur, C. Vauthier, Novel polysaccharide-decorated poly(isobutyl cyanoacrylate) nanoparticles. Pharm. Res. 20 (2003) 1786-1793.

[19] C. Damge, J. Vonderscher, P. Marbach, M. Pinget, Poly(alkyl cyanoacrylate) nanocapsules as a delivery system in the rat for octreotide, a long-acting somatostatin analogue. J. Pharm. Pharmacol. 49 (1997) 949-954.

[20] K. Langer, S. Balthasar, V. Vogel, N. Dinauer, H. von Briesen, D. Schubert, Optimization of the preparation process for human serum albumin (HSA) nanoparticles. Int. J. Pharm. 257 (2003) 169-180.

[21] S. Azarmi, Y. Huang, H. Chen, S. McQuarrie, D. Abrams, W. Roa, W.H. Finlay, G.G. Miller, R. Lobenberg, Optimization of a two-step desolvation method for preparing gelatin nanoparticles and cell uptake studies in 143B osteosarcoma cancer cells. J. Pharm. Pharm. Sci. 9 (2006) 124-132.

[22] J. Panyam, D. Williams, A. Dash, D. Leslie-Pelecky, V. Labhasetwar, Solid-state solubility influences encapsulation and release of hydrophobic drugs

from PLGA/PLA nanoparticles. J. Pharm. Sci. 93 (2004) 1804-1814.

[23] U. Bilati, E. Allemann, E. Doelker, Development of a nanoprecipitation method intended for the entrapment of hydrophilic drugs into nanoparticles. Eur. J. Pharm. Sci. 24 (2005) 67-75.

[24] K.S. Soppimath, T.M. Aminabhavi, A.R. Kulkarni, W.E. Rudzinski, Biodegradable polymeric nanoparticles as drug delivery devices. J. Control. Release 70 (2001) 1-20.

[25] D.K. Gilding, A.M. Reed, Biodegradable polymers for use in surgery. Polyglycolic/poly(lactic acid) homo- and copolymers: 1. Polymer 20 (1979) 1459-1464.

[26] K.A. Athanasiou, G.G. Niederauer, C.M. Agrawal, Sterilization, toxicity, biocompatibility and clinical applications of polylactic acid/polyglycolic acid copolymers. Biomaterials 17 (1996) 93-102.

[27] R. Jalil, J.R. Nixon, Microencapsulation using poly (L-lactic acid) III: Effect of polymer molecular weight on the microcapsule properties. J. Microencapsul. 7 (1990) 41-52.

[28] H.B. Ravivarapu, K. Burton, P.P. DeLuca, Polymer and microsphere blending to alter the release of a peptide from PLGA microspheres. Eur. J. Pharm. Biopharm. 50 (2000) 263-270.

[29] A. Goepferich, Polymer degradation and erosion. Mechanisms and applications. Eur. J. Pharm. Biopharm. 42 (1996) 1-11.

[30] S. Li, Hydrolytic degradation characteristics of aliphatic polyesters derived from lactic and glycolic acids. J. Biomed. Mater. Res. 48 (1999) 342-353.

[31] E. Walter, D. Dreher, M. Kok, L. Thiele, S.G. Kiama, P. Gehr, H.P. Merkle, Hydrophilic poly(DL-lactide-co-glycolide) microspheres for the delivery of DNA to human-derived macrophages and dendritic cells. J. Control. Release 76 (2001) 149-168.

[32] X. Luan, R. Bodmeier, Influence of the poly(lactide-co-glycolide) type on the leuprolide release from in situ forming microparticle systems. J. Control. Release 110 (2006) 266-272.

[33] Y.Y. Yang, T.S. Chung, N.P. Ng, Morphology, drug distribution, and in vitro release profiles of biodegradable polymeric microspheres containing protein fabricated by double-emulsion solvent extraction/evaporation method.

Biomaterials 22 (2001) 231-241.

[34] T. Ehtezazi, C. Washington, C.D. Melia, Determination of the internal morphology of poly (D,L-lactide) microspheres using stereological methods. J. Control. Release 57 (1999) 301-314.

[35] G. Jiang, B.H. Woo, F. Kang, J. Singh, P.P. DeLuca, Assessment of protein release kinetics, stability and protein polymer interaction of lysozyme encapsulated poly(D,L-lactide-co-glycolide) microspheres. J. Control. Release 79 (2002) 137-145.

[36] M. Morlock, T. Kissel, Y.X. Li, H. Koll, G. Winter, Erythropoietin loaded microspheres prepared from biodegradable LPLG-PEO-LPLG triblock copolymers: protein stabilization and in-vitro release properties. J. Control. Release 56 (1998) 105-115.

[37] T. Uchida, A. Yagi, Y. Oda, Y. Nakada, S. Goto, Instability of bovine insulin in poly(lactide-co-glycolide) (PLGA) microspheres. Chem. Pharm. Bull. (Tokyo) 44 (1996) 235-236.

[38] Y. Ogawa, M. Yamamoto, H. Okada, T. Yashiki, T. Shimamoto, A new technique to efficiently entrap leuprolide acetate into microcapsules of polylactic acid or copoly(lactic/glycolic) acid. Chem. Pharm. Bull. (Tokyo) 36 (1988) 1095-1103.

[39] H.K. Sah, R. Toddywala, Y.W. Chien, Biodegradable microcapsules prepared by a w/o/w technique: effects of shear force to make a primary w/o emulsion on their morphology and protein release. J. Microencapsul. 12 (1995) 59-69.

[40] N. Nihant, C. Schugens, C. Grandfils, R. Jerome, P. Teyssie, Polylactide microparticles prepared by double emulsion/evaporation technique. I. Effect of primary emulsion stability. Pharm. Res. 11 (1994) 1479-1484.

[41] I.D. Rosca, F. Watari, M. Uo, Microparticle formation and its mechanism in single and double emulsion solvent evaporation. J. Control. Release 99 (2004) 271-280.

[42] G. Crotts, T.G. Park, Preparation of porous and nonporous biodegradable polymeric hollow microspheres. J. Control. Release 35 (1995) 91-105.

[43] Y.Y. Yang, H.H. Chia, T.S. Chung, Effect of preparation temperature on the characteristics and release profiles of PLGA microspheres containing protein fabricated by double-emulsion solvent extraction/evaporation method. J.

Control. Release 69 (2000) 81-96.

[44] M. Polakovic, T. Gorner, R. Gref, E. Dellacherie, Lidocaine loaded biodegradable nanospheres. II. Modelling of drug release. J. Control. Release 60 (1999) 169-177.

[45] G. Jiang, B.C. Thanoo, P.P. DeLuca, Effect of osmotic pressure in the solvent extraction phase on BSA release profile from PLGA microspheres. Pharm. Dev. Technol. 7 (2002) 391-399.

[46] E. Leo, S. Pecquet, J. Rojas, P. Couvreur, E. Fattal, Changing the pH of the external aqueous phase may modulate protein entrapment and delivery from poly(lactide-co-glycolide) microspheres prepared by a w/o/w solvent evaporation method. J. Microencapsul. 15 (1998) 421-430.

[47] S. Giovagnoli, P. Blasi, M. Ricci, C. Rossi, Biodegradable microspheres as carriers for native superoxide dismutase and catalase delivery. AAPS PharmSciech 5 (2004) e51.

[48] K.F. Pistel, T. Kissel, Effects of salt addition on the microencapsulation of proteins using W/O/W double emulsion technique. J. Microencapsul. 17 (2000) 467-483.

[49] M.C. Julienne, M.J. Alonso, J.L. Gomez Amoza, J.P. Benoit, Preparation of poly(DL-lactide/glycolide) nanoparticles of controlled particle size distribution: application of experimental designs. Drug Dev. Ind. Pharm. 18 (1992) 1063-1077.

[50] P. Couvreur, B. Kante, M. Roland, P. Guiot, P. Bauduin, P. Speiser, Polycyanoacrylate nanocapsules as potential lysosomotropic carriers: preparation, morphological and sorptive properties. J. Pharm. Pharmacol. 31 (1979) 331-332.

[51] E. Allemann, J.C. Leroux, R. Gurny, E. Doelker, In vitro extended-release properties of drug-loaded poly(DL-lactic acid) nanoparticles produced by a salting-out procedure. Pharm. Res. 10 (1993) 1732-1737.

[52] H. Fessi, F. Puisieux, J.P. Devissaguet, N. Ammoury, S. Benita, Nanocapsule formation by interfacial polymer deposition following solvent displacement. Int. J. Pharm. 55 (1989) R1-R4.

[53] T. Jung, A. Breitenbach, T. Kissel, Sulfobutylated poly(vinyl alcohol)-graft-poly(lactide-co-glycolide)s facilitate the preparation of small

negatively charged biodegradable nanospheres. J. Control. Release 67 (2000) 157-169.

[54] S. Dreis, F. Rothweiler, M. Michaelis, J. Cinatl, Jr., J. Kreuter, K. Langer, Preparation, characterisation and maintenance of drug efficacy of doxorubicin-loaded human serum albumin (HSA) nanoparticles. Int. J. Pharm. (2007).

[55] C.V. Sternling, L.E. Scriven, Intefacial turbulence: hydrodynamic instability and the Marangoni effect. AIChE Journal 5 (1959) 514-523.

[56] B. Dimitrova, I. Ivanov, E. Nakache, Mass transport effects on the stability of emulsion: emulsion films with acetic acid and acetone diffusing across the interface. J. Dispersion Sci. Technol. 9 (1988) 321-341.

[57] T. Niwa, H. Takeuchi, T. Hino, N. Kunou, Y. Kawashima, Preparations of biodegradable nanospheres of water-soluble and insoluble drugs with DL-lactide/glycolide copolymer by a novel spontaneous emulsification solvent diffusion method, and the drug release behavior. J. Control. Release 25 (1993) 89-98.

[58] H. Murakami, M. Kobayashi, H. Takeuchi, Y. Kawashima, Preparation of poly(DL-lactide-co-glycolide) nanoparticles by modified spontaneous emulsification solvent diffusion method. Int. J. Pharm. 187 (1999) 143-152.

[59] Y. Kawashima, H. Yamamoto, H. Takeuchi, T. Hino, T. Niwa, Properties of a peptide containing DL-lactide/glycolide copolymer nanospheres prepared by novel emulsion solvent diffusion methods. Eur. J. Pharm. Biopharm. 45 (1998) 41-48.

[60] J. Molpeceres, M. Guzman, M.R. Aberturas, M. Chacon, L. Berges, Application of central composite designs to the preparation of polycaprolactone nanoparticles by solvent displacement. J. Pharm. Sci. 85 (1996) 206-213.

[61] S. Galindo-Rodriguez, E. Allemann, H. Fessi, E. Doelker, Physicochemical parameters associated with nanoparticle formation in the salting-out, emulsification-diffusion, and nanoprecipitation methods. Pharm. Res. 21 (2004) 1428-1439.

[62] S.A. Galindo-Rodriguez, F. Puel, S. Briancon, E. Allemann, E. Doelker, H. Fessi, Comparative scale-up of three methods for producing ibuprofen-loaded nanoparticles. Eur. J. Pharm. Sci. 25 (2005) 357-367.

[63] http://www.fvt.mw.tum.de/forschung/stoffuebergang/marangoni_eng.htm.

[64] J.A. Schrier, P.P. DeLuca, Porous bone morphogenetic protein-2 microspheres: polymer binding and in vitro release. AAPS PharmSciech 2 (2001) E17.

[65] J. Chesko, J. Kazzaz, M. Ugozzoli, T. O'Hagan D, M. Singh, An investigation of the factors controlling the adsorption of protein antigens to anionic PLG microparticles. J. Pharm. Sci. 94 (2005) 2510-2519.

[66] T. Jung, W. Kamm, A. Breitenbach, G. Klebe, T. Kissel, Loading of tetanus toxoid to biodegradable nanoparticles from branched poly(sulfobutyl-polyvinyl alcohol)-g-(lactide-co-glycolide) nanoparticles by protein adsorption: a mechanistic study. Pharm. Res. 19 (2002) 1105-1113.

[67] H. Larsericsdotter, S. Oscarsson, J. Buijs, Thermodynamic Analysis of Proteins Adsorbed on Silica Particles: Electrostatic Effects. J. Colloid Interface Sci. 237 (2001) 98-103.

[68] W. Norde, J. Lyklema, The adsorption of human plasma albumin and bovine pancreas ribonuclease at negatively charged polystyrene surfaces. II. Hydrogen ion titrations. J. Colloid Interface Sci. 66 (1978) 266-276.

[69] J.M. Peula, F.J. de las Nieves, Adsorption of monomeric bovine serum albumin on sulfonated polystyrene model colloids. 1. Adsorption isotherms and effect of the surface charge density. Colloids Surf. A Physicochem. Eng. Asp. 77 (1993) 199-208.

[70] S.K. Han, J.H. Lee, D. Kim, S.H. Cho, S.H. Yuk, Hydrophilized poly(lactide-co-glycolide) nanoparticles with core/shell structure for protein delivery. Sci. Tech. Adv. Mater. 6 (2005) 468-474.

[71] J. Kazzaz, J. Neidleman, M. Singh, G. Ott, D.T. O'Hagan, Novel anionic microparticles are a potent adjuvant for the induction of cytotoxic T lymphocytes against recombinant p55 gag from HIV-1. J. Control. Release 67 (2000) 347-356.

[72] M. Singh, J. Kazzaz, M. Ugozzoli, J. Chesko, D.T. O'Hagan, Charged polylactide co-glycolide microparticles as antigen delivery systems. Expert Opin. Biol. Ther. 4 (2004) 483-491.

[73] L. Tondelli, E. Canto, A. Pistagna, S. Butt, A. Tripiciano, R. Cortesi, K. Sparnacci, M. Laus, Tailor-made core-shell nanospheres for antisense oligonucleotide delivery: IV. Adsorption/release behaviour. J. Biomater.

Sci.Polym. Ed. 12 (2001) 1339-1357.

[74] K.N. Atuah, E. Walter, H.P. Merkle, H.O. Alpar, Encapsulation of plasmid DNA in PLGA-stearylamine microspheres: a comparison of solvent evaporation and spray-drying methods. J. Microencapsul. 20 (2003) 387-399.

[75] H. Tamber, P. Johansen, H.P. Merkle, B. Gander, Formulation aspects of biodegradable polymeric microspheres for antigen delivery. Adv. Drug Deliv. Rev. 57 (2005) 357-376.

[76] Y. Ataman-Onal, S. Munier, A. Ganee, C. Terrat, P.Y. Durand, N. Battail, F. Martinon, R. Le Grand, M.H. Charles, T. Delair, B. Verrier, Surfactant-free anionic PLA nanoparticles coated with HIV-1 p24 protein induced enhanced cellular and humoral immune responses in various animal models. J. Control. Release 112 (2006) 175-185.

[77] M. Singh, M. Briones, G. Ott, D. O'Hagan, Cationic microparticles: A potent delivery system for DNA vaccines. Proc. Natl. Acad. Sci. U.S.A. 97 (2000) 811-816.

[78] I. Bravo-Osuna, G. Ponchel, C. Vauthier, Tuning of shell and core characteristics of chitosan-decorated acrylic nanoparticles. Eur. J. Pharm. Sci. 30 (2007) 143-154.

[79] I. Bravo-Osuna, C. Vauthier, A. Farabollini, G.F. Palmieri, G. Ponchel, Mucoadhesion mechanism of chitosan and thiolated chitosan-poly(isobutyl cyanoacrylate) core-shell nanoparticles. Biomaterials 28 (2007) 2233-2243.

[80] A.M. De Campos, A. Sanchez, R. Gref, P. Calvo, M.J. Alonso, The effect of a PEG versus a chitosan coating on the interaction of drug colloidal carriers with the ocular mucosa. Eur. J. Pharm. Sci. 20 (2003) 73-81.

[81] I. Bertholon, G. Ponchel, D. Labarre, P. Couvreur, C. Vauthier, Bioadhesive properties of poly(alkylcyanoacrylate) nanoparticles coated with polysaccharide. J. Nanosci. Nanotechnol. 6 (2006) 3102-3109.

[82] I. Bertholon, C. Vauthier, D. Labarre, Complement Activation by Core-Shell Poly(isobutylcyanoacrylate)-Polysaccharide Nanoparticles: Influences of Surface Morphology, Length, and Type of Polysaccharide. Pharm. Res. 23 (2006) 1313-1323.

[83] I. Bravo-Osuna, T. Schmitz, A. Bernkop-Schnuerch, C. Vauthier, G. Ponchel, Elaboration and characterization of thiolated chitosan-coated acrylic

nanoparticles. Int. J. Pharm. 316 (2006) 170-175.

[84] I. Bravo-Osuna, G. Millotti, C. Vauthier, G. Ponchel, In vitro evaluation of calcium binding capacity of chitosan and thiolated chitosan poly(isobutyl cyanoacrylate) core-shell nanoparticles. Int. J. Pharm. (2007).

[85] F. Cui, F. Qian, C. Yin, Preparation and characterization of mucoadhesive polymer-coated nanoparticles. Int. J. Pharm. 316 (2006) 154-161.

[86] S. Fischer, C. Foerg, S. Ellenberger, H.P. Merkle, B. Gander, One-step preparation of polyelectrolyte-coated PLGA microparticles and their functionalization with model ligands. J. Control. Release 111 (2006) 135-144.

[87] M. Garcia-Fuentes, D. Torres, M.J. Alonso, New surface-modified lipid nanoparticles as delivery vehicles for salmon calcitonin. Int. J. Pharm. 296 (2005) 122-132.

[88] M. Garcia-Fuentes, C. Prego, D. Torres, M.J. Alonso, A comparative study of the potential of solid triglyceride nanostructures coated with chitosan or poly(ethylene glycol) as carriers for oral calcitonin delivery. Eur. J. Pharm. Sci. 25 (2005) 133-143.

[89] A. Grenha, B. Seijo, C. Remunan-Lopez, Microencapsulated chitosan nanoparticles for lung protein delivery. Eur. J. Pharm. Sci. 25 (2005) 427-437.

[90] K.A. Janes, M.P. Fresneau, A. Marazuela, A. Fabra, M.J. Alonso, Chitosan nanoparticles as delivery systems for doxorubicin. J. Control. Release 73 (2001) 255-267.

[91] Y. Kawashima, H. Yamamoto, H. Takeuchi, Y. Kuno, Mucoadhesive DL-lactide/glycolide copolymer nanospheres coated with chitosan to improve oral delivery of elcatonin. Pharm. Dev. Technol. 5 (2000) 77-85.

[92] C. Prego, M. Fabre, D. Torres, M.J. Alonso, Efficacy and mechanism of action of chitosan nanocapsules for oral peptide delivery. Pharm. Res. 23 (2006) 549-556.

[93] C. Prego, D. Torres, M.J. Alonso, Chitosan nanocapsules as carriers for oral peptide delivery: effect of chitosan molecular weight and type of salt on the in vitro behaviour and in vivo effectiveness. J. Nanosci. Nanotechnol. 6 (2006) 2921-2928.

[94] A. Vila, A. Sanchez, K. Janes, I. Behrens, T. Kissel, J.L. Vila Jato, M.J. Alonso, Low molecular weight chitosan nanoparticles as new carriers for nasal vaccine

delivery in mice. Eur. J. Pharm. Biopharm. 57 (2004) 123-131.

[95] H. Yamamoto, Y. Kuno, S. Sugimoto, H. Takeuchi, Y. Kawashima, Surface-modified PLGA nanosphere with chitosan improved pulmonary delivery of calcitonin by mucoadhesion and opening of the intercellular tight junctions. J. Control. Release 102 (2005) 373-381.

[96] L. Zhang, M. Sun, R. Guo, Z. Jiang, Y. Liu, X. Jiang, C. Yang, Chitosan surface-modified hydroxycamptothecin loaded nanoparticles with enhanced transport across Caco-2 cell monolayer. J. Nanosci. Nanotechnol. 6 (2006) 2912-2920.

[97] P. Calvo, J.L. Vila-Jato, M.J. Alonso, Cationic polymer-coated nanocapsules as ocular drug carriers. Prodeed. Int. Symp. Control. Rel. Bioact. Mater. 24th (1997) 97-98.

[98] P. Calvo, C. Remunan-Lopez, J.L. Vila-Jato, M.J. Alonso, Development of positively charged colloidal drug carriers. Chitosan-coated polyester nanocapsules and submicron-emulsions. Colloid Polym. Sci. 275 (1997) 46-53.

Chapter 2

Influence of morphology and drug distribution on the release process of FITC-dextran loaded microspheres prepared with different types of PLGA

Submitted to: *J. Microencapsulation*

Abstract

The aim of the present work was to understand the collaborative roles and the comprehensive effects of polymer nature, morphology, drug distribution, and release behavior for PLGA microspheres prepared by the double emulsion method. The morphology and drug distribution of the FITC-dextran-loaded microspheres were investigated by scanning electron microscopy (SEM) and confocal laser scanning microscopy (CLSM), respectively. The results show that the morphology and release profiles depend on the polymer nature. For the capped PLGA RG502, the porosity, pore size, and drug distribution had no pronounced influence on the release profile beyond the initial release. No significant changes in size and morphology were found, and there was negligible water uptake during the release process. PEG addition as a pore maker indicated a possible way to modify the release rate at the second release stage. However, in the case of the uncapped PLGA RG503H, release profiles were dependent upon changes in porosity, pore size, and drug loading. Increases in porosity, internal pore size, and loading resulted in a continuous release profile. Previous studies have shown the importance of different process parameters on morphology and drug release, but in this work it is clear that polymer nature is a determining factor.

Keywords: Poly(latic-co-glycolic acid), microspheres, morphology, release mechanism

1. Introduction

Polymeric microencapsulation based on biodegradable polymers has proven to be a successful technique to protect and control the delivery of bioactive proteins [1]. PLGA (polylactide-co-glycolide) copolymers are the most widely used in the development of drug-containing biodegradable microparticles because they are biodegradable, biocompatible, and have been approved for several products. The drug release mechanism from PLGA microspheres can be based on diffusion or degradation [2]. The microparticles show a tri-phasic drug release, namely, an initial release followed by a slow release phase, and a final rapid release phase. Specifically, for the release of peptides or proteins, the pore diffusion process is of great importance because polymer degradation can lead to the accumulation of acidic monomers and the subsequent generation of an acidic micro-environment inside the degrading microspheres, resulting in instability of the protein or peptide.

The release profiles of proteins depend primarily on polymer nature, morphology, and drug distribution; of these, morphology and drug distribution are determined by the process conditions. We hypothesize that drug release in the pore diffusion process is closely related to the internal and external porosity of the microspheres; therefore, it is possible to accelerate drug release during this process by changing the morphology of the microspheres. Much research has focused on modifying the release profile by varying the process parameters to create different microsphere morphology or drug distribution by w/o/w emulsion solvent evaporation methods [3-10]. However, an important question remains as to whether the influence of morphology and drug distribution on drug release at this stage is dependent on polymer nature or not, a question which had not been addressed previously.

As demonstrated in previous studies [11-16], polymer nature has a great influence on drug release in the pore diffusion process. The PLGA type (molecular weight and end-group functionality) influences morphology; for example, the hydrophilicity or hydrophobicity of the PLGA end group is an important property

affecting the hydration process during the pore diffusion phase, which influences the drug release rate from the polymer matrix. Similar modification of the morphology and drug distribution of microspheres may present different patterns of release, depending on the polymer nature. In order to fully understand the resulting influences on release profiles, the polymer nature must be considered in conjunction with these other process parameters. To the best of our knowledge, such a combined approach to observe how morphology, drug distribution, and PLGA polymer properties influence the release rate in the pore diffusion process has not been investigated before.

Taking this into account, it is imperative to further investigate the interplay of polymer properties, internal morphology, drug distribution, and their combined effects on the release process. For this purpose, FITC-dextran was encapsulated as a model hydrophilic macromolecular compound in PLGA microspheres using a w/o/w method. First, the influence of different PLGA types on the surface and internal morphology, drug distribution, and release behavior of microspheres were systematically investigated, and second, the influences of porosity, pore size, and drug distribution on the release process were studied using hydrophilic and hydrophobic PLGAs. Changes in morphology, size evolution, water uptake, and drug location during the release process were also monitored so as to further understand the collaborative influence of polymer nature, drug loading, and morphology on the release process. Scanning electron microscopy (SEM) and confocal laser scanning microscopy (CLSM) were chosen to investigate the surface and internal morphology of microspheres and drug distribution, respectively. This work is essential for designing PLGA microspheres with desired release rates. Only with this knowledge can a specific release profile be attained through the modification of morphology and drug distribution.

2. Materials and Methods:

2.1 Materials:

Fluorescein isothiocyanate labeled dextran (FITC-dextran, 40 kDa, FD40S) was

purchased from Sigma (Deisenhofen, Germany). Poly(lactic-co-glycolic acid) (PLGA Resomers® RG502, RG502H, RG503, and RG503H) were obtained from Boehringer Ingelheim (Germany). Poly(vinyl alcohol) (PVA, 88% hydrolyzed, 130 kDa, Mowiol® 18-88) was obtained from Hoechst AG (Germany).

2.2 Standard preparation method (w/o/w)

Microspheres were prepared by a modified (w/o/w) double emulsion technique [17]. The microencapsulation process was carried out at 4℃. Briefly, 0.5 g of each respective polymer was dissolved in 2.5 ml dichloromethane (DCM). Into this organic phase (o), 250 µl of an aqueous drug solution (w) was emulsified using a high speed homogenizer (Ultra-Turrax TP18/10, IKA, Germany) operating at 20 500 rpm for 30 s to form the w_1/o emulsion. This primary emulsion was injected into 200 ml of an aqueous phase containing poly(vinyl alcohol) (0.5% w/v) (external phase, w) and homogenized for 30 s (Ultra-Turrax T25, IKA, Germany) at 8000 rpm. The resulting $w_1/o/w_2$ emulsion was stirred at 200 rpm for 3 h with a propeller stirrer to allow solvent evaporation and microsphere hardening. FITC-dextran loaded microspheres were collected by filtration and washed three times with distilled water and freeze-dried for 24 h (Edwards Freeze dryer Modulyo, UK), and then dried in a vacuum oven for 8 h. Final products were stored at 4℃ in a desiccator. Nonporous microspheres were prepared by adding 10% NaCl to the outer aqueous phase. This standard protocol was varied according to the different process parameters and fomulation factors discussed below.

2.3 Characterization of microspheres

Particle size and size distribution of microspheres were analyzed by dispersing ca. 10 mg of the samples in an aqueous solution of Tween® 20 (0.1% w/v). The measurements were carried out by laser light diffraction using a Malvern Mastersizer X (Malvern Instruments, UK). Each sample was measured in triplicate.

The total drug content of the FITC-dextran loaded microspheres was analyzed by

an extraction method [17]. Briefly, 8 mg of the FITC-dextran loaded microspheres was dissolved in 0.5 ml of DCM, followed by the addition of 4 ml of PBS buffer (pH 7.4) and agitation in a rotating bottle apparatus for 15 h at 30 rpm and 37℃ (Rotatherm, Liebisch, Germany). After separation of the two phases, the FITC-dextran concentration in the aqueous phase was determined fluorometrically using an FITC-dextran calibration curve (excitation: 493 nm, emission: 515 nm, LS 50B Luminescence Spectrometer, Perkin Elmer, Germany). Each sample was measured in triplicate.

In vitro release of FITC-dextran from microspheres was determined by suspending 20 mg of microspheres in 4 ml of PBS buffer (pH 7.4) containing 0.05% NaN_3 and 0.01% Tween 80 [1]. The samples were agitated in a rotating bottle apparatus (Rotatherm) at 30 rpm and 37℃. At defined time intervals, the buffer was completely withdrawn after centrifugation (2000 rpm for 5 min) and replaced by 4 ml of fresh buffer. The concentration of FITC-dextran in the supernatant was determined fluorometrically (excitation: 493 nm, emission: 515 nm, LS 50B Luminescence Spectrometer, Perkin Elmer) using a calibration curve. Each batch was studied in triplicate.

2.4 External and internal morphology of microspheres

Scanning electron microscopy (SEM) was used to characterize the internal and external morphology of the microparticles (CamScan Series 4 Scanning Electron Microscope, Cambridge Scanning Co. Ltd., England). Samples were dried in vacuum and subsequently sputter-coated with a carbon layer at 4-6 amps for 30 seconds, then with a gold layer at 2 amps for 30 seconds at 5×10^{-5} Pa (Edwards Auto 306 Vacuum Coater, Edwards, Germany). For the internal morphology, the cryo-cutting technique described by Ehtezazi et al. [18] was applied to prepare the cross sections of the microspheres for SEM investigation.

2.5 Drug distribution

The distribution of FITC-dextran within the microspheres was observed with a Carl Zeiss LSM 5100 confocal laser scanning microscope (Germany). The cross sections of PLGA microspheres were placed onto a glass slide, and the fluorescent image was taken (excitation: argon laser 488 nm, emission: optical filter set, long pass 505 nm, pinhole: 120).

2.6 Differential scanning calorimetry (DSC)

The drug status in the microspheres was investigated using a DSC7 calorimeter (Perkin Elmer). Thermograms covered the range of –10°C to 160°C with heating and cooling rates of 20°C/min. The melting point was determined from the endothermic peak of the DSC curve recorded in the first heating scan. The glass transition temperatures (Tg) were recorded from the second heating scan.

2.7 Water uptake and size evolution

Defined amount of microspheres were suspended in 7 ml of PBS, and the mixture was stirred at 30 rpm, 37°C. At pre-determined time intervals, the samples were centrifuged and the size of the microspheres was measured as described above. The size evolution at time t compared to time 0 was defined as:

$$Size\ evolution = \frac{size(t)}{size(0)} \times 100\%$$

Additional microspheres were collected periodically and the surface water was removed by filtration and the wet weight (Ww) of the microspheres was recorded. The samples were dried under vacuum to a constant weight and the dry weight (Wd) was recorded. The water uptake was then calculated as:

$$Water\ uptake = \frac{Ww - Wd}{Wd} \times 100\%$$

2.8 Calculations and Statistics

Results are presented as the mean ± standard deviation from at least three separate measurements. Significance between the mean values was calculated using ANOVA one-way analysis (Origin 7.0, Northampton, MA, USA). Probability values $P < 0.05$ were considered significant.

3. Results and discussion

3.1 The Effect of polymer molecular weight and end group

The polymers used in the present study were PLGAs with different molecular weight and end-group functionality. Properties for the four types of polymers used in this study are listed in Table 1. The polymers RG503 and RG503H have higher molecular weights than RG502 and RG502H; the "H" in the polymer name indicates uncapped (free) carboxyl termini, as opposed to having capped (ester) termini. FITC-dextran loaded microspheres are prepared with the standard preparation protocol.

When using the same preparation conditions, Table I shows that the size of the microspheres increased with increasing polymer molecular weight. For polymers of the same molecular weight, the microparticles prepared with capped polymers were larger than particles prepared with the uncapped polymers.

Figure 1 shows that more porous structures were observed for PLGAs with higher molecular weight, and relatively denser, less porous structures were seen for microparticles prepared from with the low molecular weight PLGAs. The influence of the PLGA end group on morphology cannot be generalized. The higher molecular weight RG503H microspheres showed a more porous surface and lower internal porosity; in contrast, RG503 microspheres showed less pores on the surface and a higher internal porosity. In the case of the lower molecular weight polymers, a different finding was observed. End-capped polymer (RG502) resulted in denser structure with less pores on the surface, when compared to uncapped polymer (RG502H). These

results suggest that the influence of the PLGA end group on the structure of microspheres depends on the PLGA molecular weight.

A possible explanation of these results is that double emulsion droplet size and stability is the decisive factor for the size and structure of microspheres [19], and this depends on the viscosity of organic phase and the interfacial tension of internal/outer water phase and organic phase. Higher molecular weight polymers (RG503 and RG503H) yield a more viscous solution, which leads to bigger emulsion droplets and a relatively stable double emulsion, which corresponds to the increased size and more porous structure. Simultaneously, the uncapped polymer (RG503H) is more hydrophilic than the capped polymer [20], which facilitates improved convection between the internal aqueous phase and the outer aqueous phase, which leads to the lower internal porosity and more pores on the surface.

However, the less viscous solutions of lower molecular weight PLGAs reduce the stability of the double emulsion. In this case, the more hydrophilic uncapped polymer (RG502H) decreases the interfacial tension, which improves the stability of double emulsion, and ultimately, results in higher porosity in the microspheres compared to the capped polymer (RG502). For RG502, its more hydrophobic properties, together with its lower viscosity generates a less stable double emulsion such that the internal water phase merges together, resulting in a capsule structure in a few cases. This internal water phase then connects with the outer water phase, which results in the denser structure observed for most micropsheres. This morphology was confirmed by the SEM images of micropsheres prepared with RG502. Confocal microscopy revealed that at a low theoretical drug loading (1%), the drug was uniformly distributed in the polymer matrix for all polymer types.

All microspheres showed a fast initial release phase, followed by a slower zero-order release phase, except for RG502H. Due to the faster degradation of RG502H, a full tri-phasic release profile was observed during the study duration, as shown in Figure 2. The initial release rate of microspheres is in the order of RG502H>RG503H>RG502>RG503. Regression equations for the second release

phase are shown in Table I according to a zero-order release model. The release rates of the uncapped polymers RG502H (1.106) and RG503H (0.724) are much greater relative to the capped polymers RG502 (0.286) and RG503 (0.161). In addition, the capped polymers with different molecular weights showed similar release rates at this second stage, irrespective of their differences in morphology.

It is known that size and surface morphology are key factors for the initial release rate. For polymers having the same end group, low molecular weight polymers result in a higher burst release because of the smaller microparticle size, which provides more surface area for drug diffusion [21]. For particles of similar size, microspheres prepared with uncapped polymer (RG503H) showed a higher release rate, as compared to the end-capped polymer (RG502). This finding can probably be explained by the more hydrophilic nature of the uncapped polymer and the porous structure of the microspheres, both of which facilitated water uptake from the release medium, resulting in a higher initial burst. The slower release rate observed for the end-capped polymer can be attributed to the delayed hydration of the microparticles because of the polymer's more hydrophobic character and the presence of fewer pores on the surface.

These results suggest that polymer nature plays an important role in the preparation of microspheres, which results in different morphologies and release rates. It is feasible that by selecting PLGAs of different molecular weights or different end groups, microspheres of a desired morphology or release rate could be manufactured.

Since the size of microspheres prepared from RG502 and RG503H was comparable (around 30 μm), and these two types polymers bear different end groups, they were chosen for the subsequent studies to investigate the combined effects of polymer end group, structure of microspheres, and drug distribution on the release process.

Polymer	Mw[c]	Inherent viscosity[d] (dl/g)	Acid number[e]	Microparticle size (μm)	Zero-order regression at second phase[f]
RG 502[a]	10 754	0.24	0.94	31.2 ± 0.5	$Q = 0.286t + 13.33$ ($R^2 = 0.974$)
RG 503[a]	31 281	0.41	0.72	47.8 ± 0.9	$Q = 0.161t + 2.71$ ($R^2 = 0.931$)
RG 502H[b]	10 777	0.19	15.1	24.8 ± 0.2	$Q = 1.106t + 14.44$ ($R^2 = 0.931$)
RG 503H[b]	28 022	0.38	4.60	35.6 ± 0.3	$Q = 0.724t + 15.80$ ($R^2 = 0.989$)

Table I. Physicochemical properties of poly(lactide-co-glycolide) PLGA, microparticle size, and second phase release rates.

All the data are from Boehringer Ingelheim Pharma GmbH and Co. KG.

[a] Non-H-series with ester termini.

[b] H-series with free carboxyl termini.

[c] Weight average molecular weight.

[d] 0.1% solution in chloroform, at 25 °C.

[e] mg KOH/g PLGA.

[f] Calculated from data in Figure 2 between 1 – 21 days, except for RG502H (1 – 11 days).

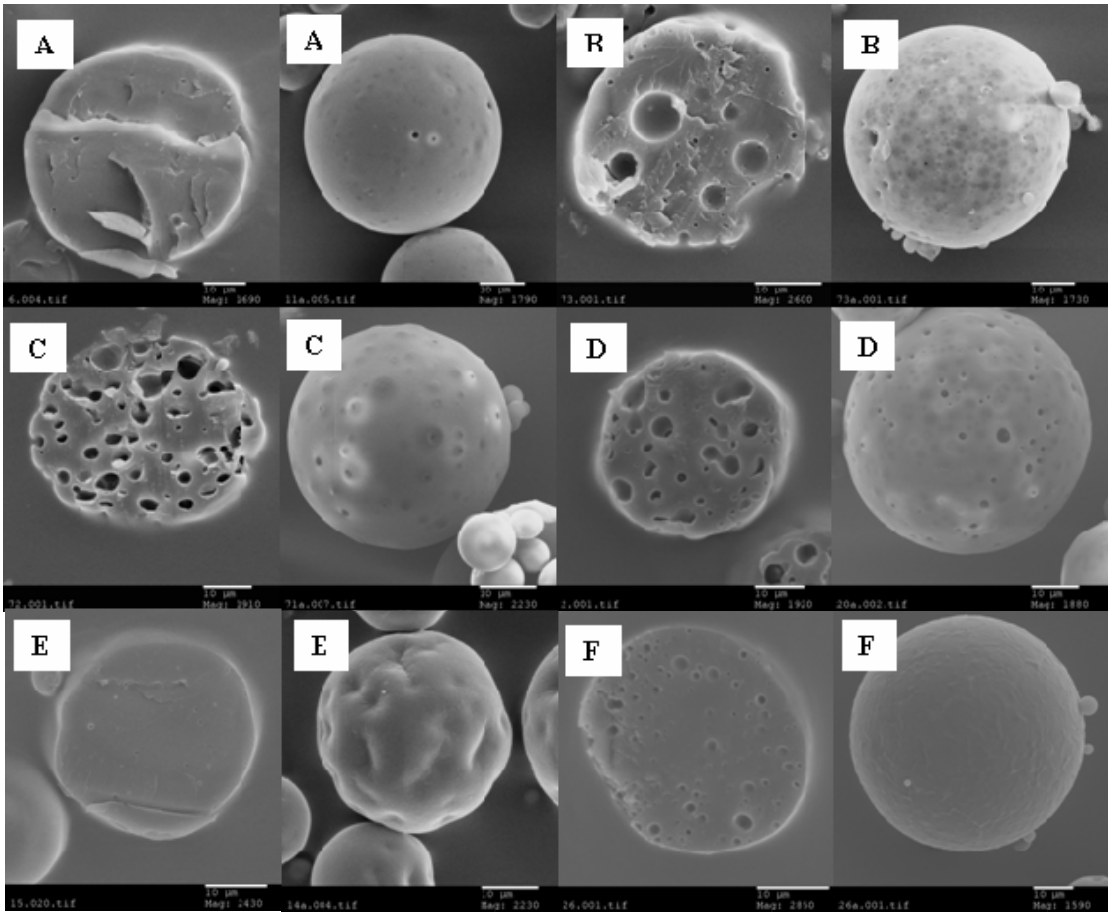

Figure 1. Surface scanning electronic micrographs of microspheres fabricated from different polymer types: RG502 (A), RG502H (B), RG503 (C), and RG503H (D). Both internal (cross-section, left) and external (right) morphologies are shown for porous microspheres prepared by the standard protocol. Nonporous RG503H micropsheres prepared with 10% NaCl in the external aqueous phase are shown at drug loading of 1% (E) and 10% (F).

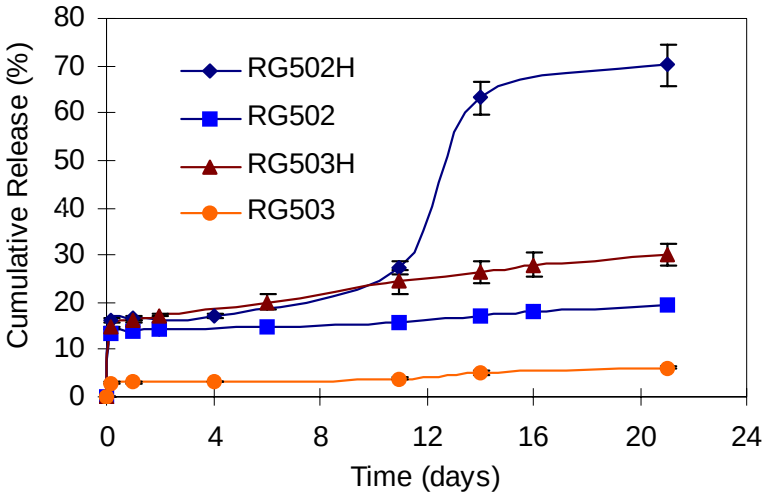

Figure 2. In vitro release profiles of the microspheres prepared from different polymers using the standard protocol.

3.2 Influence of porosity

Because the drug diffusion process is dependent on the porous structure of microspheres [2], the effect of porosity on the release process was investigated for PLGAs with different end groups . According to previous reports [6-8,22], the addition of salt to the external water phase (w_2) resulted in denser structures; therefore, nonporous and porous microspheres were prepared with polymers RG502 and RG503H using the standard protocol with and without the addition of 10% NaCl, respectively.

As expected, the addition of NaCl resulted in improved microsphere characteristics such as a dense morphology, and a nonporous and rugged surface for both formulations studied, as shown in in the SEM images in Figure 1E. Upon NaCl addition, the size of microspheres also decreased from 31.2 μm to 27.1 μm for RG502, and from 35.6 μm to 25.0 μm for RG503H.

Figure 3 shows that porosity influences the release rate both at the initial and the second release phases of RG503H particles. By reducing the porosity of the microspheres, the initial burst release was reduced by half, from 14.7% for the porous particles to 6.6% for the nonporous particles. The nonporous RG503H particles displayed a higher release rate during the second stage, however, such that the cumulative release at 21 h was about 30% for both the porous and nonporous microspheres.

In the case of the RG502 microspheres, a more drastic drop in the initial release resulted when the porosity of the particles was reduced. The burst release decreased from 13.6% for the porous RG502 microspheres to just 0.5% for the nonporous microspheres. Unlike what was observed for the RG503H particles, the release rates at the second stage were not significantly different for the RG502 particles ($P > 0.05$). In summary, making the particles less porous had significant results in reducing the burst release for both polymers, but the porosity only affected the second phase release rate for the RG503H particles.

These results are consistent with previous reports of a significant reduction in the initial burst with a decrease in porosity [9]. It is also worth mentioning that upon comparison of microspheres of similar size and morphology, the nonporous microspheres prepared from RG503H still exhibited a higher initial release (6.6%) than the nonporous microspheres of RG502 (0.5%). This is possibly due to the fact that the end groups of RG503H are more hydrophilic relative to RG502, which leads to a relatively loose structure during preparation and the association of more hydrophilic

drug substance on the surface. The higher release rate observed at the second release stage for the nonporous RG503H microspheres can be attributed to greater water uptake and higher swelling when compared to RG502 microspheres (see Figures 4 and 5). The water uptake after 15 days was similar for both the porous and nonporous RG503H microspheres (106.4% and 105.5%, respectively), and significant size increases were observed after 14 days in both cases, from 35.6 μm to 47.7 μm for the porous particles and from 25.0 μm to 35.7 μm for the nonporous particles.

The drug diffusion rate from this swelling matrix is not dependent on the porosity but on the concentration of drug in the microspheres. Based on the same drug loading, a lower burst release leads to a relatively higher drug concentration in the polymer matrix at the second stage; this concentration gradient results in a higher release rate for the nonporous RG503H microspheres. Morphology changes of RG503H microspheres are shown in Figure 6a. During the release process, no significant changes were observed for nonporous microspheres except for the size before the onset of the degradation. After incubating 15 days, a denser crust and a number of small pores were formed. In contrast, big cavities were formed in the porous microshperes after 15 days.

In the case of the RG502 microspheres, the sharp decrease in the initial release for the nonporous particles can be attributed to the smaller size, higher density, and hydrophobicity. The water uptake curve in Figure 5a shows no significant water uptake for either the porous or nonporous RG502 microspheres. This is also in agreement with the SEM pictures, which show marginal changes in the structure for both the porous

and nonporous particles during the release process shown in Figure 6(b). Figure 5b also shows that the size of these microspheres was not significantly different after 21 days ($P>0.05$).

Due to the hydrophobic character of the polymer, there is very little water penetration, exchange between the microspheres and the medium, or changes in structure. Irrespective of the porous or nonporous structure of the microspheres, the polymer nature limits the dissolution and diffusion of the drug from the polymer network until degradation sets in. This can explain the lower release rates observed for this end-capped polymer during the second release stage. To summarize these results for both RG502 and RG503H, porosity plays an important role in the release process; however, the effects of porosity are dependent upon the polymer nature.

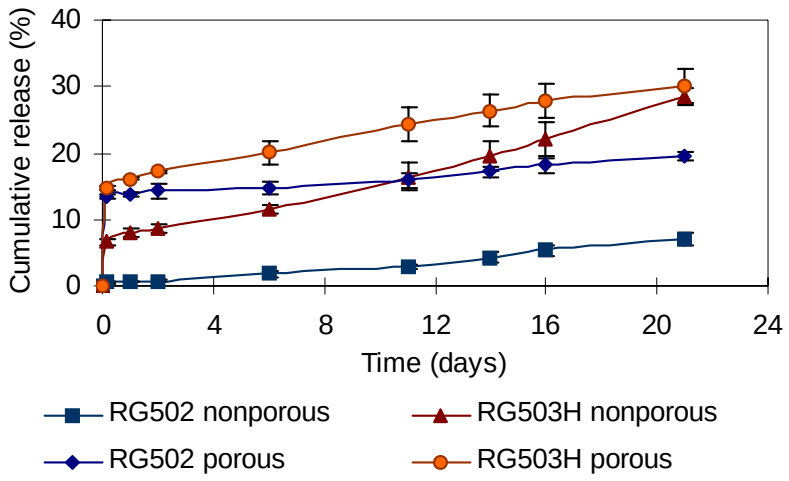

Figure 3. Release profiles of porous and nonporous microspheres prepared with RG502 and RG503H.

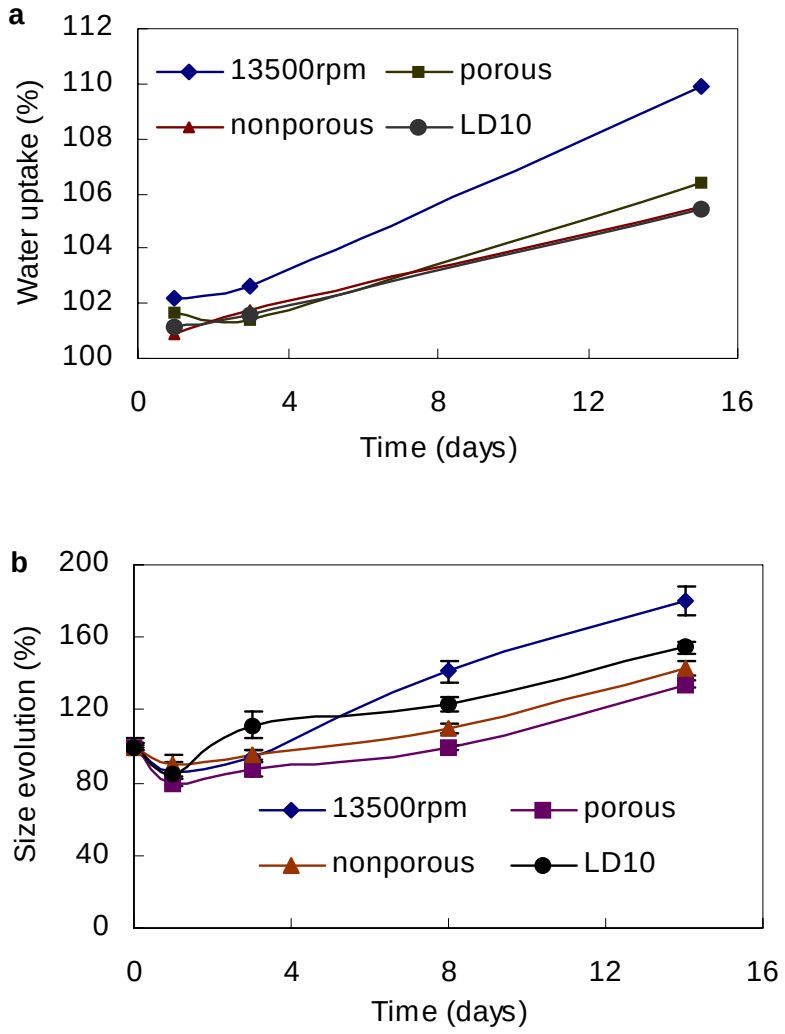

Figure 4. Water uptake (a) and size evolution (b) of RG503H microspheres during the release process. The standard protocol was varied as follows: 13500 rpm: primary emulsion homogenization speed changed to 13,500 rpm to increase pore size; Porous: standard protocol; Nonporous: NaCl added to the outer aqueous phase; LD10: drug loading of 10% with NaCl addition in the outer aqueous phase.

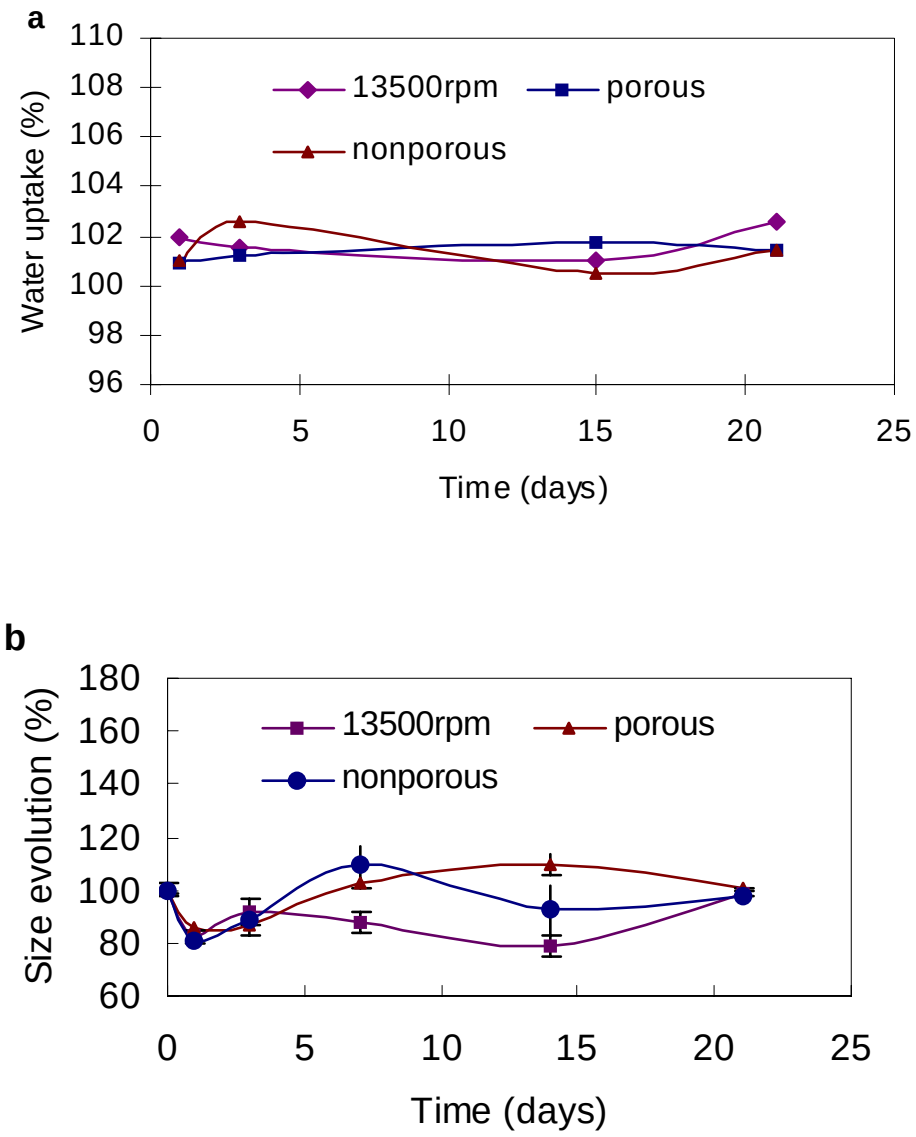

Figure 5. Water uptake (a) and size evolution (b) of RG502 microspheres during the release process. 13500 rpm: primary emulsion homogenization speed changed to 13,500 rpm to increase pore size; Porous: standard protocol; Nonporous: NaCl added to the outer aqueous phase.

a

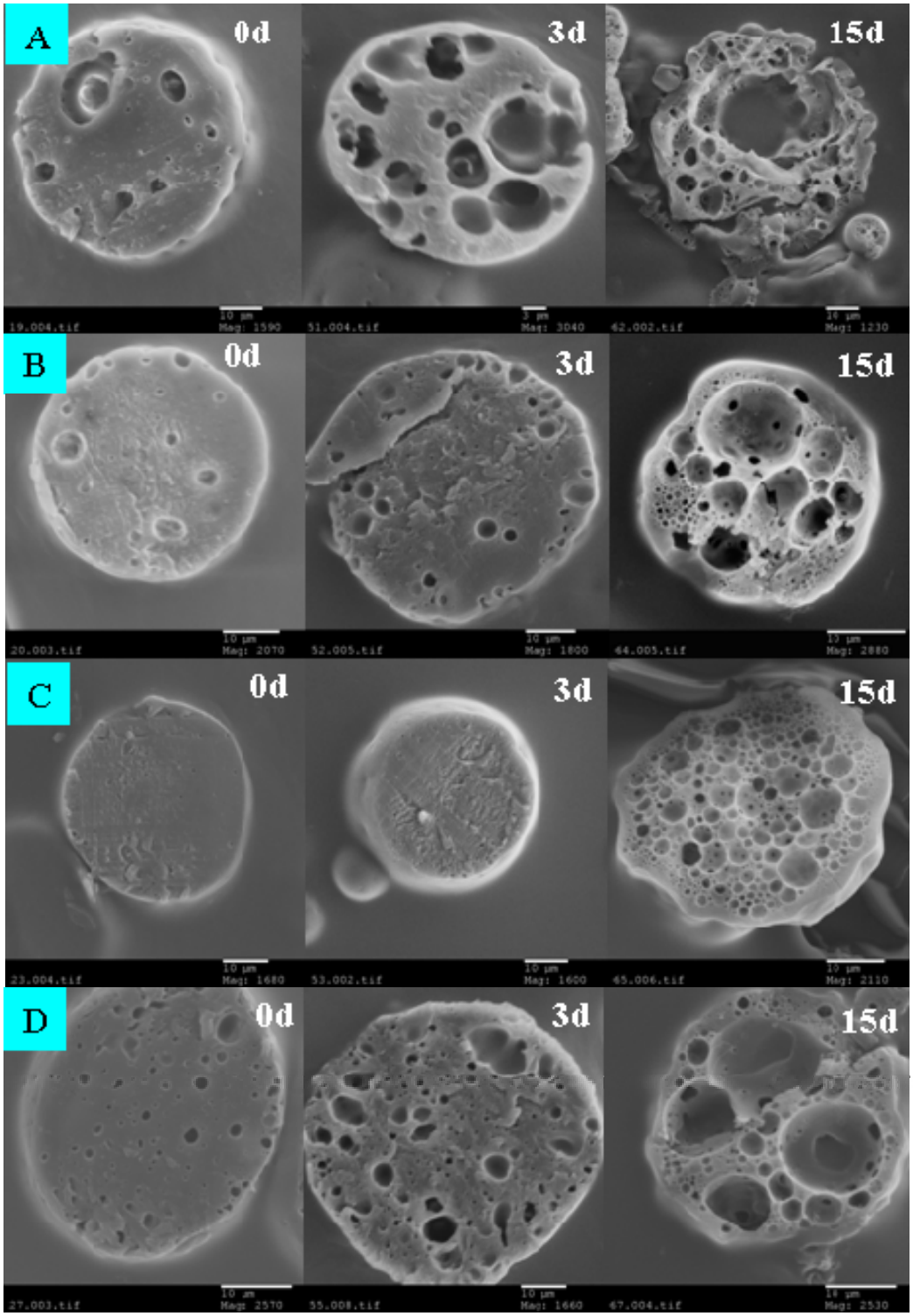

b

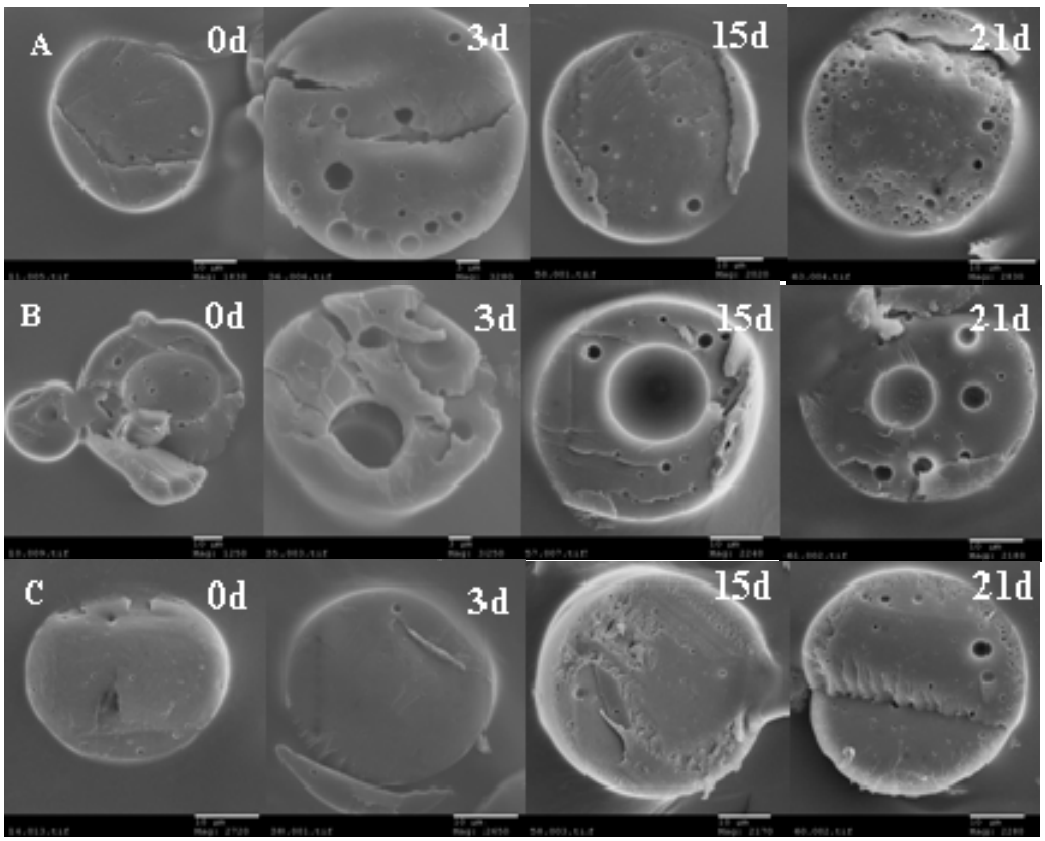

Figure 6. Scanning electronic micrographs of microspheres prepared from RG503H (a) and RG502 (b) during the release process. A: standard preparation protocol; B: standard protocol with a lower homogenization speed (13,500 rpm); C: standard protocol with 10% NaCl in the outer aqueous phase; D: drug loading of 10% with NaCl addition in the outer aqueous phase (for RG503H only).

3.3 The influence of pore size

The homogenization speed of the primary emulsion has a significant effect on microsphere morphology, as it provides the energy to disperse the internal aqueous phase in the organic phase [3,23]. Ehtezazi et al. found that formulations prepared at a lower speed contain larger and more broadly distributed pores than those prepared at higher speeds [18]. In order to investigate the influence of pore size distribution and polymer nature on the release process, porous microspheres were prepared with the

standard protocol by homogenizing the primary emulsion at different speeds with the polymers RG502 and RG503H.

The shear rates did not affect the size distribution patterns in this study, which is similar to the findings reported for BSA encapsulation in the literature [3]. Figure 7A shows the effects of homogenization speed on the structure of microspheres prepared with the polymer RG502. At speeds of 9 500 rpm and 13 500 rpm, a "microcapsule" structure results with average diameters of 26 ± 9 μm and 21 ± 6 μm, respectively, as measured from at least ten SEM images. Upon increasing the homogenization speed, the structure of the microspheres changed from the "microcapsule" type to a matrix-structure. At the speed of 20 500 rpm, a denser structure was observed with less microcapsule structure. In the case of the PLGA RG503H microspheres shown in Figure 7B, homogenizing at 13 500 rpm resulted in pores as large as 10-14 μm, but at 20 500 rpm, the pores were in the range of 3-5μm, with some surface pores less than 2 μm. This reconfirms that the homogenization speed is a successful way to modify the internal structure.

An increase in homogenization speed leads to homogeneous drug distribution, which is demonstrated by confocal microscopy in Figure 7 and confirms the report of Yan et al. [24]. At lower homogenization speeds, most of the drug reservoirs are larger than 2 μm, and some are even larger than 5μm.

Figure 8 shows that for the polymer RG502, microcapsules produced at low shear rate showed a higher initial release, whereas matrix-structure microspheres exhibited a lower burst release. However, no significant difference was observed in the second release phase for microspheres produced at different homogenization speeds ($P > 0.05$). No significant water uptake or size evolution had been observed for RG502 microspheres ($P > 0.05$, see Figure 5). Due to the hydrophobic nature of the polymer, hydration and swelling do not affect the behavior of these microspheres; therefore,

differences in pore size have no influence on water uptake, size evolution, or release rates. Figure 6 shows no obvious changes in morphology during the 21-day incubation for all RG502 formulations.

In the case of RG503H, the pore size has a less pronounced effect on the initial release rate compared to RG502. However, Figure 8 shows that the release rate increased as a function of pore size at the second release stage. The water uptake and size evolution were substantially higher for the RG503H microspheres with larger pores (the 13,500 rpm data series in Figure 4). The larger pore sizes and the hydrophilic nature of this uncapped PLGA facilitate the matrix water uptake process, and this faster hydration resulted in a higher swelling ratio. Figure 6 shows that incubation for 15 days, the microspheres with smaller pores displayed an almost spherical morphology, whereas microspheres with larger pores had a more distorted morphology. Larger pores and larger drug reservoirs were created at lower homogenization speeds, and these pores became even larger after the drug was released.

In summary, pore size showed a pronounced influence on the burst release but negligible influence on the release rate at the second release stage for RG502 microspheres. The opposite was observed for RG503H microspheres, where a marginal influence on the initial release and a greater effect at the second release stage were observed.

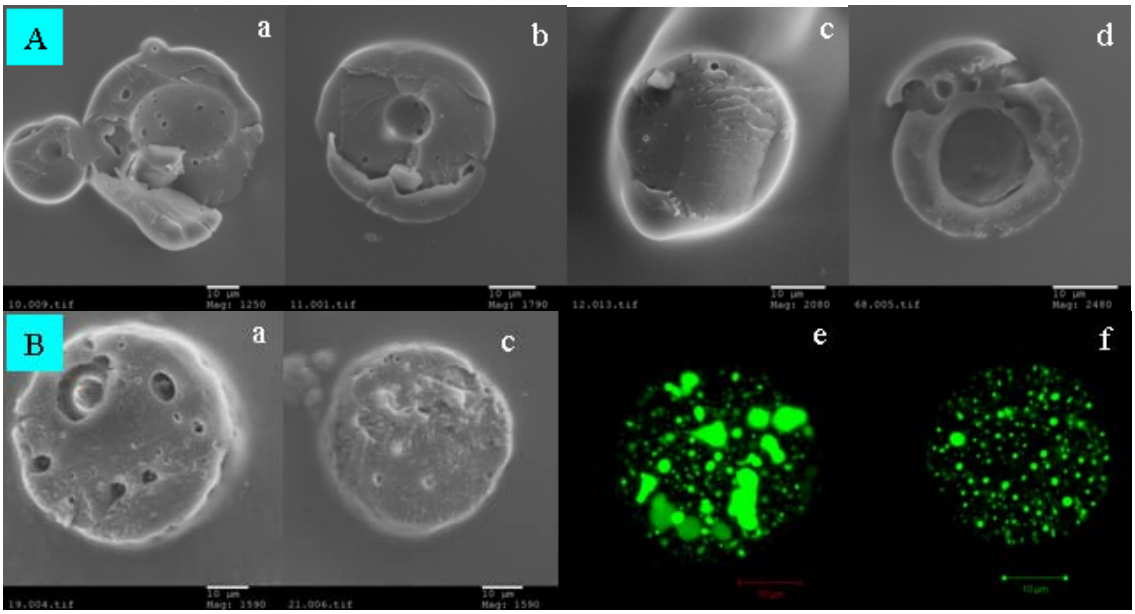

Figure 7. Scanning electronic micrographs of microsphere cross-sections. Microspheres were prepared from RG502 (A) or RG503H (B) at different homogenization speeds of the primary emulsion: 13,500 rpm (a), 20,500 rpm (b), and 24,000 rpm (c). Frame (d) shows RG502 particles with PEG addition (PEG: PLGA ratio of 20%). Frames (e) and (f) show CLSM images of RG503H microspheres prepared at 13,500 rpm and 20,500 rpm, respectively, with a drug loading of 1%

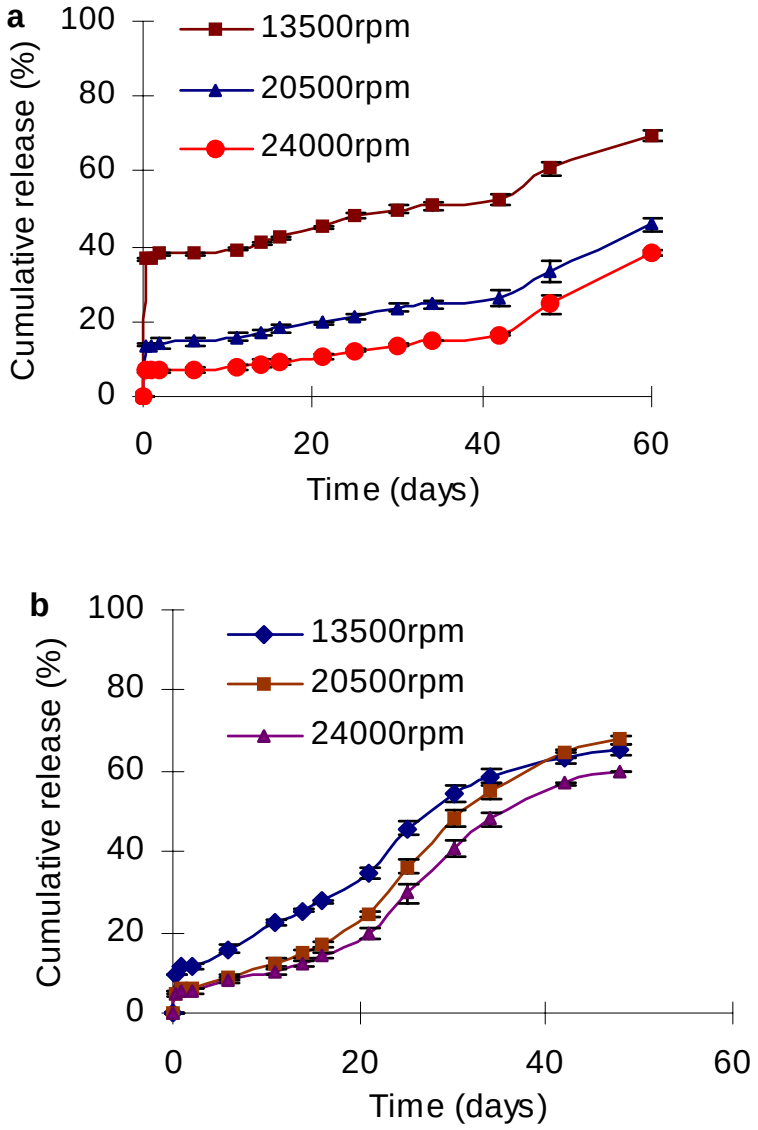

Figure 8. In vitro release profiles of FITC-dextran loaded microspheres prepared from RG502 (a) or RG503H (b) at different primary emulsion homogenization speeds.

3.4 Influence of drug loading on microsphere properties

Drug loading is a critical factor for microsphere delivery systems. It has been reported that drug loading can influence the location of the drug in the matrix, the drug release profile, and the formation of water channels during the release process [21,25,26]. In order to investigate the combined effect of drug loading and polymer

nature on the release process for microspheres of similar structure, nonporous RG502 and RG503H microspheres were prepared at different theoretical drug loading values, and the release profiles, morphology, size evolution, and water uptake during the release process were studied.

Increased drug loading resulted in slightly increased particle size and increased microsphere porosity – even with the addition of NaCl in the external aqueous phase (see Figure 1F). At low drug loading (1%), confocal laser scanning microscopy (CLSM) shows that the FITC-dextran was uniformly distributed in the microspheres as small drug strands less than 0.5μm, whereas at higher drug loading, the FITC-dextran was distributed as much bigger drug strands greater than 1μm (images not shown). DSC studies found that at all drug loading levels for both polymers the drug was molecular dissolved in the polymer matrix, except for drug loadings of 20% and 30% in RG502. These results are in good agreement with a previous report that at low nominal drug loading, fluconazole was incorporated in an amorphous state or in a molecular dispersion in the microsphere matrix, but at high nominal drug loading, part of the drug was in a crystalline form [27]. LeCorre et al. have also observed relatively highly loaded drug existing in a particulate dispersion instead of a molecular dispersion [26].

For RG502 microspheres, increased drug loading led to a higher burst release, as shown in Figure 9; however, the drug loading had little effect on the release rate at the second release phase even when the drug loading was increased to 30%. This result confirmed the findings of Sah et al., that the concentration gradient does not influence the drug release until the onset of polymer degradation [25].

In contrast, for microspheres prepared with RG503H, drug loading had a less pronounced effect on intial release, and higher release rates resulted from higher drug loading. At drug loading of 10%, a continuous release was observed over a period of 60 days. This is similar to the report of Sandor et al., who observed that higher

loaded microspheres, which have more interconnecting channels, did not exhibit the pronounced shift from diffusion-based to polymer degradation-based release that was seen with lower loaded microspheres [28].

The influence of drug loading on the release profile is dependent on the PLGA nature. The hydrophilic property of RG503H facilitates the matrix hydration and swelling process. Within this swelling structure, drug particles are dissolved and more apt to congregate. At high drug loading, large clusters of drug can thus extend from the surface deep into the matrix, which leads to increased release times [29]. For the more hydrophobic RG502, the swelling of matrix is the limiting step because of the delayed hydration process. The drug is thereby trapped in the matrix and kept in the solid state even at high drug loading. This hypothesis was tested by visualizing the changes of size and morphology during the release process.

Morphology changes of microspheres prepared from RG503H are shown in Figure 6a. At a FITC-dextran drug loading of 10%, rapid morphological changes are observed during the release process [30]. After incubation in the release medium for 15 days, a crust structure is obtained. The thickness of the crust decreases during the release process, and larger voids were observed, which can be ascribed to degradation and subsequent drug evacuation.

The water uptake during incubation shown in Figure 4a was similar for both loaded and unloaded RG503H microspheres. Figure 4b shows that during the release process, the size of the microspheres loaded with drug swelled to a larger size. The higher drug loading thus facilitates the formation of diffusion channels in the relatively hydrophilic polymer matrix, which results in a fast release rate.

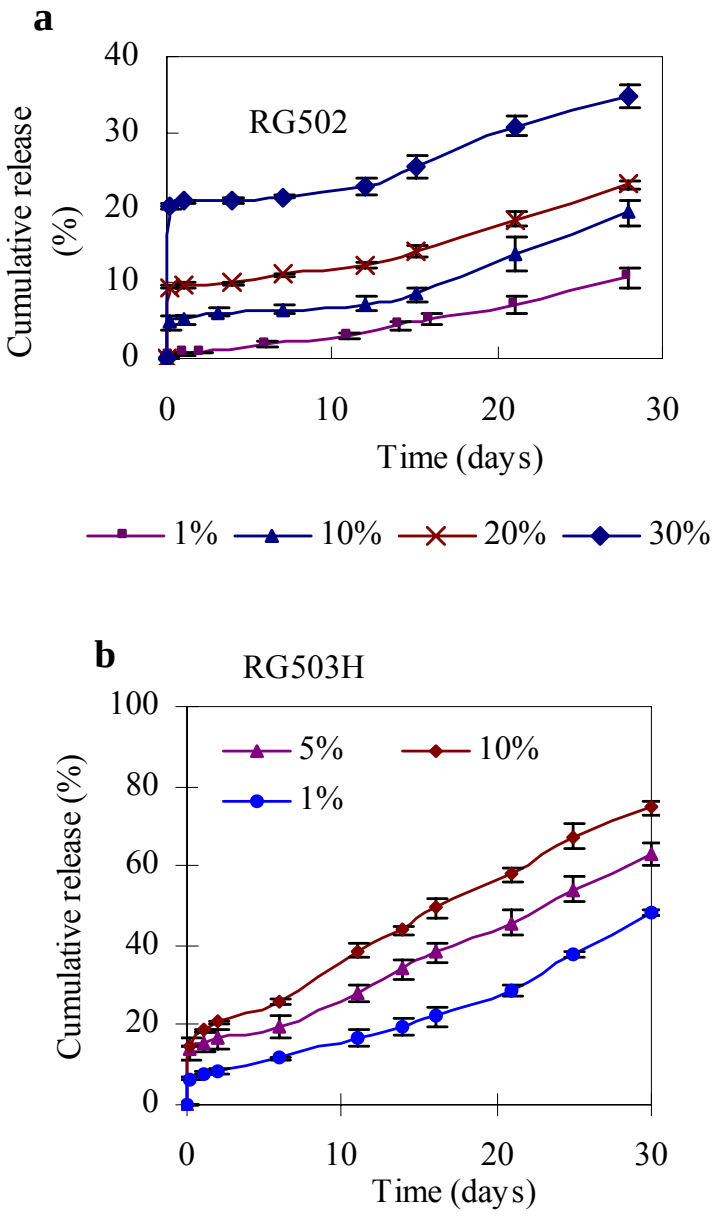

Figure 9. In vitro release profiles of FITC-dextran loaded microspheres prepared from RG502 (a) or RG503H (b) at different drug loading values.

3.5 Influence of PEG addition

From the above studies, when using the end capped polymer RG502, the release rate at the second release stage is difficult to tailor through the modification of porosity, pore size, and drug loading. Therefore, PEG was introduced into the microsphere formulation as a pore maker in order to alter the release rate. The polymer blend

microspheres were prepared by dissolving PEG6000 and RG502 in the organic solvent at different ratios with the addition of 10% NaCl in the outer aqueous phase. The resulting release profiles and the structure of the microspheres were investigated.

The addition of PEG decreased the size of the particles, which is similar to the findings of Dorati et al. [5]. This can be explained by the loss of PEG during the organic solvent evaporation process. At low ratios of PEG addition, using both PEG and NaCl in the preparation process resulted in microspheres with a smooth, non-porous surface and a compact internal structure (images not shown), but higher ratios of PEG (20%, 30%), even in the presence of NaCl, led to a dramatic change from a matrix structure to a capsule structure, as shown in Figure 7d, together with a high burst release. The release patterns obtained upon the addition of PEG are shown in Figure 10. Higher amounts of PEG6000 make the microspheres more hydrophilic, promoting higher release rates through channels formed from the dissolution of PEG in the polymer matrix [31]. The results demonstrate that in order to achieve a specific release profile, the ratio of PEG: PLGA should be optimised.

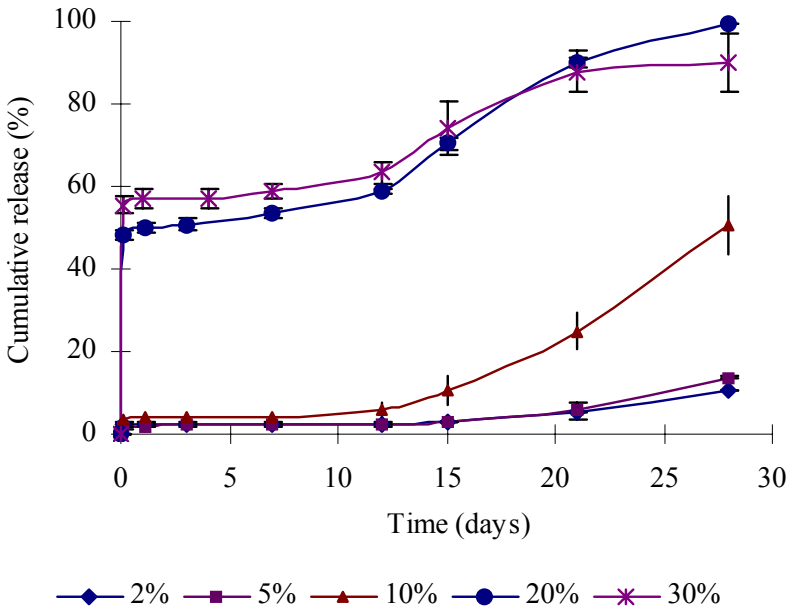

Figure 10. In vitro release profiles of RG502 microspheres loaded with 1% FITC-dextran prepared with the addition of PEG as a polymer blend, presented as ratio (%) of PEG:PLGA.

4. Conclusions

A deep understanding of microsphere structure, drug distribution, and the effects of PLGA nature is necessary for the design of microspheres with desired release profiles. The current investigation of particle morphology and release kinetics highlights the importance of polymer nature in the resulting structures and release mechanisms. The effects of certain defined process parameters and formulation factors on microsphere characteristics turned out to be dependent upon polymer properties. Microsphere characteristics including porosity, pore size, and drug distribution have a more pronounced effect on the initial release and only a marginal effect on the release rate at the second release phase for the end-capped polymer RG502. In contrast, for the hydrophilic polymer RG503H, continuous release can be achieved with the increase of porosity, pore size, and drug loading. The release rate at the second release phase is more difficult to modify when using the hydrophobic polymer RG502, as compared to the hydrophilic polymer RG503H. PEG addition is a possible technique for improving the release rate of RG502 microspheres. Morphological characterization of the FITC-dextran loaded microparticles during the release process provided deep insights on the release behavior, and the information resulting from this analysis will assist in the establishment of suitable release models.

References

[1] K. Frauke Pistel, A. Breitenbach, R. Zange-Volland, T. Kissel, Brush-like branched biodegradable polyesters, part III. Protein release from microspheres of poly(vinyl alcohol)-graft-poly(D,L-lactic-co-glycolic acid). J. Control. Release 73 (2001) 7-20.

[2] T. Ehtezazi, C. Washington, Controlled release of macromolecules from PLA microspheres: using porous structure topology. J. Control. Release 68 (2000) 361-372.

[3] H.K. Sah, R. Toddywala, Y.W. Chien, Biodegradable microcapsules prepared by

a w/o/w technique: effects of shear force to make a primary w/o emulsion on their morphology and protein release. J. Microencapsul. 12 (1995) 59-69.

[4] G. Crotts, T.G. Park, Preparation of porous and nonporous biodegradable polymeric hollow microspheres. J. Control. Release 35 (1995) 91-105.

[5] R. Dorati, I. Genta, L. Montanari, F. Cilurzo, A. Buttafava, A. Faucitano, B. Conti, The effect of gamma-irradiation on PLGA/PEG microspheres containing ovalbumin. J. Control. Release 107 (2005) 78-90.

[6] T. Uchida, K. Yoshida, S. Goto, Preparation and characterization of polylactic acid microspheres containing water-soluble dyes using a novel w/o/w emulsion solvent evaporation method. J. Microencapsul. 13 (1996) 219-228.

[7] T. Uchida, K. Yoshida, A. Ninomiya, S. Goto, Optimization of preparative conditions for polylactide (PLA) microspheres containing ovalbumin. Chem. Pharm. Bull. (Tokyo) 43 (1995) 1569-1573.

[8] K.F. Pistel, T. Kissel, Effects of salt addition on the microencapsulation of proteins using W/O/W double emulsion technique. J. Microencapsul. 17 (2000) 467-483.

[9] G. Jiang, B.C. Thanoo, P.P. DeLuca, Effect of osmotic pressure in the solvent extraction phase on BSA release profile from PLGA microspheres. Pharm. Dev. Technol. 7 (2002) 391-399.

[10] S. Mao, J. Xu, C. Cai, O. Germershaus, A. Schaper, T. Kissel, Effect of WOW process parameters on morphology and burst release of FITC-dextran loaded PLGA microspheres. Int. J. Pharm. 334 (2007) 137-148.

[11] A. Porjazoska, K. Goracinova, K. Mladenovska, M. Glavas, M. Simonovska, E.I. Janjevic, M. Cvetkovska, Poly(lactide-co-glycolide) microparticles as systems for controlled release of proteins -- preparation and characterization. Acta. Pharm. 54 (2004) 215-229.

[12] A. Frank, S.K. Rath, S.S. Venkatraman, Controlled release from bioerodible polymers: effect of drug type and polymer composition. J. Control. Release 102 (2005) 333-344.

[13] F. Lagarce, O. Cruaud, C. Deuschel, M. Bayssas, G. Griffon-Etienne, J. Benoit, Oxaliplatin loaded PLAGA microspheres: design of specific release profiles. Int. J. Pharm. 242 (2002) 243-246.

[14] M.J. Alonso, R.K. Gupta, C. Min, G.R. Siber, R. Langer, Biodegradable microspheres as controlled-release tetanus toxoid delivery systems. Vaccine 12 (1994) 299-306.

[15] K. Makino, Mogi, T., Ohtake, N., Yoshida, M., Ando, S.,, T. Nakajima, Ohshima, H., Pulsatile drug release from poly(lactide-co-glycolide) microspheres: how does the composition of the polymer matrixes affect the time interval between the initial burst and the pulsatile release of drugs? Colloid. Surf. B: Biointerfaces 19 (2000) 173-179.

[16] X. Luan, R. Bodmeier, Influence of the poly(lactide-co-glycolide) type on the leuprolide release from in situ forming microparticle systems. J Control Release 110 (2006) 266-272.

[17] K.F. Pistel, B. Bittner, H. Koll, G. Winter, T. Kissel, Biodegradable recombinant human erythropoietin loaded microspheres prepared from linear and star-branched block copolymers: influence of encapsulation technique and polymer composition on particle characteristics. J. Control. Release 59 (1999) 309-325.

[18] T. Ehtezazi, C. Washington, C.D. Melia, Determination of the internal morphology of poly (D,L-lactide) microspheres using stereological methods. J. Control. Release 57 (1999) 301-314.

[19] N. Nihant, C. Schugens, C. Grandfils, R. Jerome, P. Teyssie, Polylactide microparticles prepared by double emulsion/evaporation technique. I. Effect of primary emulsion stability. Pharm. Res. 11 (1994) 1479-1484.

[20] J.A. Schrier, P.P. DeLuca, Porous bone morphogenetic protein-2 microspheres: polymer binding and in vitro release. AAPS PharmSciech 2 (2001) E17.

[21] Y.Y. Yang, T.S. Chung, N.P. Ng, Morphology, drug distribution, and in vitro release profiles of biodegradable polymeric microspheres containing protein

fabricated by double-emulsion solvent extraction/evaporation method. Biomaterials 22 (2001) 231-241.

[22] S. Takada, T. Kurokawa, K. Miyazaki, S. Iwasa, Y. Ogawa, Utilization of an amorphous form of a water-soluble GPIIb/IIIa antagonist for controlled release from biodegradable microspheres. Pharm. Res. 14 (1997) 1146-1150.

[23] Y. Ogawa, M. Yamamoto, H. Okada, T. Yashiki, T. Shimamoto, A new technique to efficiently entrap leuprolide acetate into microcapsules of polylactic acid or copoly(lactic/glycolic) acid. Chem. Pharm. Bull. (Tokyo) 36 (1988) 1095-1103.

[24] C. Yan, Resau,J.H.,Hewetson,J.,West,M.,Rill,W.L.,Kende,M., Characterization and morphological analysis of protein loaded poly(lactide-co-glycolide) microspheres prepared by water-in-oil-in-water emulsion technique. J.Control. Release 32 (1994) 231-241.

[25] T.R. Sah HK, Chien YW., The influence of biodegradable microcapsule formulations on the controlled release of a protein. J. Control. Release 30 (1994) 201-211.

[26] P. Le Corre, J.H. Rytting, V. Gajan, F. Chevanne, R. Le Verge, In vitro controlled release kinetics of local anaesthetics from poly(D,L-lactide) and poly(lactide-co-glycolide) microspheres. J. Microencapsul. 14 (1997) 243-255.

[27] P.A. Rivera, M.C. Martinez-Oharriz, M. Rubio, J.M. Irache, S. Espuelas, Fluconazole encapsulation in PLGA microspheres by spray-drying. J. Microencapsul. 21 (2004) 203-211.

[28] M. Sandor, D. Enscore, P. Weston, E. Mathiowitz, Effect of protein molecular weight on release from micron-sized PLGA microspheres. J. Control. Release 76 (2001) 297-311.

[29] M.S. Hora, R.K. Rana, J.H. Nunberg, T.R. Tice, R.M. Gilley, M.E. Hudson, Release of human serum albumin from poly(lactide-co-glycolide) microspheres. Pharm. Res. 7 (1990) 1190-1194.

[30] S.W. Sun, Y.I. Jeong, S.W. Jung, S.H. Kim, Characterization of FITC-albumin encapsulated poly(DL-lactide-co-glycolide) microspheres and its release

characteristics. J. Microencapsul. 20 (2003) 479-488.

[31] C. Perez-Rodriguez, N. Montano, K. Gonzalez, K. Griebenow, Stabilization of alpha-chymotrypsin at the CH2Cl2/water interface and upon water-in-oil-in-water encapsulation in PLGA microspheres. J. Control. Release 89 (2003) 71-85.

Chapter 3

Charged nanoparticles as protein delivery systems: A feasibility study using lysozyme as model protein.

Submitted to: *European Journal of Pharmaceutics and Biopharmacy*

Abstract

The aim of this study was to investigate the feasibility of negatively charged nano-carriers (nanoparticles), consisting of polymer blends of poly(lactide-co-glycolide) (PLGA), and poly(styrene-co-4-styrene-sulfonate) (PSS), to improve the loading capacity and release properties of a positively charged model protein, lysozyme, through an adsorption process. Negatively charged nanoparticles were prepared by a solvent displacement method using polymer blends (RG502H and PSS). The system was characterized by dynamic light scattering analysis regarding size, size distribution, and zeta potential. Morphology of these particles was investigated using transmission electron microscopy (TEM), scanning electron microscopy (SEM) and atomic force microscopy (AFM). The loading capacity of lysozyme was evaluated as a function of polymer blend ratio, protein concentration, pH, and ionic strength; in vitro release profiles were also studied. The results show that negatively charged nanoparticles were obtained using polymer blends of PLGA and PSS, characterized by increased net negative surface charge with increasing ratios of PSS. Moreover, protein loading capacity increased as function of PSS/PLGA ratio. Increased pH facilitated the adsorption process and improved the loading capacity. Maximum loading efficiency was achieved at salt concentrations of 50mM. In vitro release of lysozyme from the polymer blend nanoparticles was dependent on drug loading and full bioactivity of lysozyme was preserved throughout the process. These findings suggest that this is a feasible method to prepare nanoparticles with high negative surface density to efficiently adsorb positively charged protein through electrostatic interactions.

Keywords: Charged nanoparticles; Lysozyme, Electrostatic interaction; protein delivery; Charge density

1. Introduction

Recent years have seen increasing interest in polymeric nanoparticles as carriers for hydrophilic macromolecules such as proteins, vaccines, and polynucleotides [1,2]. Numerous investigations have shown that nanoparticles can not only improve the stability of therapeutic agents against enzymatic degradation and control the release of therapeutic agents, but they can also be delivered to distant target sites either by localized delivery using a catheter-based approach with a minimal invasive procedure, or they can be conjugated to a biospecific ligand which could direct them to the target tissue or organ [1,3]. Drugs or antigens can either be entrapped in the polymer matrix, encapsulated in a liquid core, surrounded by a shell-like polymer membrane, or bound to the particle surface by adsorption [4]. For an effective nanoparticulate delivery system, the nanoparticle size and loading must be adjusted carefully, and protein stability during preparation and release must be ensured. Some reported methods for preparing nanoparticles from biodegradable polymers include: emulsification solvent evaporation [5], monomer emulsion polymerization [6], salting out [7], and nanoprecipitation [8].

The w/o/w double emulsion technique has been widely used for protein micro- and nano-encapsulation. Unfortunately, this method requires high shear forces and organic solvents, both of which are usually detrimental to proteins. Solvent displacement has become a popular alternative for this purpose. This technique does not rely on shear stress to produce nanoparticles, but takes advantage of differences in the interfacial tension, a phenomenon also designated as the Marangoni effect [9,10]. However, the use of this technique may expose the protein to organic solvent during nanoparticle preparation or to high acidity if the release of the protein does not outpace the polymer degradation [11]. Moreover, the solvent displacement method typically results in low encapsulation efficiency for water soluble drugs [12]. Therefore, we have investigated a method to associate the protein to the nanoparticle surface by adsorption. This technique can be performed in an aqueous solution and at a low

temperature, thus improving the prospects for preserved activity of sensitive drug molecules.

However, a successful nanoparticulate system should have a high loading capacity to reduce the dose of the carrier required for administration. As previously reported, lower loading efficiency was observed for the adsorption process compared to the encapsulation method, and the capacity of adsorption is related to the hydrophobicity of the polymer and the specific area of the NPs [2]. In terms of the protein adsorption process, both Coulomb (electrostatic) and van der Waals interactions (hydrophobic) are thought to be governing factors for the adsorption of proteins. However, the hydrophobic nature of polymer results in the denaturation and aggregation of proteins [13,14]. This highlights the importance of electrostatic interactions in the process of protein adsorption. The fundamental electrostatic interactions between particles and proteins have not been fully investigated so far, and little is known about the particle properties that are critical to adsorption efficiency and the protein bioactivity [15].

Based on these considerations, we have undertaken this work to explore the potential of negatively charged nanoparticles as a delivery vehicle for positively charged proteins, with the goal to attain a high level of protein loading with full bioactivity. Negatively charged sulfobutylated branched polyesters SB-PVA-g-PLGA were successfully used for nanoparticle preparation and protein adsorption with tetanus toxoid [4,16]. In order to guide further modification of this polymer, investigations regarding the influence of charge density on nanoparticle properties and protein interactions are of importance. For this purpose, PSS, a partially sulfonated polystyrene containing sulfonic acid groups attached to the backbone, was selected to modify the charge density of PLGA nanoparticles, intended to prepare nanoparticles of varying negative charge density. Lysozyme, a 14.3 kDa basic protein with a isoelectric point of 11, was employed in this study as a model positively charged protein because of its detailed characterization and the straightforward assessment of its biological activity [17].

The first aim of this study was to establish the model consisting of negatively charged nanocarriers, prepared from a blend of PLGA and PSS using a solvent displacement method. The second step was to test the hypothesis that this strategy would result in improved loading efficiency and bioactivity preservation for adsorbed lysozyme. Finally, changes in pH and ionic strength were investigated to gain insight into the surface-protein and protein-protein electrostatic interactions.

2. Materials and Methods

2.1 Materials

Poly(lactic-co-glycolic acid) (PLGA Resomer® RG502H) was supplied by Boehringer Ingelheim (Germany). Poly(styrene-co-4-styrene-sulfonate) (PSS, Parent polystyrene Mn=133 200, Mw/Mn=1.04, Sulfonation Degree: 50 mol% by Titration, Mn=184 400, Mw=191 800) was purchased from Polymer Source, Inc. (Dorval, Canada). The Micro BCA protein assay kit was from Pierce Chemical (Bonn, Germany). Hen egg white lysozyme, *Micrococcus lysodeikticus*, and Cytochrome c from bovine heart (12 327 kDa, pI 10) were obtained from Sigma-Aldrich Chemie GmbH (Germany). Bovine serum albumin (BSA, 66.4 kDa, pI 4.7) was purchased from Hoechst Behring (Marburg, Germany). All other chemicals were purchased from Sigma, of analytical grade, and used without further purification.

2.2 Preparation of PLGA-PSS nanoparticles

Nanoparticles were prepared by a solvent displacement technique, as described previously [4,18]. Briefly, 10.0 mg of polymer at different mass ratios of PSS to PLGA (RG502H) were dissolved in 1 ml of acetone at 25°C. The resulting solution was subsequently injected to a magnetically stirred (500 rpm) 5 ml aqueous phase of filtrated double distilled water (pH 7.0, conductance 0.055 μS/cm, 25°C) using an electronically adjustable single-suction pump to inject the organic solution into the aqueous phase through an injection needle (Sterican 0.55×25mm) at a constant flow rate (10.0 ml/ min). After the injection of the organic phase the resulting colloidal

suspension was stirred for 8 h under reduced pressure to remove the organic solvents. Particles were characterized and used directly after the preparation.

2.3. Physicochemical and morphological characterization of negatively charged nanoparticles

2.3.1. Particle size and Zeta potential measurements

The average particle size and zeta potential of the NPs were measured using a Zetasizer Nano ZS/ZEN3600 (Malvern Instruments, Malvern, UK). Particle size and polydispersity were determined using non-invasive back scatter (NIBS) technology, which allows sample measurement in the range of 0.6 nm – 6 μm. Freshly prepared particle suspensions (800 μl) were placed in a folded capillary cell without dilution. The measurement was carried out using a 4mW He-Ne laser (633nm) as light source at a fixed angle of 173°. The following parameters were used for experiments: medium refractive index 1.330, medium viscosity 0.88 mPa s, dielectric constant 78.54, temperature 25°C. Each size measurement included at least 10 runs. All measurements were carried out in triplicate, and the results were expressed as the mean size ± S.D.

Zeta potential was measured with a combination of laser Doppler velocimetry and phase analysis light scattering (PALS). A Smoluchowsky constant F (K_a) of 1.5 was used to calculate zeta potential values from the electrophoretic mobility. All measurements were carried out at 25°C in triplicate, and the results were expressed as the mean ± S.D.

2.3.2. Scanning electron microscopy (SEM)

Prior to SEM observation, nanoparticle suspensions were diluted 1/5 with ultrapure water, and a drop of diluted suspension was then directly deposited on a polished aluminum sample holder. Samples were dried in vacuum and subsequently sputter-coated with a carbon layer at 4-6 amps for 30 seconds then with a gold layer at 2 amps for 30 seconds at 5×10^{-5} Pa (Edwards Auto 306 Vacuum Coater, Edwards, Germany). Subsequently, the morphology of nanoparticles was observed at 3 kV using a scanning electron microscope (SEM, S-4200, Hitachi, Japan).

2.3.3. Transmission electron microscopy (TEM)

The samples were prepared by coating a copper grid (200 mesh covered with Formvar/carbon) with a thin layer of dilute particle suspension. After negative staining with 2% (w/v) phosphotungstic acid for 2 min, the copper grid was then dried at room temperature before measurement. Nanoparticles were investigated using transmission electron microscopy (TEM, Zeiss EM 10) at an accelerating voltage of 300 kV.

2.3.4. Atomic force microscopy (AFM)

To obtain information about the substructure and topography of the dried nanoparticles, AFM measurements were carried out in air under normal atmospheric conditions, using a NanoWizard (JPK Instruments, Berlin, Germany). Imaging was performed in contact mode using force in the range of 1-10 nN with pyramidal silicon nitride tips mounted on cantilevers of spring constant 0.036 Nm^{-1}. Height measurements and surface roughness were obtained using NanoWizard AFM image analysis software (JPK Instruments, version 2.1).

2.3.5. Differential scanning calorimetry (DSC)

Polymer films cast from 10% (w/v) acetone solutions on Teflon® plates were allowed to dry for 24 h under reduced pressure. Residual solvents were then removed in vacuum at room temperature until constant weights were obtained. Differential scanning calorimetry (DSC) was conducted under a nitrogen atmosphere using a DSC7 calorimeter (Perkin Elmer) in sealed aluminum pans, relative to indium and gallium standards. Thermograms covered a range of −20 to 200°C with heating and cooling rates of 10°C/min. Glass transition temperatures (T_g) were determined from the second run.

2.4. Loading capacity of PLGA–PSS nanoparticles for lysozyme

Nanoparticle suspensions of defined concentrations were incubated with defined amounts of lysozyme for 5 h at 4°C. For investigations with Cytochrome C and Bovine

serum albumin (BSA), one-milliliter portions of NP suspension (1mg/ml) were incubated with defined amounts of protein at 4°C for 5 h in pH 7.0 PBS buffer (15 mM). The amount of absorbed protein on the nanoparticles was calculated by measuring the difference between the amount of protein added to the nanoparticles solution and the measured non-entrapped protein remaining in the aqueous phase. After incubation, samples were centrifuged for 30 min at 13 000 rpm (25°C), and the supernatant was checked for the non-bound protein by bicinchoninic acid (BCA) assay with measurement at 570 nm. For each protein concentration, a control tube was prepared without any nanoparticles to account for any protein loss due to adsorption to the Eppendorf tubes. Protein loading efficiency was calculated as follows:

$$\text{Protein loading efficiency} = \frac{\text{Total amount of protein} - \text{Free protein}}{\text{Total amount of protein}} \times 100\%$$

2.5. In vitro release of lysozyme from nanoparticles

For the release studies, protein loaded nanoparticle suspensions were incubated in PBS buffer (pH 7.4) containing 0.05% NaN_3 and 0.01% Tween® 80 by Rotatherm at 37°C. At predetermined intervals, 1 ml aliquots were withdrawn and centrifuged (13 000rpm, 30 min), after which the total protein content in the supernatant was determined by the BCA assay. All experiments were performed in triplicate.

2.6. In vitro bioactivity of Lysozyme

Lysozyme activity was determined using the decrease in optical dispersion at 450 nm of a *M. luteus* (*lysodeikticus*) suspension. Briefly, a 2.5 ml aliquot of *M. lysodeikticus* cell suspension (0.24 mg/ml in 66 mM PBS, pH 6.24) was incubated with either 50 μl of aqueous lysozyme solutions obtained from the nanoparticles during the *in vitro* protein release tests or with lysozyme standard solutions (1–100μl). The decrease in absorbance intensity at 450 nm over time was related to the bioactivity of the lysozyme against the *M. lysodeikticus* cells. The relative bioactivity of lysozyme was calculated from the slope of the linear part of the curve (absorbance versus time)

according to the technique described by van de Weert et al. [19].

2.7. Statistical analysis

Results are presented as the mean ± S.D. from at least three measurements. Statistical analysis was performed using one-way analysis of variance (ANOVA) followed by Tukey's post-test to determine the level of significance among various groups (Origin 7.0 SRO, Northampton, MA, USA). Differences were considered to be statistically significant at a level of $p \leq 0.05$.

3. Results and Discussion

3.1 Solubility of PSS and compatibility of PSS and PLGA

As indicated in the introduction, the purpose of this work was to investigate the feasibility of the interaction between oppositely charged nanoparticles and proteins. With this concept in mind, the negative charge density of nanoparticles was varied by adding different amount of PSS in the polymer matrix. The solvent displacement technique was chosen to prepare nanoparticles because of certain advantages, e.g., narrow size distributions and the ability to prepare particles without the use of high shear stress and surfactants [4].

3.1.1 Solubility of PSS in organic solvent and aqueous phase

Solvent displacement is based on the precipitation of a dissolved polymer in solution upon addition to a miscible, surfactant-containing or free solution which is a non-solvent for the polymer [4]. Using this technique, organic solvents, such as acetone, dimethyl sulfoxide (DMSO*)*, tetrahydrofuran (THF), and ethanol, are frequently used to dissolve the polymer; Poloxamer- or PVA-containing aqueous phases are commonly employed as the non-solvent.

The solubility of PSS was investigated at room temperature in different organic solvents and in acetate buffer at different pH values. PSS was totally dissolved in acetone, ethanol, and DMSO at 20 mg/ml. In the case of THF and dichloromethane,

however, 5 mg/ml PSS was insoluble even after incubation at 37°C between 24-48 hours. The solubility of PSS in acetone at room temperature was determined to be 0.53 ± 0.01 g/ml.

PSS swelled in acetate buffer of pH 3-12. A clear solution was observed at pH 2.26 at the concentration of 10 mg/ml. Based on these results, it could be concluded that it is feasible to prepare PLGA/PSS nanoparticles with solvent displacement in a wide pH range.

3.1.2 Compatibility of PSS and PLGA

PLGA and PSS were chosen in this work to mimic a charged polymer for preparation of nanoparticles of varying charge density. Both polymers were co-dissolved in organic solvent, and upon diffusion of the organic phase into water, both polymers formed nanoparticles. In order to verify that no phase separation occurred and that a homogeneous polymer blend structure is formed during the aggregation process, DSC experiments were carried out to investigate the compatibility of PLGA and PSS.

Different ratios of these polymers were dissolved in acetone and polymer blend films were prepared after evaporation of organic solvent. DSC experiments were performed for polymer blend films and placebo nanoparticles. For all samples, only one Tg was observed in the thermogramme, indicating that no phase separation occurred and a homogeneous polymer blend was obtained. The Tg of pure PLGA (RG502H) is 42.23°C, and when the ratio of PSS in the polymer blend increased, Figure 1 shows that the Tg gradually decreased, to 34.14°C at 80% PSS, even though the Tg of pure PSS is much higher (156.34°C). In the case of placebo nanoparticles, a decrease in Tg from 44°C to 39°C was observed with the increase of PSS from 0% to 10%, which is in agreement with the observations of the polymer blend films. These results demonstrate the homogeneous structure of polymer blends from PLGA and PSS, and the decrease in Tg indicated the possible interaction of PSS and PLGA.

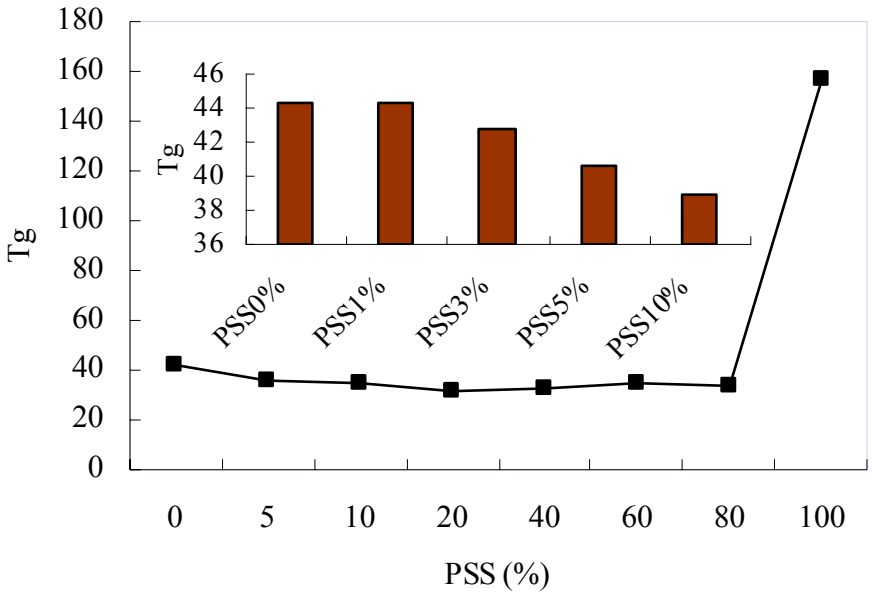

Figure 1. Glass transition temperature (Tg) of polymer blend films with varied amount of PSS. The inset shows the Tg of nanoparticles with different amount of PSS.

3.2. Characterization of PLGA–PSS blend nanoparticles

Nanoparticles were prepared with a polymer blend of PSS and PLGA at different mass ratios, following the same standard preparation protocol in order to exclude any influence of technological aspects. Preliminary experiments showed that high amounts of PSS (20%, 30%) led to much higher increased particle size (>300 nm) and larger polydispersity (> 0.4), and a plateau in the zeta potential, which could be attributed to the swelling of PSS in water and saturation of functional groups on the nanoparticle surface. Therefore, in order to investigate the variable charge density of nanocarriers with minimal influence of swelling or increased particle size, polymer blend nanoparticles were examined at ratios of PSS to PLGA between 0% and 10%.

The particle size, polydispersity index, and zeta potential values of the nanoparticles in this range are presented in Table 1. The size and zeta potential were

significantly influenced by blending PLGA with PSS. A mass ratio of 10% PSS to PLGA resulted in an increase in the mean particle size from 122 to 200 nm as a consequence of PSS swelling in water. The polydispersity index was less than 0.25 in all cases, indicating narrow size distributions.

As expected, the zeta potential decreased with increasing amounts of PSS. The sulfonic acid functional groups modified the charge density of nanoparticles characterized with strongly increased negative charge upon addition of PSS (to < –50mV). The pH of nanoparticles suspensions decreased from pH 6.5 for pure PLGA to pH 4.2 for the polymer blend containing 10% PSS. The nanoparticles in the present study were found to be stable in dispersion state at room temperature for at least 24 hours, even without using surfactant during the preparation process, due to the high absolute values of zeta potential.

SEM and TEM images are shown in Figure 2. In general, SEM micrographs revealed a compact and spherical structure independent of PLGA–PSS ratio, with a size distribution confirming the size measurements by PCS. TEM micrographs also demonstrated well-defined spherical particle morphologies, with a more stained outer layer that could be attributed to the orientation of PSS on the surface due to the hydrophilic property of the sulfonic acid groups. AFM images in Figure 2 showed smooth nanoparticle surface without any noticeable pinholes or cracks.

Mass ratio PSS: RG502H (%)	Size (nm)	Polydispersity Index (PdI)	Zeta potential (mV)
0	122 ± 1.4	0.09 ± 0.01	-32.28 ± 1.77
1	143 ± 5.6	0.010 ± 0.01	-40.23 ± 2.37
3	165 ± 3.4	0.11± 0.02	-48.73 ± 0.61
5	180 ± 15.7	0.11 ± 0.02	-52.26 ± 1.92
10	200 ± 10.8	0.13 ± 0.03	-56.48 ± 0.26

Table 1 Characteristics of polymer blend nanoparticles prepared from different mass ratios (% PSS in PLGA), n = 3.

3.3. Lysozyme loading capacity of the polymer blend nanoparticles

As mentioned previously, the primary aim of this study was to improve protein loading efficiency via electrostatic interactions. Nanoparticle surface charge density was modified successfully using PLGA and PSS polymer blends, and these nanoparticles were used to investigate the loading capacity of lysozyme, a model electropositive protein. The interactions of oppositely charged protein and nanoparticle were evaluated in terms of the particle size, zeta potential, and loading efficiency.

3.3.1. Characteristics of protein loaded nanoparticles

A 1 mg/mL nanoparticle suspension (10% PSS) was incubated with different mass ratios of protein. After incubation with lysozyme solution, the nanoparticles were evaluated in terms of size, zeta potential, and adsorption efficiency. Figure 3 shows that the zeta-potential of polymer blend nanoparticles increased with increasing protein concentrations. Between 0% and 10% theoretical drug loading, a linear relationship was observed between protein concentration and zeta potential (R^2=0.999). Further

increases in lysozyme concentration led to sharply elevated zeta potential up to the 40% mass ratio of lysozyme to nanoparticles. The plateau value around 35 mV indicates saturation of the particle surface. This reversal of surface charge from negative to positive confirms the adsorption of lysozyme to the nanoparticle surface.

Figure 3 also shows that nanoparticle size increased linearly between 0% and 10% lysozyme (R^2=0.994). At the mass ratio of 20%, the zeta potential is close to zero; obvious flocculation was observed due to the lack of charge stabilization and the size could not be measured. At higher protein concentrations as mass ratio of 40%, increased particles size as 242.7 nm was detected compared to 198.3 nm for placebo nanoparticles.

After protein loading at the 40% mass ratio, the SEM images in Figure 2 still show well-defined nanoparticle structure similar to the placebo particles, and no aggregates were observed. Upon close observation of the TEM image, double layers were seen in the protein-loaded nanoparticles when the samples were treated with negative staining. The inner white region corresponds to the polymeric nanoparticle core, and the hydrophilic nanoparticle shell is colored dark grey. The outer layer shows the protein on the nanoparticle surface, and excess unbounded protein appears in the stained background. The AFM image of the protein loaded particles reveals a slightly rougher surface than the blank particles.

The loading efficiency was dependent on a lysozyme concentration. More specifically, at 50 μg/ml lysozyme (corresponding to a 5% mass ratio), the adsorption efficiency was 53%, but this value increased with increasing protein concentration, to a maximum of 100% loading efficiency at 250 μg/ml lysozyme (25% mass ratio). This increase in loading efficiency may be explained by the improved mobility of ions in the incubation medium and the slightly elevated ionic strength in the presence of protein molecules. Figure 5 shows that for 10% PSS, at lysozyme concentrations above 250 μg/ml, the amount of protein adsorbed on the nanoparticle surface reached a plateau. Therefore, concentrations above this saturation point resulted in decreased loading efficiency.

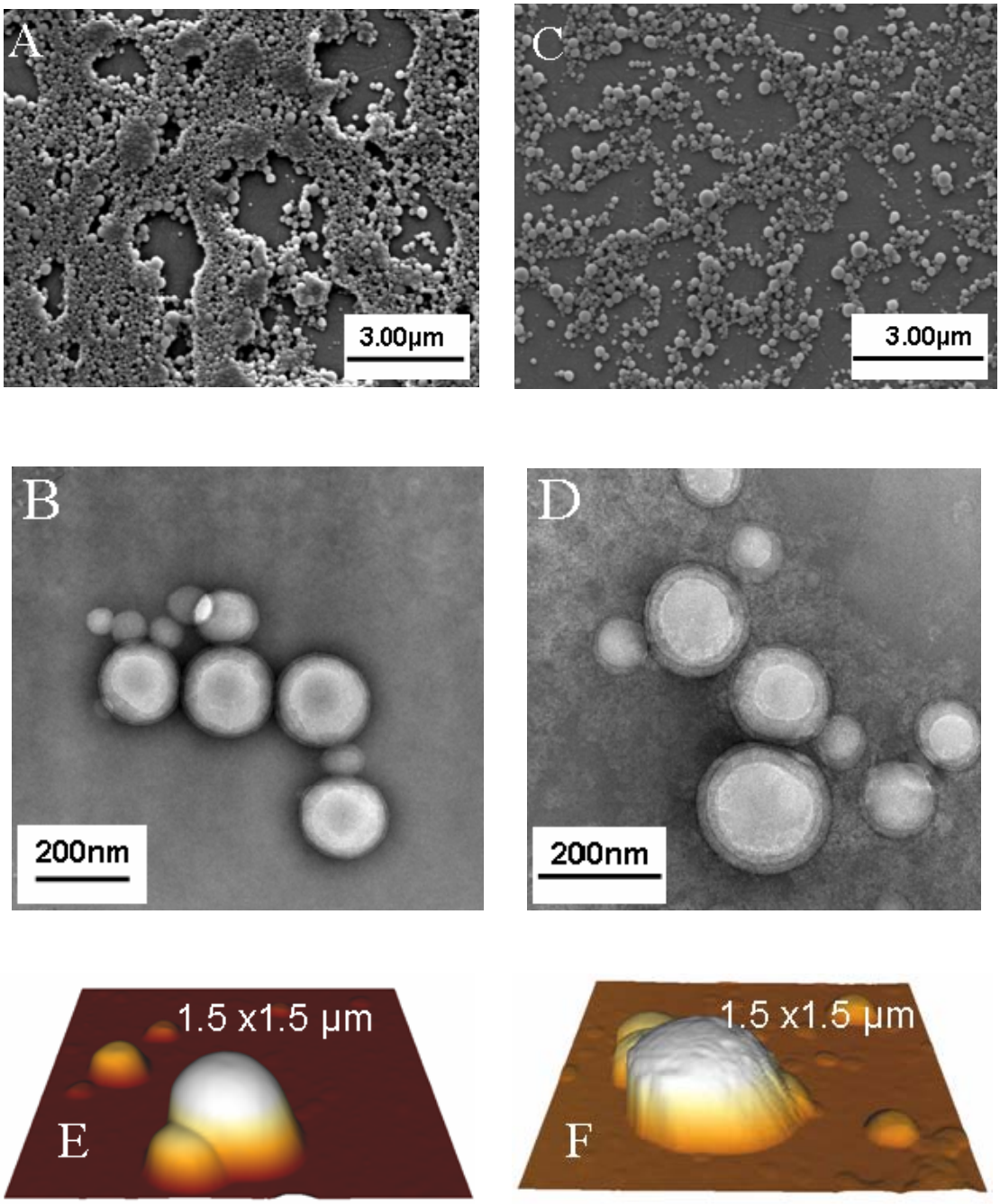

Figure 2. Micrographs of placebo and lysozyme-loaded nanoparticles prepared from PLGA–PSS (10%). (A) SEM (B) TEM (E) AFM for placebo nanoparticles, and (C) SEM (D) TEM (F) AFM for protein-loaded nanoparticles at 40% theoretical drug loading.

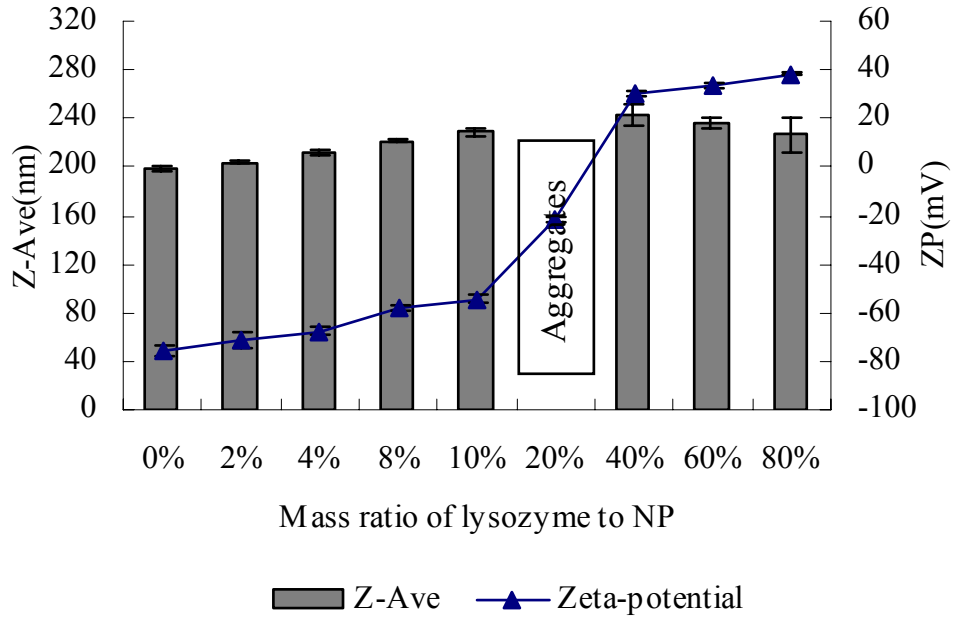

Figure 3. Size and ζ-potential of PLGA/PSS (10% PSS) nanoparticles after incubation with lysozyme at different concentrations. Error bars indicate the standard deviation (n = 3).

3.3.2. Effect of polymer ratio of PSS to PLGA

Figure 4 shows the zeta potential values resulting from lysozyme loading at various mass ratios to nanoparticle suspensions prepared at different polymer ratios. As expected, the zeta potential increased with increased drug loading in all cases, with maximum values between 30 and 40 mV. As the amount of PSS increased from 0% to 10%, the "isoelectric point" of the protein loaded nanoparticles shifted from around 2% to 30% lysozyme (mass ratio). This suggests that increased amounts of PSS augmented the net negative charge on the surface of the nanoparticles, thus requiring larger amounts of positively charged lysozyme in order to neutralize the surface charge. In contrast, the zeta potential of nanoparticles containing no PSS (pure RG502H) had already reversed to a positive value at a theoretical drug loading of only 4%.

The loading capacity of nanoparticles at different polymer ratios in Figure 5 is remarkably high with these polymer blend nanoparticles, compared to reports of similar work. According to Jung et al [18], the maximum amount of tetanus toxoid adsorbed onto nanoparticles prepared with the SB(43)-PVA-PLGA10 polymer is about 60 μg/mg nanoparticles. However, the polymer blend nanoparticles in this work have a loading capacity as high as 250 μg/mg nanoparticles. Increased amounts of PSS resulted in a higher loading capacity, as the increased density of charge-containing surfaces offer more potential binding sites for coulombic interactions with the protein molecules. The electrostatic properties of both the charged surface and the charged protein molecule play an important role in the overall protein adsorption process. This result is also in agreement with the findings of Wittemann et al. [20-25], in which spherical polyelectrolyte brushes (SPBs) can trap high amounts of protein within the brush. SPBs consist of solid polymer cores, poly(styrene), for example, onto which linear polyelectrolyte chains such as poly(styrene sulfonic acid) are grafted. Norde and Lyklema [26,27] also studied the adsorption behavior of HSA and bovine pancreas nuclease at negatively charged polystyrene surfaces using potentiometric titration, in which they postulated the formation of ion pairs between sulfate groups on the polystyrene surface and positively charged protein groups. In contrast, RG502H demonstrated comparatively low protein loading capacity; in this case, particle aggregates were observed in the nanoparticles suspension at a theoretical loading as low as 5%.

At steady state, the adsorbed amount of lysozyme, Γ was established as a function of the lysozyme equilibrium concentration c_e , and an adsorption isotherm (Γ vs. c) was constructed. These lysozyme adsorption data were then fitted to the

Langmuir equation expressed by equation (1), where Γ is the amount of adsorbed protein, c_e is the equilibrium protein concentration in the incubation medium, b is a coefficient related to the affinity between the nanoparticles and protein, and Q_0 is the maximum adsorption capacity.

$$\frac{c_e}{\Gamma} = \frac{1}{Q_0 b} + \frac{c_e}{Q_0}$$

eq. (1)

The parameters for this equation appear in Table 2, where the linear regression analysis shows a good fit, with all correlation coefficients (R^2) greater than 0.999. The results indicate that under the conditions of this experiment, the protein adsorbs as a monolayer around the particles. Multilayer formation, as described by the Freundlich isotherm, was not observed even at higher protein concentrations, which is in accordance with previous work [18]. Moreover, the data fitted to the Langmuir model reflect the increased affinity (constant b) of the positively charged protein to the nanoparticle surfaces upon increased amounts of negatively charged sulfonic groups (PSS content). Chesko et al. also have reported that data for protein binding to anionic PLGA/DDS microparticles fits the Langmuir model, providing evidence that a monolayer of adsorbed protein is formed [28]. However, our adsorption data did not fit the Langmuir isotherm over the entire concentration range, possibly due to stronger electrostatic interactions between the protein and the sulfonic acid groups on the nanoparticle surface.

Polymer	Q_0 (μg/mg nanoparticles)	b (ml/mg)	K_a	ΔG^o (kJ/mol)	R^2
RG502H	77.5	0.276	21.41	-7.06	0.9998
PSS:PLGA 1%	119.1	0.301	35.84	-8.24	0.9996
PSS:PLGA 3%	172.4	0.433	74.63	-9.931	0.9997
PSS:PLGA 10%	250.0	0.851	212.76	-12.34	0.9995

Table 2. Langmuir equation parameters and free energy for the adsorption of lysozyme onto PLGA-PSS nanoparticles.

Q_0 : maximum adsorption capacity
b : affinity constant of lysozyme for the nanoparticles
K_a: equilibrium association constant, $K_a = Q_0 b$
ΔG^o : Gibbs free energy, $\Delta G^o = -RT\ln K_a$

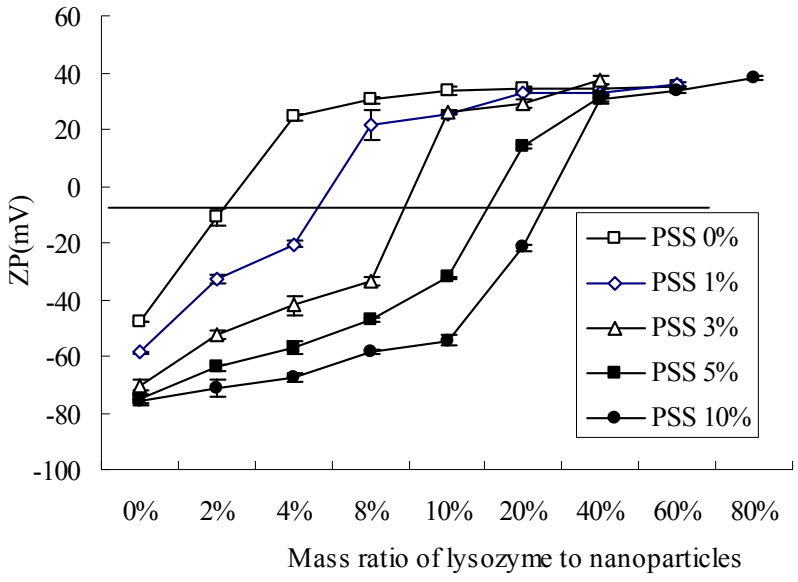

Figure 4. ζ-potentials of PLGA/PSS nanoparticles at different ratios of PSS to PLGA after incubation with lysozyme at different concentrations. Values are given as mean ± SD (n = 3).

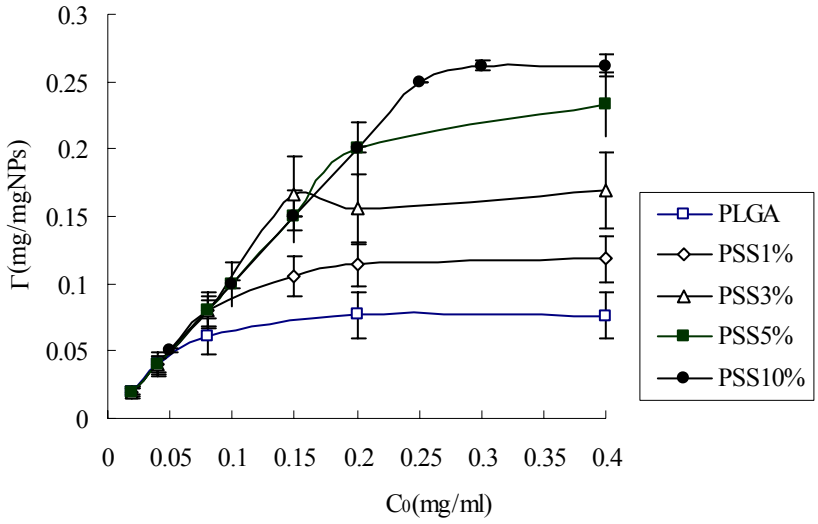

Figure 5. Amount of lysozyme adsorbed to the surface of PLGA/PSS nanoparticles at different ratios of PSS to PLGA and at different lysozyme concentrations. Error bars indicate the standard deviation (n = 3).

3.3.3. Effect of pH

Protein adsorption to hydrophobic polymers has frequently been investigated based on interactions between the hydrophobic domains of the protein and the hydrophobic polymer surface. Hydrophilic surfaces usually repel hydrophobic protein segments and decrease protein adsorption. In our study, however, the surface association between the negatively charged particles and the positively charged protein is hypothesized to be driven by the electrostatic interaction. In the incubation medium, both the particles and the protein surface charge are neutralized by counter ions. This affects the ζ-potential, which leads to charge redistribution and/or charge transfer between the polymeric surface and the protein molecule. To further investigate the adsorption mechanisms and to evaluate the important parameters in this adsorption process, the influence of pH in the incubation medium was studied.

Figure 6 shows the ζ-potential profiles as a function of incubation medium pH for unloaded polymer blend nanoparticles. As expected, the ζ-potentials decreased at higher pH values due to the increasing dissociation of the sulfonic acid groups at the

nanoparticle surface. The resulting increase in negative charge density on the nanoparticle surface at elevated pH supplied more binding sites for the positively charged protein. Upon summing up all charged amino acids and taking into account their dissociation ratios according to refs [29] and [30], the net positive charge of lysozyme decreases at higher pH, suggesting that more protein is required to neutralize the negatively charged nanoparticle surface. This leads to an increase in loading efficiency at higher pH, as seen in Figure 6, from 65.5% at pH 4.52 to 100% at the higher pH values. These results suggest that electrostatic interactions dominate the adsorption process and that the surface charge density at a given pH governs the maximum amount of protein adsorbed.

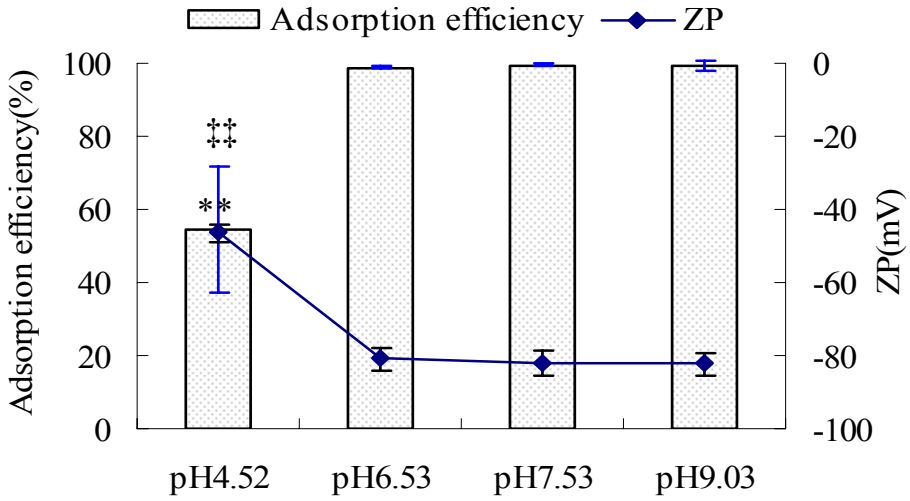

Figure 6. ζ-potentials (ZP) of PLGA/PSS (PSS10%) nanoparticles and adsorption efficiency of lysozyme at different pH values for 40% theoretical protein loading. Error bars indicate the standard deviation (n = 3). $P < 0.01$ ‡‡ for ζ-potential and ** for adsorption efficiency .

3.3.4. Effect of ionic strength

As ionic strength can have a shielding effect on electrostatic forces, the influence of ionic strength on nanoparticles properties and protein adsorption was studied by incubating the nanoparticles with various concentrations of NaCl. Figure 7 shows that particle size was not influenced by ionic strength, and other than a jump in zeta potential from –67 to –46 mV (at 0 and 1 mM), there was little change in zeta potential at higher ionic strength values.

Figure 8 shows that increases in ionic strength caused increased adsorption efficiency between 0 and 50 mM. At higher salt concentrations, a slight decrease in loading efficiency was observed. The trend was similar for both theoretical drug loading values (60% and 80%). In other words, maximum lysozyme absorption was attained at a salt concentration of 50 mM. This observation indicates that in addition to electrostatic effects, hydrophobic interactions may still play a role in this adsorption process especially at lower ionic strength. It has been previously reported that increases in ionic strength could promote the hydrophobic interactions of dye molecules with a poly(GMA) surface [31]. Similarly, enhanced adsorption of negatively charged BSA to negatively charged planar surfaces composed of poly(styrene sulfonic acid) or silica is only observed at higher ionic strength [32]. Zhang et al also reported maximum BSA adsorption at a salt concentration of 200 mM [33]. In summary, while electrostatic interactions play an important role in protein adsorption, hydrophobic interactions also contribute at lower ionic strength values.

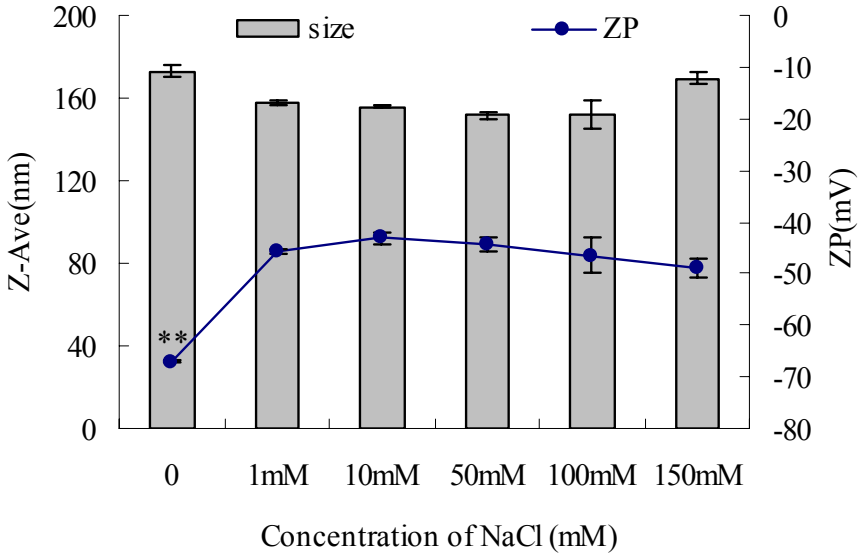

Figure 7. Size (Z-Ave) and ζ-potential (ZP) of PLGA/PSS nanoparticles (10% PSS) at different salt concentrations. Error bars indicate the standard deviation (n = 3). ** $P < 0.01$ for ζ-potential at NaCl concentration 0mM compared to all other NaCl concentrations.

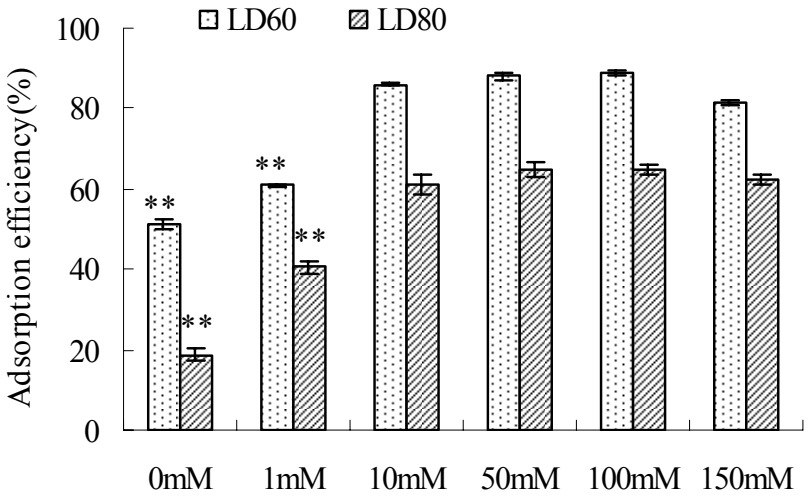

Figure 8. Adsorption efficiency of protein on PLGA/PSS (10% PSS) nanoparticles as a function of salt concentration at theoretical drug loading of 60% (LD60) and 80% (LD80). Error bars indicate the standard deviation (n = 3). ** $p < 0.01$ for adsorption efficiency at NaCl concentration of 0 and 1mM compared to other NaCl concentrations.

3.4. Adsorption of BSA and Cytochrome c

It has been clearly demonstrated that the higher negative charge density of nanoparticles favor loading of the electropositively charged model protein lysozyme. As part of this feasibility study, and to gain further insights into the process of protein adsorption to these PLGA/PSS nanoparticles, investigations were carried out using proteins with different properties. Cytochrome c (pI 10, Mw 12.3 kDa) was chosen as a protein with similar properties to lysozyme (pI 10.7, Mw 14.6 kDa), and BSA (bovine serum albumin) was chosen as a model negatively charged protein. BSA adsorption has been previously characterized by hydrophobic interactions with particles [32,33]. In addition to studies with the PLGA/PSS (10%) blend nanoparticles, the adsorption process was also compared to pure PLGA nanoparticles. These studies are important for understanding the interactions of nanoparticles and proteins, and their resulting applications for protein loading.

As seen in Figure 9 (A) and (B), the surface negative charges were neutralized by cytochrome c for both types of nanoparticles. In the case of polymer blend nanoparticles, the zeta potential increased gradually as the concentration of cytochrome c increased, leveling off at –18 mV at 300 μg/ml. In contrast, for PLGA nanoparticles, the zeta potential increased more sharply at lower concentrations of cytochrome c, and was already near the plateau value at 150 μg/ml, indicating a faster neutralization of surface charge. Upon comparing Figures 9 (A) and 9 (B) , one can see that due to the higher surface charge density on the PLGA/PSS particles compared to PLGA particles, more cytochrome c is required to neutralize the charge on the former.

Negligible changes in size were observed for PLGA/PSS nanoparticles ($P>0.05$) after incubation with cytochrome C. In contrast, flocculation occurred with the PLGA nanoparticles at protein concentrations of 200-250μg/ml, and aggregates were observed upon incubation with 300-400μg/ml cytochrome c. The reduced net charge on the surface and the accompanying reduction in repulsive forces between the particles led to this aggregation.

Previous studies have reported the complexation of cytochrome c with sulfonated polystyrene nanoparticles through electrostatic interactions [34,35]. Surprisingly, in this work, the maximum amount of cytochrome c adsorbed is lower for the PLGA/PSS nanoparticles (24 μg/mg) than for the PLGA nanoparticles (103 μg/ml), even though the PLGA/PSS nanoparticles carried more net negative charge. Therefore, it can be deduced that the interaction of lysozyme with PLGA/PSS nanocarriers is highly affected by the surface charge [36], but for cytochrome c, the electrostatic interaction is not the primary driving force for adsorption. Bayraktar et al. [37] suggest that facial specificity for nanoparticle binding is apparently determined by a fine balance between electrostatics and hydrophobicity; for cytochrome c, a combination of hydrophobic and coulombic interactions would lead to better binding efficiency. Rezwan et al. also suggest that electrostatic interactions seem to govern protein adsorption in the cases where the protein and material surfaces are very hydrophilic [38].

After incubation of both types of nanoparticles with BSA, no noticeable aggregates nor obvious changes in zeta potential were observed at any of the BSA concentrations studied. No adsorption of BSA was achieved for PLGA/PSS particles, but a small amount of BSA (about 15 μg/mg) adsorbed to the PLGA particles (see Figures 9 C and D). It has been previously reported that proteins can overcome repulsive electrostatic interactions and still adsorb [28], but this adsorption is not as effective as observed near the isoelectric point or at a pH which allows for opposite (attractive) charges. These results suggest that electrostatics play a dominant role in driving adsorption, but additional noncoulombic factors such London, van der Waals, and hydrophobic forces also play a role.

In the previously mentioned report concerning slightly sulfonated polystyrene particles [34], the ionic groups on the particle surface stabilize the hydrophobic core of polystyrene chains. It can be deduced by analogy that for the PLGA/PSS particles in this work, the higher density of sulfonate functional groups on the surface leads to more hydrophilicity than exhibited by the pure PLGA particles. For this reason, the

PLGA particles are able to participate in more hydrophobic interactions in the adsorption process, and, in the case of BSA adsorption, overcome electrostatic repulsion.

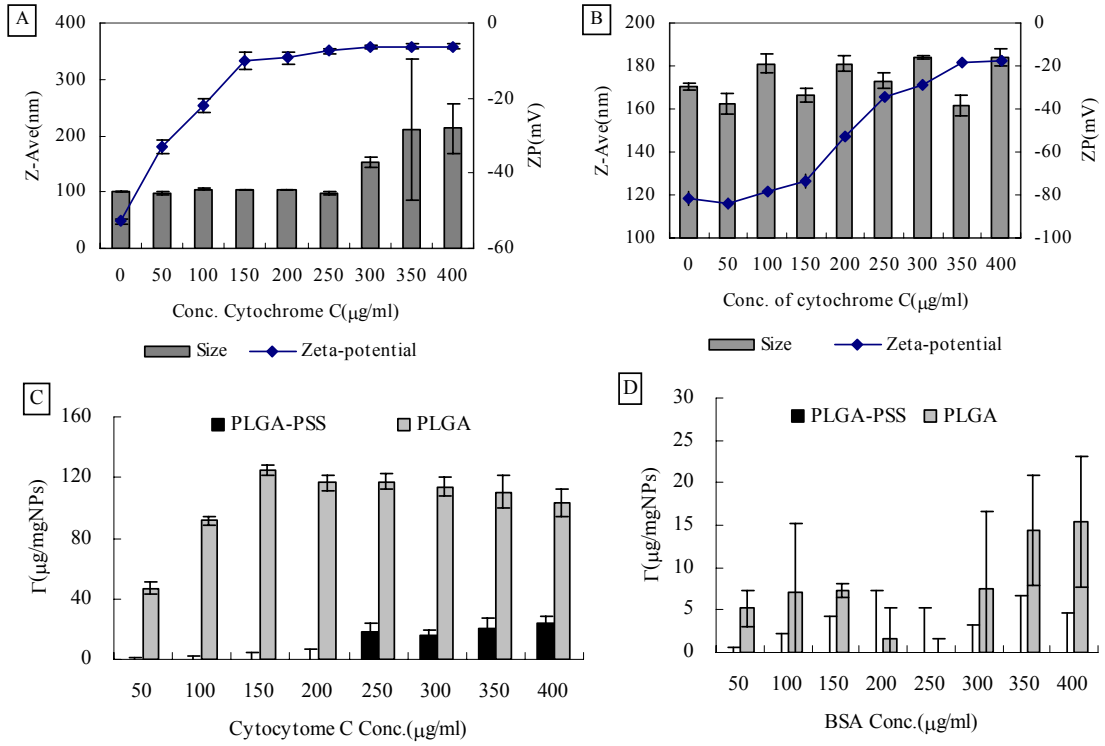

Figure 9. Size and zeta-potential of PLGA (A) or PLGA/PSS (B) nanoparticles after incubation with cytochrome c. Loading capacity of cytochrome c (C) and BSA(D) to PLGA and PLGA/PSS nanoparticles (NPs) (n=3).

3.5. Release and bioactivity

In vitro experiments monitoring the release of lysozyme from nanoparticles at different theoretical drug loadings were performed in pH 7.4 PBS. During these experiments, the stability of the lysozyme solution was investigated as control. No significant differences ($p>0.05$) were observed in lysozyme concentrations at each time point during the release process as measured by both BCA assay and bioactivity, which indicates that the sampling process had no effect on lysozyme bioactivity.

Figure 10 shows the release of lysozyme from three different nanoparticle formulations.

It can be seen that the release rate of protein from PLGA/PSS nanoparticles at 10% loading was much faster than that at 40% loading. The increased amount of protein loaded decreased the release rate. Possible explanation is that the increased amount of lysozyme in the 40% loading sample enhanced the interaction between the protein and the nanoparticles, which led to the slower release. In addition, the coating of protein adsorbed to the nanoparticle surface can decrease the diffusion of protein by reducing the porosity or decreasing the swelling of the nanoparticles. This dependence of release on loading amount is in agreement with a previous report [39], in which chloroquine phosphate was loaded onto gelatin nanoparticles through similar adsorption method and also released faster at a lower drug loading.

The release of lysozyme from the 5%-loaded RG502H nanoparticles is slower than the 10%-loaded polymer blend particles. This probably reflects the differences in the protein-particle interaction mechanisms. Hydrophobic forces play a more important role for the PLGA particles than for the PLGA/PSS nanoparticles, and the release rate from the PLGA particles can be attributed to these hydrophobic interactions. In contrast, electrostatic interactions between the hydrophilic surface of the polymer blend nanoparticles and lysozyme are of more importance for the PLGA/PSS system.

In order to verify that the particle preparation and release process do not denature the protein, the bioactivity of released lysozyme was determined. Figure 11 shows the concentration and bioactivity of lysozyme released from 40%-loaded nanoparticles. There were no significant differences between the two measures at any of the time points ($P>0.05$), which confirms that no lysozyme denaturation was detected during the process of adsorption onto the nanoparticles or during the release. Based on these data, it may be concluded that this is a facile and feasible method for preparing protein-loaded nanoparticles.

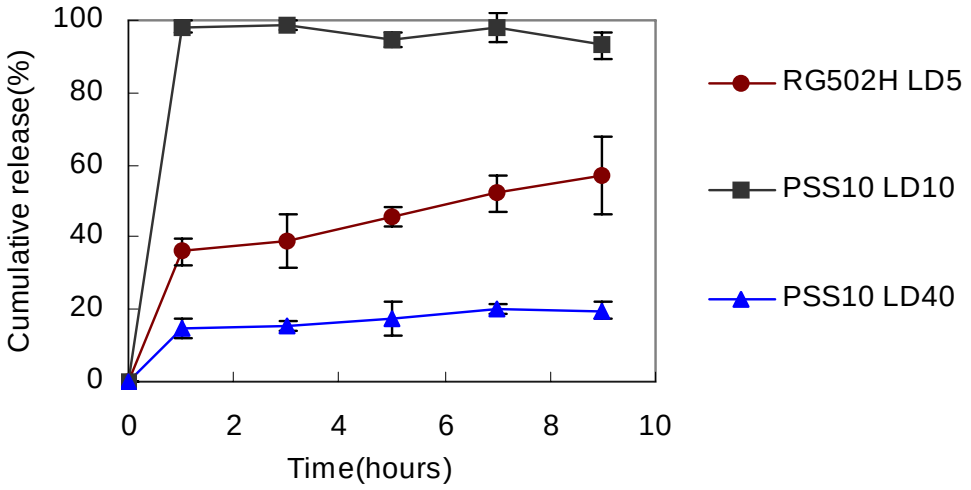

Figure 10. In vitro release profiles of lysozyme from PLGA and PLGA/PSS nanoparticles at different theoretical drug loading values. RG502H LD5: PLGA nanoparticles with theoretical drug loading of 5%; PSS10LD10 and PSS10LD40: PLGA-PSS nanoparticles at a ratio of 10% of PSS to PLGA, with theoretical drug loadings of 10% and 40%, respectively. Each data point represents mean ± standard deviation (n = 3).

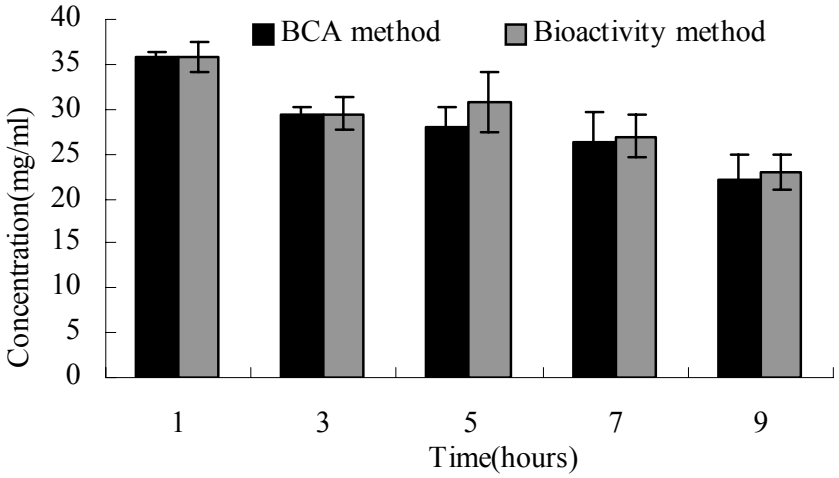

Figure 11. Comparison of the concentrations and bioactivity of lysozyme released from PLGA-PSS nanoparticles (10% PSS, 40% theoretical protein loading), as measured by BCA assay and activity against *Micrococcus lysodeikticus* cell walls, respectively (n=3).

4. Conclusions

In the present report we describe the feasibility of employing a model negatively charged nanocarrier system, consisting of a polymer blend of PLGA and PSS, for increasing the loading capacity of the model positively charged protein lysozyme based on the increased negative charge density of the nanoparticles. Investigations of pH and ionic strength suggest that electrostatic interactions primarily govern the adsorption process, but that hydrophobic interactions also play a minor role. Moreover, studies involving the adsorption behavior of cytochrome c and BSA corroborate the key role of electrostatic interactions for the adsorption of hydrophilic electropositive protein to hydrophilic negatively charged nanoparticles. The release rate of lysozyme from nanoparticles was dependent on drug loading, and the preservation of full protein bioactivity was demonstrated. Taken together, our results suggest a feasible method to improve the loading capacity of proteins based on the electrostatic interactions between oppositely charged proteins and nanoparticles. Further studies involving new types of negatively charged polymers recently developed in our research group are currently in progress.

Acknowledgments

Cuifang Cai would like to acknowledge the German Academic Exchange Service (Deutsche Akademische Austauschdienst, DAAD) for the financial support. We thank Johannes Sitterberg for the AFM images, and Michael Hellwig for his assistance about TEM and SEM images.

References

[1] J. Panyam, V. Labhasetwar, Biodegradable nanoparticles for drug and gene delivery to cells and tissue, Adv. Drug Deliv. Rev. 55 (2003) 329-347.

[2] K.S. Soppimath, T.M. Aminabhavi, A.R. Kulkarni, W.E. Rudzinski, Biodegradable polymeric nanoparticles as drug delivery devices, J. Control. Release 70 (2001) 1-20.

[3] A. Brunner, K. Maeder, A. Goepferich, pH and osmotic pressure inside biodegradable microspheres during erosion, Pharm. Res. 16 (1999) 847-853.

[4] T. Jung, A. Breitenbach, T. Kissel, Sulfobutylated poly(vinyl alcohol)-graft-poly(lactide-co-glycolide)s facilitate the preparation of small negatively charged biodegradable nanospheres, J. Control. Release 67 (2000) 157-169.

[5] M.C. Julienne, M.J. Alonso, J.L. Gomez Amoza, J.P. Benoit, Preparation of poly(DL-lactide/glycolide) nanoparticles of controlled particle size distribution: application of experimental designs, Drug Dev. Ind. Pharm. 18 (1992) 1063-1077.

[6] P. Couvreur, B. Kante, M. Roland, P. Guiot, P. Bauduin, P. Speiser, Polycyanoacrylate nanocapsules as potential lysosomotropic carriers: preparation, morphological and sorptive properties, J. Pharm. Pharmacol. 31 (1979) 331-332.

[7] E. Allemann, J.C. Leroux, R. Gurny, E. Doelker, In vitro extended-release properties of drug-loaded poly(DL-lactic acid) nanoparticles produced by a salting-out procedure, Pharm. Res. 10 (1993) 1732-1737.

[8] H. Fessi, F. Puisieux, J.P. Devissaguet, N. Ammoury, S. Benita, Nanocapsule formation by interfacial polymer deposition following solvent displacement, Int. J. Pharm. 55 (1989) R1-R4.

[9] C.V. Sternling, L.E. Scriven, Intefacial turbulence: hydrodynamic instability and the Marangoni effect, AIChE Journal 5 (1959) 514-523.

[10] B. Dimitrova, I. Ivanov, E. Nakache, Mass transport effects on the stability of emulsion: emulsion films with acetic acid and acetone diffusing across the interface, J. Dispersion Sci. Technol. 9 (1988) 321-341.

[11] J.A. Schrier, P.P. DeLuca, Porous bone morphogenetic protein-2 microspheres: polymer binding and in vitro release, AAPS PharmSciech 2 (2001) E17.

[12] T. Niwa, H. Takeuchi, T. Hino, N. Kunou, Y. Kawashima, Preparations of biodegradable nanospheres of water-soluble and insoluble drugs with DL-lactide/glycolide copolymer by a novel spontaneous emulsification solvent diffusion method, and the drug release behavior, J. Control. Release 25 (1993) 89-98.

[13] X. Li, Y. Zhang, R. Yan, W. Jia, M. Yuan, X. Deng, Z. Huang, Influence of process parameters on the protein stability encapsulated in poly-DL-lactide-poly(ethylene glycol) microspheres, J. Control. Release 68 (2000) 41-52.

[14] W. Lu, T.G. Park, Protein release from poly(lactic-co-glycolic acid) microspheres: protein stability problems, PDA J. Pharm. Sci. Technol. 49 (1995) 13-19.

[15] K. Rezwan, L.P. Meier, L.J. Gauckler, Lysozyme and bovine serum albumin adsorption on uncoated silica and AlOOH-coated silica particles: the influence of positively and negatively charged oxide surface coatings, Biomaterials 26 (2005) 4351-4357.

[16] T. Jung, W. Kamm, A. Breitenbach, K.D. Hungerer, E. Hundt, T. Kissel, Tetanus toxoid loaded nanoparticles from sulfobutylated poly(vinyl alcohol)-graft-poly(lactide-co-glycolide): evaluation of antibody response after oral and nasal application in mice, Pharm. Res. 18 (2001) 352-360.

[17] R. Ghaderi, J. Carlfors, Biological activity of lysozyme after entrapment in poly(d,l-lactide-co-glycolide)-microspheres, Pharm. Res. 14 (1997) 1556-1562.

[18] T. Jung, W. Kamm, A. Breitenbach, G. Klebe, T. Kissel, Loading of tetanus toxoid to biodegradable nanoparticles from branched poly(sulfobutyl-polyvinyl

alcohol)-g-(lactide-co-glycolide) nanoparticles by protein adsorption: a mechanistic study, Pharm. Res. 19 (2002) 1105-1113.

[19] M. Van de Weert, J. Hoechstetter, W.E. Hennink, D.J. Crommelin, The effect of a water/organic solvent interface on the structural stability of lysozyme, J. Control. Release 68 (2000) 351-359.

[20] A. Wittemann, M. Ballauff, Secondary structure analysis of proteins embedded in spherical polyelectrolyte brushes by FT-IR spectroscopy, Anal. Chem. 76 (2004) 2813-2819.

[21] C. Czeslik, R. Jansen, M. Ballauff, A. Wittemann, C.A. Royer, E. Gratton, T. Hazlett, Mechanism of protein binding to spherical polyelectrolyte brushes studied in situ using two-photon excitation fluorescence fluctuation spectroscopy, Phys. Rev. E 69 (2004) 021401.

[22] S. Rosenfeldt, A. Wittemann, M. Ballauff, E. Breininger, J. Bolze, N. Dingenouts, Interaction of proteins with spherical polyelectrolyte brushes in solution as studied by small-angle x-ray scattering, Phys. Rev. E 70 (2004) 061403.

[23] B. Haupt, T. Neumann, A. Wittemann, M. Ballauff, Activity of enzymes immobilized in colloidal spherical polyelectrolyte brushes, Biomacromolecules 6 (2005) 948-955.

[24] P.M. Biesheuvel, A. Wittemann, A modified box model including charge regulation for protein adsorption in a spherical polyelectrolyte brush, J. Phys. Chem. B 109 (2005) 4209-4214.

[25] K. Anikin, C. Rocker, A. Wittemann, J. Wiedenmann, M. Ballauff, G.U. Nienhaus, Polyelectrolyte-mediated protein adsorption: fluorescent protein binding to individual polyelectrolyte nanospheres, J. Phys. Chem. B 109 (2005) 5418-5420.

[26] W. Norde, J. Lyklema, The adsorption of human plasma albumin and bovine pancreas ribonuclease at negatively charged polystyrene surfaces. II. Hydrogen ion titrations, J. Colloid Interface Sci. 66 (1978) 266-276.

[27] W. Norde, J. Lyklema, The adsorption of human plasma albumin and bovine pancreas ribonuclease at negatively charged polystyrene surfaces. I. Adsorption isotherms. Effects of charge, ionic strength, and temperature, J. Colloid Interface Sci. 66 (1978) 257-265.

[28] J. Chesko, J. Kazzaz, M. Ugozzoli, T. O'Hagan D, M. Singh, An investigation of the factors controlling the adsorption of protein antigens to anionic PLG microparticles, J. Pharm. Sci. 94 (2005) 2510-2519.

[29] K. Rezwan, L.P. Meier, L.J. Gauckler, A prediction method for the isoelectric point of binary protein mixtures of bovine serum albumin and lysozyme adsorbed on colloidal titania and alumina particles, Langmuir 21 (2005) 3493-3497.

[30] P.M. Biesheuvel, P. Stroeve, P.A. Barneveld, Effect of Protein Adsorption and Ionic Strength on the Equilibrium Partition Coefficient of Ionizable Macromolecules in Charged Nanopores, J. Phys. Chem. B 108 (2004) 17660-17665.

[31] Y.C. Liu, E. Stellwagen, Accessibility and multivalency of immobilized Cibacron blue F3GA, J. Biol. Chem. 262 (1987) 583-588.

[32] S. Robinson, P.A. Williams, Inhibition of Protein Adsorption onto Silica by Polyvinylpyrrolidone, Langmuir 18 (2002) 8743-8748.

[33] S. Zhang, Y. Sun, Further studies on the contribution of electrostatic and hydrophobic interactions to protein adsorption on dye-ligand adsorbents, Biotechnol. Bioeng. 75 (2001) 710-717.

[34] J. Gong, P. Yao, H. Duan, M. Jiang, S. Gu, L. Chunyu, Structural Transformation of Cytochrome c and Apo Cytochrome c Induced by Sulfonated Polystyrene, Biomacromolecules 4 (2003) 1293-1300.

[35] L. Liang, P. Yao, J. Gong, M. Jiang, Interaction of apo cytochrome c with sulfonated polystyrene nnanoparticles, Langmuir 20 (2004) 3333-3338.

[36] P. Calvo, J.L. Vila-Jato, M.J. Alonso, Effect of lysozyme on the stability of polyester nanocapsules and nanoparticles: stabilization approaches,

Biomaterials 18 (1997) 1305-1310.

[37] H. Bayraktar, C.-C. You, V.M. Rotello, M.J. Knapp, Facial Control of Nanoparticle Binding to Cytochrome c, J. Am. Chem. Soc. 129 (2007) 2732-2733.

[38] K. Rezwan, A.R. Studart, J. Voros, L.J. Gauckler, Change of zeta potential of biocompatible colloidal oxide particles upon adsorption of bovine serum albumin and lysozyme, J. Phys. Chem. B 109 (2005) 14469-14474.

[39] F.Q. Hu, G.F. Ren, H. Yuan, Y.Z. Du, S. Zeng, Shell cross-linked stearic acid grafted chitosan oligosaccharide self-aggregated micelles for controlled release of paclitaxel, Colloids Surf. B 50 (2006) 97-103.

Chapter 4

Layer-by-layer nanostructured protein loaded nanoparticles: A feasibility study using lysozyme as model protein and chitosan as coating material

In preparation for *European Journal of Pharmaceutics and Biopharmaceutics*

Abstract

We have previously demonstrated that negatively charged nanoparticles consisting of PLGA and poly(styrene-co-4-styrene-sulfonate) (PSS) showed considerably high loading capacity for positively charged model protein lysozyme depending on the surface charge density of nanoparticles. Here our objective was to investigate a layer-by-layer structured protein nanocarrier using chitosan and its derivatives as coating for protein loaded PLGA/PSS nanoparticles. Nanoparticles were prepared by a solvent displacement method. Loading with electropositively charged model protein lysozyme and followed chitosan coating were performed through electrostatic interaction between oppositely charged nanoparticles-protein, and nanoparticles-chitosan. The influence of chitosan composition, concentration and initial protein loading on the properties of nanoparticles was evaluated in terms of size, zeta-potential and dissociation of lysozyme. Furthermore, the effect of coating on protein release and stability of nanoparticles were also investigated. The results showed that increased size and inversion of zeta-potential of particles, as well as TEM micrographs evidenced the coating of chitosan on the surface. In addition, dissociation of lysozyme was dependent on polymer composite, irrespective of initial protein loading. Moreover, with this polymer coating more stable particles were obtained in PBS, without burst release within 24 hours. In conclusion, these studies showed the feasibility of designing a layer-by-layer protein nanocarrier with chitosan and its derivatives as coating material on the surface of protein loaded nanoparticles through electrostatic interaction. In light of these results, these novel polymer coated protein loaded nanoparticles with layer-by-layer nanostructure could be considered as promising new protein delivery systems with enhanced properties, i.e. protection of protein, controlled release, stability, and combined with beneficial properties of coated polymer, i.e. surface charge, mucoadhesivity, hydrophilicity and penetration enhancement for chitosan.

Keywords: Chitosan coating; Nanoparticles; Lysozyme; Electrostatic interaction; Protein carrier

1. Introduction

Significant advances in biotechnology have resulted in the discovery of a large number of therapeutic and antigenic proteins [1]. Despite the important efforts dedicated to the design of protein delivery systems, delivery of these proteins to specific sites of action in an active form, at an appropriate concentration and for an appropriate duration still remains a challenge especially since the labile structure of proteins are prone to be hydrolytic and enzymatic degradation [2].

New delivery strategies, intended to enhance the efficacy of these macromolecules, have been extensively described [3]. Among them, polymeric nanoparticles have shown a certain degree of success for the delivery of proteins and vaccines to the systemic circulation and to the immune system. Since size and surface properties, i.e. surface charge and hydrophobicity, of nanoparticles have been recognized as crucial charcteristics, especially, surface modified colloidal carriers such as nanoparticles were demonstrated to be a promising and useful tool in the development of drug carrier systems with the intention of administering biotechnology engineered products. They present several characteristics that make them suitable candidates to develop efficient mucosal administration forms, to achieve long circulation time after parental administration, to modify the body distribution, and to offer drug protection against *in vivo* acid and enzymatic degradation [4]. Some of the widely used surface-coating materials are: polyethylene glycol (PEG), polyethylene oxide (PEO), poloxamer, poloxamine, polysorbate (Tween-80) and lauryl ethers (Brij-35) [5].

Although the oral, nasal and pulmonary routes are most common and convenient routes compared to injection for delivering the macromolecules, peptide and protein drugs are degraded before they reach the blood stream and cannot cross the mucosal barriers [6]. Taking this challenge, the mucoadhesive polymer-coated nanoparticles colloidal carriers were thought to solve these problems. Besides their mucoadhesive properties, these polymer coatings could also protect the peptide against proteolytic enzymes and/or to enhance the transport of the peptide through the

intestinal mucosa. Among them, chitosan coated nanoparticles draw a great interest in this field.

Chitosan is a biocompatible and hydrophilic polysaccharide of low toxicity [7], comprising copolymers of glucosamine and *N*-acetylglucosamine. To improve solubility at physiological pH , chitosan derivatives, *N*-trimetyl chitosan (TMC) and PEGylated TMC, have been synthesized and showed positive properties such as lower cytotoxicity [8]. Chitosan has bioadhesive properties due to electrostatic interactions with sialic groups of mucins in the mucus layer. It was also demonstrated that chitosan can enhance the absorption of hydrophilic molecules by promoting a structural reorganization of the tight junction-associated proteins [9]. Due to the mucoadhesivity and ability to enhance the penetration of large molecules across mucosal surfaces [10], development of chitosan and its derivatives coated nanoparticles has been the subject of many studies in recent years [4,9,11-21].

We investigated the feasibility of negatively charged PLGA/PSS nanoparticles as protein carrier. The charge density of nanoparticles could be modulated by adjusting the polymer ratio of PLGA to PSS (a partially sulfonated polystyrene containing sulfonic acid groups attached to the backbone). Lysozyme, as a model electropositively charged protein, was absorbed onto the negatively charged nanoparticles through electrostatic interaction. This is a facile method to prepare protein loaded nanoparticles with full preserved bioactivity and high protein loading. However, it has been clearly demonstrated that through adsorption loading method fast detachment and the instability of protein still remain a challenge, because protein was supposed to be located on the surface of nanoparticles [5]. Therefore, a feasibility was carried out to further investigate the surface modification with polymer coating intended to solve this problem.

Although it is well known that chitosan can be degraded by lysozyme in serum [22], in this work lysozyme loaded nanoparticles were evaluated after chitosan coating immediately and the in vitro release also was investigated within 24 hours. Moreover, the degradation of chitosan by lysoyzme has been studied and negligible degradation

within 48 hours was observed. Hence, chitosan could be chosen as coating materials in this feasibility study, along with model protein lysozyme.

As demonstrated before, the overall surface charge of lysozyme loaded PLGA/PSS nanoparticles can be varied depending on the protein loading; thus, this surface charge surplus of nanoparticles facilitates further surface modifications. As such, at low drug loading the negative charge surplus of protein loaded nanoparticles can be used to deposit alternating layers of polycations on the surface. This formation of surface coating is supposed to be mediated by the interaction between the negatively charged protein-loaded nanoparticles and the positively charged polymer molecules.

This layer-by-layer structure is preferable for the protection of protein and inhibition of burst release. Furthermore, when chitosan and its derivatives were selected as coating materials, this polymer coating also can improve the potential performance of nanoparticles in vivo as mentioned above. Bearing this concept in mind, in this work, chitosan and its derivatives coated lysozyme loaded nanoparticles were evaluated in terms of protein loading and nanoparticles properties. Moreover, the interaction of protein-chitosan, protein-nanoparticles, and protein-nanoparticles during coating process was studied to gain further insight into the underlying mechanism.

Taken together, the aims of the present work were, first, to prepare chitosan coated lysozyme loaded nanoparticles and characterize this layer-by-layer structure protein delivery nanocarrier; and, second, to investigate the influence of chitosan composition, concentration and initial protein loading on the properties of nanoparticles. Finally, the effect of this polymer coating on release and stability of nanoparticles were also evaluated. To the best of our knowledge, similar reports have not been published so far. It is also expected that the results of this study will impact the design of nanoparticles for protein delivery system in the future.

2. Materials and methods

2.1.Materials

Poly(lactic-co-glycolic acid) (PLGA Resomers®RG502H) was supplied by

Boehringer Ingelheim (Germany). Poly(styrene-co-4-styrene-sulfonate) (PSS, Sample# P6117-SSO3H, Parent polystyrene Mn=133 200, Mw/Mn=1.04, Sulfonation Degree: 50mol% by Titration, Mn=184 400, Mw=191 800) was purchased from Polymer Source, Inc.(Germany). The Micro BCA protein assay kit was purchased from Pierce Chemical (Bonn, Germany). Hen egg white lysozyme was obtained from Sigma-Aldrich Chemie GmbH (Germany). Bovine serum albumin (BSA) was purchased from Hoechst Behring (Marburg, Germany).

Three different commercially available chitosans F-LMW (150kDa), F-MMW (400 kDa), F-HMW (600kDa), with a nominal degree of deacetylation of 84.5%, 84.7%, and 85.0% respectively, were purchased from Fulka (Neu-Ulm, Germany). Trimethyl chitosan (TMC) derivatives were synthesized in a two-step synthesis [23]. In this study, degree of quaternization of TMC is 40%. PEGylated TMC copolymer, PEG(550)-g-TMC400 was synthesized by grafting poly(ethylene glycol) (PEG) 550 Da onto TMC 400 kDa according to the method described previously [8]. The following nomenclature for the copolymers was adopted: PEG(X)n-g-TMC(Y), where X designates the MW of PEG in Da, Y denotes the MW of TMC in kDa, and the subscript n represents the average number of PEG chains per TMC macromolecule of Y kDa. All other chemicals were purchased from Sigma, of analytical grade, and used without further purification.

2.2. PLGA/PSS Nanoparticles preparation

Nanoparticles were prepared by a solvent displacement technique, described in detail elsewhere [24,25]. Briefly, 10.0 mg of polymer at different mass ratio of PLGA (RG502H) to PSS were dissolved in 1 ml of acetone at 25°C. The resulting solution was subsequently injected to a magnetic stirred (500rpm) aqueous phase 5 ml of filtrated and double distilled water (pH 7.0, conductance 0.055 μS/cm, 25°C) using a special apparatus. The apparatus consists of an electronically adjustable single-suction pump which was used to inject the organic solution into the aqueous phase through an injection needle (Sterican 0.55×25mm) at constant flow rates (10.0 ml/ min). The

pump rate was regulated and constantly monitored by an electric power control. After the injection of the organic phase the resulting colloidal suspension was stirred for 8 h under reduced pressure to remove the organic solvents. Particles were characterized and used directly after the preparation. Specifically, based on previous experiment, in this study, the mass ratio 10% of PSS:PLGA was chosen to prepare polymer blend nanoparticles for the further protein loading and chitosan coating.

2.3. Preparation of protein-loaded PLGA/PSS nanoparticles

Nanoparticle suspensions of defined concentrations were incubated with defined amounts of lysozyme for 5 h at 4°C. The amount of absorbed protein on the nanoparticles was calculated by measuring the difference between the amount of protein added to the nanoparticles solution and the measured non-entrapped protein remaining in the aqueous phase. After incubation, samples were centrifuged for 30 min at 13 000 rpm (25°C), and the supernatant was checked for the non-bound protein by bicinchonic acid assay (BCA). For each protein concentration, a control tube was prepared without any nanoparticles to account for any protein loss due to adsorption to the Eppendorf tubes. In order to investigate the deposition of alternating layers of polycations utilizing the negative charge surplus of nanoparticles at lower protein loading, in this study, initial theoretical protein loading 10% of lysozyme was selected. Protein loading efficiency was calculated as follows:

$$\text{Protein loading efficiency} = \frac{\text{Total amount of protein} - \text{Free protein}}{\text{Total amount of protein}} \times 100\%$$

2.4. Preparation of polymer coated proteins

Chitosan and its derivatives coated nanoparticles were produced by simple adsorption of the positively charged polymer to the negatively charged protein loaded Nanoparticles. The protein loaded nanoparticles were incubed with chitosan solution (5mM acetate buffer pH 5.5) at room temperature 1 hour. These freshly prepared samples were evaluated with regard to the size and zeta-potential. With respect to the

lysozyme loading, samples were centrifuged for 30 min at 13 000 rpm (25°C), and the supernatant was checked for the non-bound protein by bicinchonic acid assay (BCA) and loading of lysozyme was measured and calculated as described in methods section 2.3.

2.5. Particle size and Zeta potential measurements

The average particle size and zeta potential of the nanoparticles were measured using a Zetasizer Nano ZS/ZEN3600 (Malvern Instruments, Malvern, UK). Particle size and polydispersity were determined using non-invasive back scatter (NIBS) technology, which allows sample measurement in the range of 0.6nm - 6μm. Freshly prepared particles suspension (800 μl) was placed in a green disposable zeta cell (folded capillary cell DTS 1060) without dilution. The measurement was carried out using a 4mW He-Ne laser (633nm) as light source at a fixed angle 173°. The following parameters were used for experiments: medium refractive index 1.330, medium viscosity 0.88 mPa s, a dielectric constant of 78.54, temperature 25°C. Each size measurement was performed at least 10 runs. All measurements were carried out in triplicate directly after NP preparation, and the results were expressed as mean size ± S.D.

After the size measurement, zeta potential was measured with the M3-PALS Technique (a combination of laser Doppler velocimetry and phase analysis light scattering (PALS). A Smoluchowsky constant F (K_a) of 1.5 was used to achieve zeta potential values from electrophoretic mobility. Each zeta-potential measurement was performed automatically at 25°C. All measurements were carried out in triplicate directly after NP preparation, and the results were expressed as mean size ± S.D.

2.6. Transmission electron microscopy (TEM)

The samples were prepared by coating a copper grid (200 mesh and covered with Formvar/carbon) with a thin layer of dilute particle suspension. After negative staining with 2% (w/v) (pH 7.4) phosphotungstic acid for 2 min, the copper grid was

then dried at room temperature before the measurement. Nanoparticles were investigated using transmission electron microscopy (TEM) (Zeiss EM 10) at an accelerating voltage of 300 kV.

2.7. Scanning electron microscopy (SEM)

In order to perform the SEM observation, nanoparticle suspension was fist diluted with ultrapure water (1/5), and then a drop of the diluted nanoparticle suspension was then directly deposited on a polished aluminum sample holder. Samples were dried in vacuum and subsequently sputter-coated with a carbon layer at 4-6 AMPS for 30 seconds then with a gold layer at 2 AMPS for 30 seconds at 5×10^{-5} Pa (Edwards Auto 306 Vacuum Coater, Edwards, Germany). The morphology of nanoparticles was observed at 3 kV using a scanning electron microscope (SEM; S-4200, Hitachi, Japan).

2.8. In vitro release of lysozyme from nanoparticles

For the release studies, protein loaded nanoparticle suspensions were incubated in phosphate buffered saline (PBS) (pH 7.4) containing 0.05% NaN_3 and 0.01% Tween® 80 by Rotatherm at 37°C. At predetermined intervals, 1 ml aliquots were withdrawn and centrifuged (13 000rpm, 30min), after which the total protein content in the supernatant was determined by the bicinchonic acid assay method. All experiments were performed in triplicate.

2.9. Statistical analysis

All experiments were done in triplicate under the same condition. The results were expressed as means ± standard deviation (SD), and the significance of differences among the groups were determined by *t*-test. Probability values ($p < 0.05$) were considered as significant.

3. Results and Discussion

The main goal of the present work was to explore the feasibility of chitosan coating performed through electrostatic interactions onto protein loaded nanoparticles, intending to design a layer-by-layer nanostructure for protein delivery. Considering this strategy, negatively charged protein loaded nanoparticles would be preferable for this coating process, when chitosan, a cationic polymer, was selected as a coating material. In our previous work, it has been previously shown that the surface charge of lysozyme loaded PLGA/PSS nanoparticles is dependent on the loading of lysozyme. At lower protein loading, protein loaded PLGA/PSS nanoparticles still present a negatively charged surface characterized by negative zeta-potential. Based on our previous experimental data, in this work, nanoparticles with ratio of PSS to PLGA 10% at theoretical protein loading 10% were selected to perform the further coating of chitosan. As shown before, placebo PLGA/PSS (PSS10%) nanoparticles displayed a zeta-potential as –56mV, after incubation with lysozyme at this drug loading the particles still showed negative zeta-potential as -36mV, together with the loading efficiency about 85.71%. Thus, with this negative charge surplus, nanoparticles can be used to deposit alternating layer of chitosan.

3.1. Preparation and characterization of chitosan (CS) coated lysoyzme loaded nanoparticles

Protein loaded nanoparticles were incubated in a solution containing chitosan 150 kDa with different concentrations from 0 to 1.92 mg/ml. The effect of CS concentration on the properties of the lysozyme loaded nanoparticles is shown in Fig.1. The results indicate that the concentration of CS had a significant influence on the particle size and zeta-potential of all the resulting formulations investigated. More specifically, the size of the CS-coated nanoparticles linearly increased upon addition of increasing amounts of CS from 244nm to 606nm (R^2=0.9671) within the range of chitoan concentrations from 0 to 1.92mg/ml. It was noted that aggregates were formed at the concentration of chitosan 60μg/ml; as a consequence, the size of nanoparticles

could not be measured at this point. Combined with the monitoring of zeta-potential shown in Fig.1 B, this aggregation could be explained by neutralized surface of nanoparticles, due to lack of charge stabilization with zeta-potential close to zero. However, further increasing the CS concentration up to120 μg/ml led to an inversion of the zeta-potential, and aggregation decreased. These results could be attributed to the high zeta-potential value induced by an excess of chitosan which let to stronger electrostatic repulsive force to prevent aggregation of particles. Overall, this increase in size after incubation with chitosan confirmed the deposition of chitosan on surface of nanoparticles. In agreement with the results presented in this work, other authors have also demonstrated that size of chitosan coated nanocapsule was significantly larger than that of the uncoated nanoparticles [19,26]. Additionally, the polydispersity index of chitosan coated nanoparticles remarkably increased from 0.116 for the uncoated particles to around 0.4 for chitosan coated nanoparticles, indicating a broad size distribution after incubation with chitosan solution.

As can be noted in Fig.1 B, Zeta-potential of protein loaded PLGA/PSS (PSS10%) nanoparticles was inverted from negative (–36 mV) to positive values up to 46 mV upon addition of increasing amounts of CS to the incubation medium. At the concentration of CS 60 μg /ml, the zeta-potential was neutralized, whereas at a CS concentration of 120 μg /ml, an inversion of zeta-potential was detected. The positive value was further slightly increased at CS concentration of 240 μg/ml. Thereafter, a stable value at around 45 mV was reached. Indeed, further increased concentration only resulted in an increased size, and no further changes in zeta-potential were found in this experiment. This was probably due to the saturation of CS association on the surface. The results of the zeta-potential of the nanoparticles before and after the incubation with chitosan also confirmed that this cationic polysaccharide was located at the surface of the nanoparticles, which is consistent with the previous finding of Garcia-Fuentes et al [18].

After incubation with chitosan, the loading of lysoyzme was also evaluated. As

can be seen in Fig. 4, the amount of lysozyme associated onto the nanoparticles first increased from 85.7 μg /mg to 96.5 μg /mg at lower concentration of chitosan solution in the range of 0～60 μg /mg, and thereafter followed by a remarkably reduction from 96.5 μg /mg to 52.4 μg /mg with the further increased concentration of chitosan. This could be explained that at lower concentration of chitosan, increasing of CS concentration elevated the motility of ions in incubation medium which facilitated the adsorption process. These results are consistent with the influence of ionic strength on loading efficiency investigated before, in which increased ionic strength at lower concentration (<50mM) led to the improvement of adsorption efficiency of lysozyme. The latter reduction of the lysozyme association at higher concentration of chitosan solution was attributed to a competition between chitosan and lysozyme, both positively charged, in their association to the surface of the nanoparticles. Similarly, Garcia-Fuentes et al have also previously reported that competition of sCT and CS in the association with lipids resulted in the detachment of sCT [18].

In the present study, the morphology of CS-coated nanoparticles with different amounts of chitosan was investigated using SEM and TEM techniques. The micrographs are shown in Fig. 2. Generally, the particles showed a compact and spherical structure. It was also noteworthy that aggregates were evidenced by SEM images after incubation with chitosan solution at concentration of 60 μg/ml, which was in agreement with the result of size distribution measured by PCS as illustrated in Fig. 1. By contrast, at the CS concentration of 120 μg /ml, no aggregates but very well individualized particles were found in SEM images, corresponding to a monodomal size distribution measured by PCS. However, the particle diameters appeared lower than the hydrodynamic diameters measured in aqueous suspension. This difference was also noticed for chitosan coated nanoparticles by many other authors [4,27], which could be attributed to the swelling of nanoparticles in suspension when particles were measured with PCS. On the contrary, for SEM sample preparation, nanoparticles were previously dried in the vacuum which led to shrinkage of nanoparticles. More

importantly, in this formulation, not only chitosan, but also PSS, which swell in the water, should be responsible for this enlargement of size in the suspension.

Compared with SEM, TEM technique allowed the close observation of particles; hence, more information about the size and structure of particles could be obtained. As seen in Fig.1 C and D, the difference in the structure of uncoated and chitosan coated nanoparticles was highlighted. For the uncoated protein loaded nanoparticles shown in Fig. 2 (C), a thin dark layer around the nanoparticles was visualized and suggested the protein location around the surface of nanoparticles. In contrast, in the case of chitosan coated nanoparticles, a thicker layer was observed and at the concentration of chitosan 120 μg/ml, and thickness of the outer layer is about 15 nm. Compared to the size measurement using PCS, at this concentration the size should be 353 ±13.8 nm, which is much larger than that of the uncoated particles with 244.7 ±2.1 nm. Theoretically, the chitoan layer of nanoparticles should be around 100 nm, which is much higher than 15 nm. This discrepancy confirmed the size shrinkage of nanoparticles in SEM images is primarily due to chitosan condensation at dry state. Bravo-Osuna et al [14] have also reported that chitosan coated nanoparticles showed a gel layer surrounding the nanoparticles retaining the dye, allowing visualization of chitosan coating. However, this TEM appearance is inconsistent with the observation reported by Garcia-Fuentes et al [18], where chitosan coating could not be clearly identified in the TEM images. This probably is attributed to different amount of chitosan attached onto the surface of nanoparticles; moreover, in our study, protein was presumed to be located on the surface, which retaining the dye surrounding the nanoparticles let to the augment of external layer thickness. Therefore, it is possible to deduce that negligible external layer can be detected in TEM images when lower amount of chitosan is attached to the surface of Nanoparticles because of the shrinkage of chitosan at dry state.

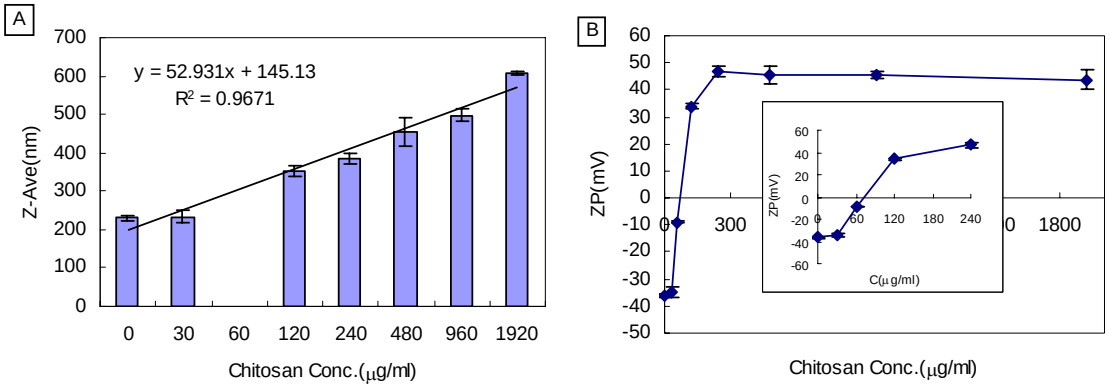

Figure 1. Size (A) and zeta-potential (B) of chitosan coated lysozyme loaded nanoparticles at different chitosan concentration: polymer ratio of PLGA: PSS 10% at initial theoretical lysoyzme loading 10% (mean ± S.D., *n*=3)

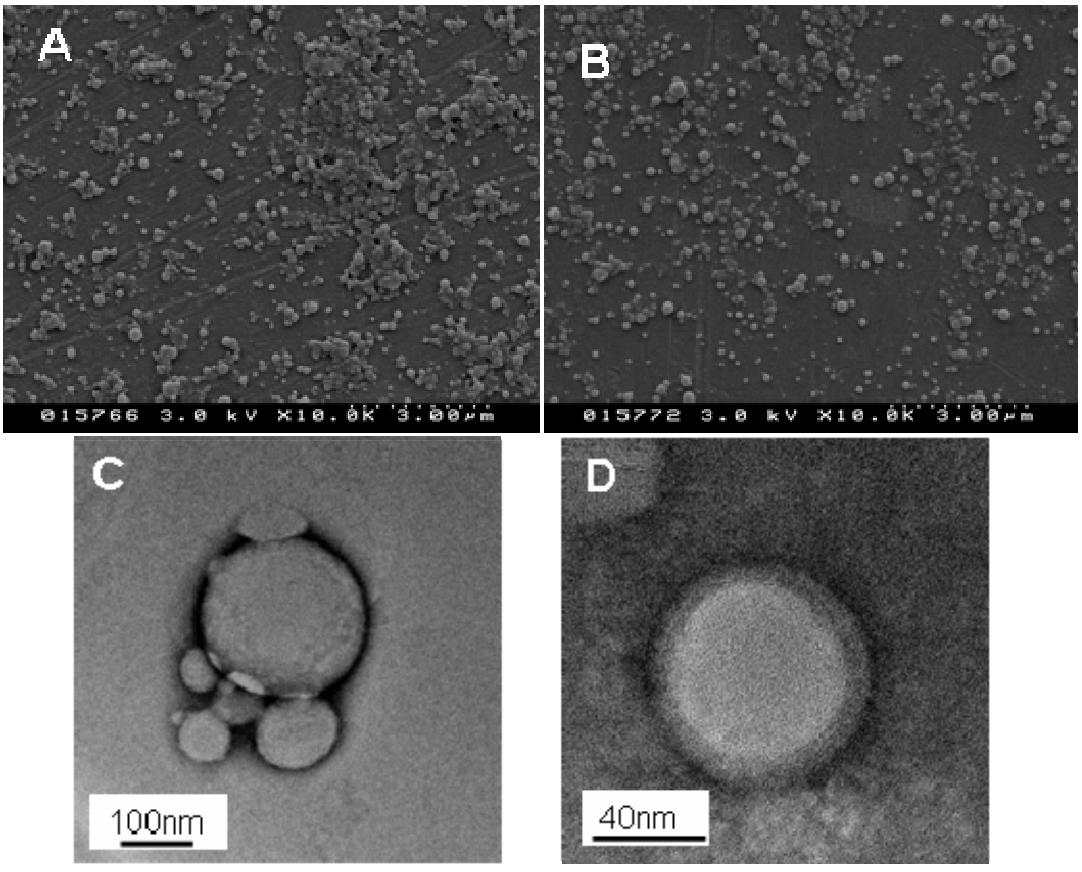

Figure 2. Scanning electron micrographs and transmission electron micrographs of chitosan coated nanoparticles, SEM: A: chitosan 60 μg/ml B: chitosan 120 μg/ml; TEM: C: uncoated lysozyme loaded Nanoparticles, D: nanoparticles with chitosan coating at the concentration of chitosan 120 μg/ml.

3.2. Effect of chitosan molecular weight

The molecular weight of chitosan has been considered to influence the stability of the DNA/chitosan or peptide/chitosan complex, transfection efficiency, and immune response of tetanum toxin[4]. Taking potential application of this protein nanocarrier into account and as a feasibility study of layer-by-layer protein delivery nancarrier, the deposition behavior of chitosan with different molecular weight (150 kDa, 400 kDa, 600 kDa) on this lysozyme loaded PLGA/PSS nanoparticles was investigated in terms of properties of nanoparticles and protein loading. For this purpose protein loaded nanoparticles were incubated in solution containing chitosan with different molecular weight at room temperature for 1 hour; thereafter, size, zeta-potential, and loading efficiency of lysozyme were evaluated as described above.

As shown in Fig.3, increased size of the polymer-coated nanoparticles was observed with increased concentration of polymer solution irrespective of the chitosan molecular weight. On the other hand, chitosan coating led to augmentation of size relative to uncoated nanoparticles; meanwhile it is also worthwhile to mention that the size increment was dependent on the chitosan molecular weight. Size of chitosan 400 kDa coated nanoparticles is significantly higher than that of chitosan 150 kDa at every concentration point using two sample paired t-test ($P<0.01$). Similarly, in the case of chitosan 400 kDa, slight aggregation was also observed at the concentration of 60 μg/ml, reflected in the abnormal large size of measured at this point. By contrast, for chitosan 600 kDa only under a narrow range of concentration, stable nanparticles could be obtained illustrated in Fig. 3. C. Prego. et al also have reported that the thickness of the coating is greatly dependent on the chitosan molecular weight [19]. These results could be explained by the fact that the thickness of the chitosan coating is expected to be dependent on the chain length of chitosan molecules. Additionally, these results also suggest a chitosan coating with desirable

thickness is possible to be achieved by varying the chitosan concentration and/or molecular weight.

Figure 3 B demonstrates that the zeta potential was inverted from highly negative values for the uncoated nanoparticles (about −36 mV) to highly positive values for chitosan coated nanoparticles (about +40 mV) with the increase of chitosan concentration irrespective of the molecular weight. More specifically, for chitosan 600 kDa, at the lower concentration of 30 μg/ml, zeta-potential has been neutralized compared to at 60 μg/ml for chitosan 150 kDa and 400 kDa. This results indicate that based on same concentration, higher molecular weight chitosan provides higher accessibility of positive binding site resulting in a fast neutralization of surface negative charge of particles.

The results of lysozyme loading after polymer coating are shown in Fig.4. The dissociation effect showed chitosan molecular weight dependent. More specifically, lower molecular weight chitosan (150 kDa) showed remarkably lower association of lysozyme compared to higher molecular weight chitosan (400 kDa, 600 kDa). This indicates that the higher molecular weigh chitosan with higher binding site accessibility and long chain length was not able to displace lysozyme to the same extent as lower molecular weight chitosan with short chain length. This might be explained by the faster neutralized surface charge of nanoparticles by adsorption of higher molecular weight chitosan, indicating of the reduced amount of higher molecular weight chitosan required to form the coating as compared to the lower molecular weight. However, different result was found by C. Prego et al [19] that chitosan oligomer nanocapsules showed slightly higher encapsulation efficiency. This inconsistence might be attributed to the different distribution of protein in the particles. In this work, protein was supposed to be located on the surface of nanoparticles which is sensitive to the competition with chitosan for the binding onto the surface of nanoparticles. On the contrary, in the research of C. Prego et al, sCT was encapsulated in the nanoparticles for which the dissociation was dependent on the charge density of coated polymer not the amount of coated polymer.

Additionally, irregular loading capacity of lysozyme was presented for higher

molecular weight chitosan 600 kDa, which could be due to the undetectable particles at the lower concentration because of the aggregation and at higher concentration because of the higher viscosity of solution.

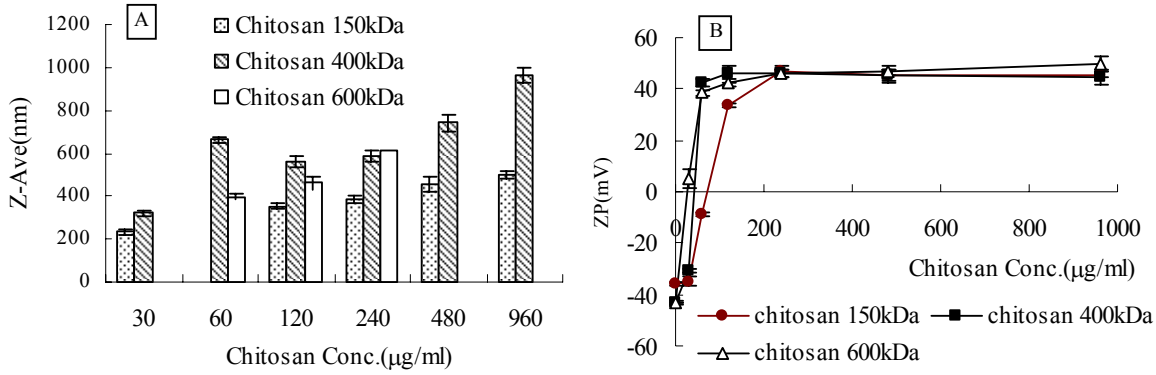

Figure 3 Size (A) and zeta-potential (B) of lysozyme loaded PLGA/PSS (PSS10%) nanoparticles after incubation with different molecular weight chitosan at different concentration (mean ± S.D., *n*=3).

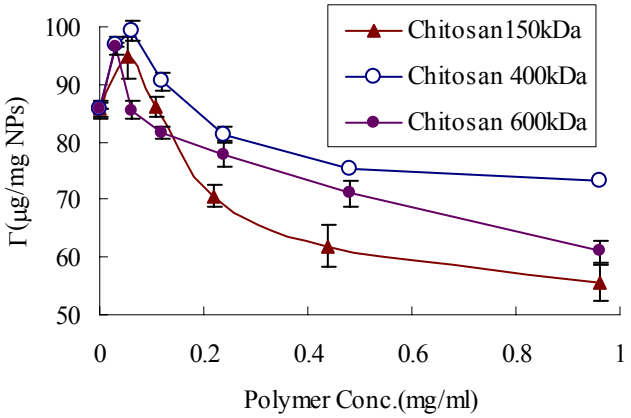

Figure 4 Loading amount of lysozyme of nanoparticles after incubation with different molecular weight chitosan at different concentration (mean ± S.D., *n*=3).

3.3. Effect of polymer structure of chitosan

It has been demonstrated that the polymer nature of surface coating is of prime important for the performance of nanoparticle protein delivery in vivo. Because of solubility limition in narrow pH ranges of chitosan, chitosan derivatives, i.e. TMC and PEGly-TMC, were extensively synthesized and investigated regarding

physicochemical properties. With the introduce of PEG chains in the chitosan molecules, it has been found that PEG-g-TMC copolymers were completely water-soluble over the entire pH range of 1-14 regardless of the PEG MW and showed a lower cytotoxicity [8]. Moreover, it has been reported that PEG-coated nanoparticles render the system stable under the harsh conditions of gastrointestinal tract [18], and because of the this steric PEG barrier the rapid uptake of nanoparticles by the mononuclear phagocyte system would be prevented resulting in prolonged circulation in vivo [28]. However, whether this PEG-g-TMC combine the property of chitosan and PEG or not, and whether using this polymer as coating materials of nanoparticles endow nanoparticles different properties or not, i.e. surface charge, hydrophilic, size, stability, et al, have not yet been studied so far. Therefore, in this feasibility study, preliminary investigation of different chitosan derivatives coated nanoparticle was performed.

In this experiment, TMC400 kDa, $PEG(550)_{83}$-TMC400 and $PEG(550)_{148}$-TMC400 , which have been recently described, were selected to perform the coating process of particles following the standard protocol. As can be seen in Fig.5, the size of the coated nanoparticles increased upon addition of increasing amounts of coating materials. No significant difference in size was observed among all formulations. With this polymer coating, the zeta-potential underwent also an inversion from negative to positive, and then leveled off at the value of -38 mV, which is lower relative to -45 mV for chitosan coating. Indeed, with the graft of PEG chains, the charge density of chitosan decreased. It was also reported that increased chains of PEG in the polymer resulted in reduced zeta-potential of chitosan and insulin complex [8]. However, between $PEG(550)_{83}$-TMC400 and $PEG(550)_{148}$-TMC400 coated nanoparticles, no significant difference in size and zeta-potential was detected. This finding can probably be explained by lower molecular weight of PEG with short chain length which is not long enough to shield the charge of chitosan. Overall, the changes in particle size and the inversion of the surface charge indicated that chitosan derivatives coating formed the third layer of this nanocarrier successfully.

Concerning the loading of lysozyme shown in Fig.6, the amount of lysozyme associated after incubation with chitosan derivatives showed similar tendency compared to chitosan upon increasing concentration of polymer. Interestingly, amount of lysozyme associated with the coating of chitosan derivatives is far lower than that of chitosan. Indeed, taking polymer concentration at 960μg/ml as example, loading amount of lysozyme is 74.42 μg, 57.25 μg, 44.22 μg and 36.57 μg for chitosan 400 kDa, TMC(400), $PEG(550)_{83}$-TMC400 and $PEG(550)_{148}$-TMC400, respectively. Since the competition between protein and polymer in binding onto nanoparticles is supposed to be depending on the charge density, TMC with higher charge density could displace protein more effectively than PEG-TMC. However, lysozyme is presumed to be located on the surface of nanoparticles, which is easier to be displaced by chitosan or its derivatives. In this case, the charge density is not the key factor for lysozyme loading. because of lower charge density of PEG-TMC, more amount of polymer is required to neutralize the surface negative charge of nanoparticles, which led to the higher detachment of protein. In fact, these results are also in good agreement with the influence of chitosan molecular weight. To conclude, chitosan derivatives coating led to lower lysoyzme association efficiency in this study.

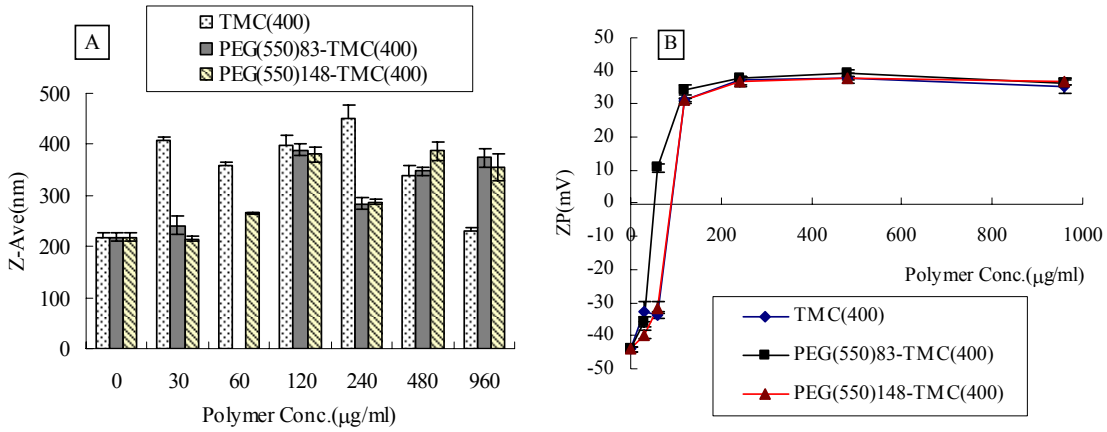

Figure 5. Changes in size (A) and zeta-potential (B) of nanoparticles after incubation with chitosan derivatives at different concentration (mean ± S.D., *n*=3).

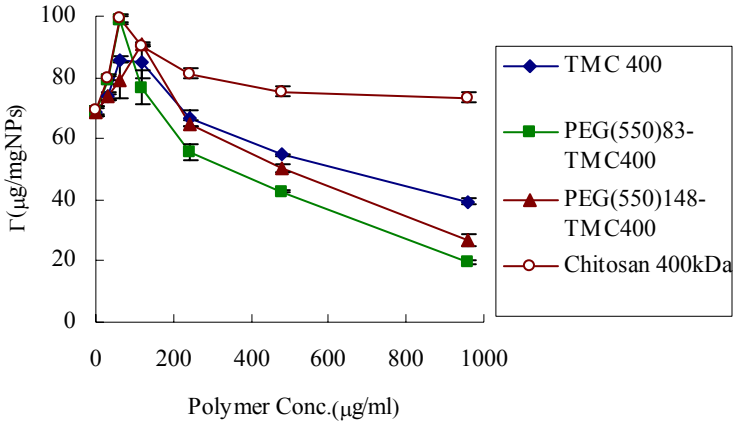

Figure 6. Loading amount of lysozyme after incubation with chitosan derivatives at different concentration (mean ± S.D., *n*=3).

3.4. Influence of initial protein loading of lysozyme

As shown in above, chitosan coating led to the detachment of lysozyme, which was not expected concerning this protein delivery strategy. During protein adsorption and chitosan coating, the negative charges on the surface of particles get through a neutralization process. When lysozyme occupies all negative binding sites of nanoparticles, this latter chitosan coating might lead to the detachment because of competition between lysozyme and chitosan. If surface binding sites have not been totally occupied by lysozyme at the first step, the further coating process might lead to the binding of chitosan on the rest negative sites on the surface and no detachment of lysoyzme occur. With this idea in mind, we attempted to prepare nanoparticles with different initial lower theoretical protein loading 2.5% and 5%, compared to 10% for the standard protocol. After incubation with chitosan solution, the properties of chitosan coated nanoparticles were evaluated in terms of size, zeta-potential and loading capacity of lysozyme.

As expected, lower lysozyme loaded nanoparticles showed slightly decreased size and higher net negative charge on the surface relative to the standard protocol. After incubation with chitosan solution, as illustrated in Fig. 7 (A), similar tendency of zeta-potential changes was observed for nanoparticles independent of different initial protein loading. Indeed, negatively charged surface of the protein loaded

nanoparticles was neutralized by positively charged chitosan for all formulations. Because of the difference in negative charge surplus of nanoparticles induced by the different protein loading, different amount of chitosan was required to neutralize the surface charge of nanoparticles, and this was reflected by different chitosan concentration at which the zeta-potential of particles shifted from negative to positive. More specifically, zeta-potential of nanoparticles with higher initial theoretical protein loading shifted to positive at lower chitosan concentration solution, i.e. for 10% protein drug loading at the chitosan concentration 30 μg/ml, by contrast, for protein drug loading 2.5%, 5% at chitosan concentration 60 μg/ml. With further increased chitosan concentration, a plateau of zeta-potential about 50 mV was reached irrespective of the initial protein loading.

With respect to the size changes depicted in Fig. 7 (B), no significant difference in size ($P>0.05$) was observed for all formulation. With the increase of chitosan coating particles size increased as described above. Within the range of all concentrations investigated, stable nanoparticles were obtained for all formulations except for nanoparticles with initial drug loading 10% at chitosan concentration 30 μg/ml. These results suggest that size of nanoparticles is primarily dependent on the chitosan concentration; and protein loading plays a minor role in this increment in size. This could be well explained by the smaller molecular weight of lysozyme (14.3 kDa) compared to chitosan (400 kDa). Moreover, higher accumulation of chitosan molecules on the surface formed a gel layer, which is more pronounced than the protein layer.

Regarding the influence of different initial drug loading on the lysozyme detachment after incubation with chitosan solution, the results obtained were rather unexpected. Figure 8 demonstrates the lysozyme loading underwent a short increase up to 100% association efficiency and followed by a linear reduction with the increase of chitosan concentration irrespective of different initial drug loading. Total amount of lysozyme in the formulation with lower initial protein loading 2.5% was displaced at chitosan concentration 960μg/ml. In fact, the results indicate a stronger electrostatic interaction of chitosan-particles than protein-particles. This might be attributed to the

difference in the positive charge density of protein and chitosan. Based on this data, the conclusion can be drawn that during chitosan coating process detachment of protein from particles is not dependent on initial protein loading, but mostly dependent on the chitosan concentration.

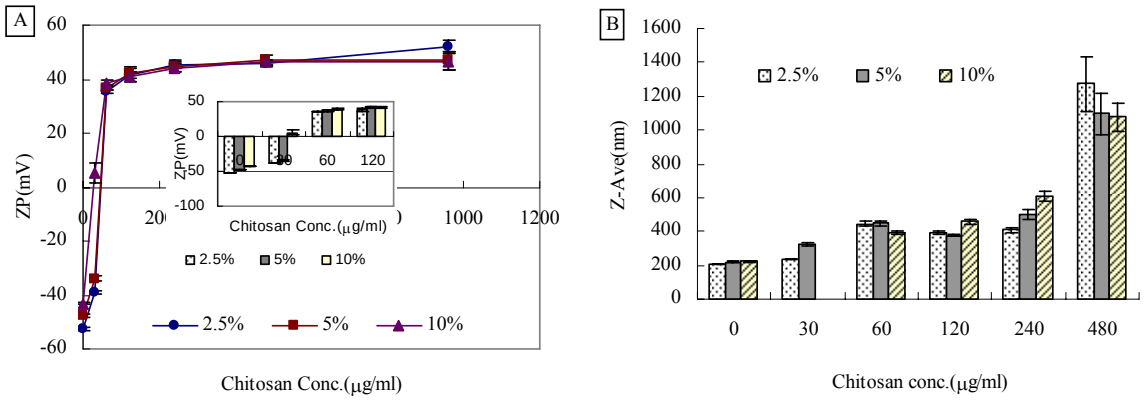

Figure 7. Size (A) and zeta-potential (B) of at different initial theoretical drug loading after incubation with chitosan solution (mean ± S.D., *n*=3).

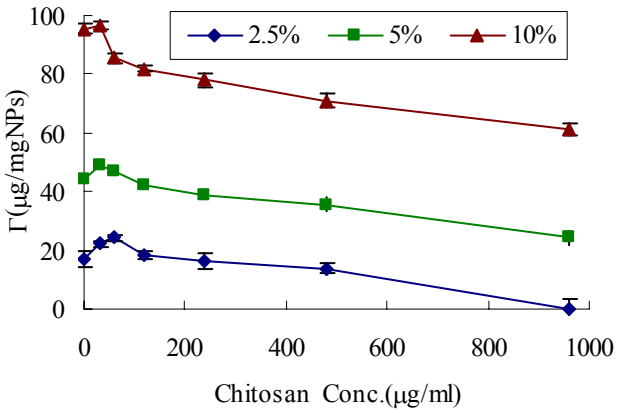

Figure 8. Loading amount of lysozyme on chitosan coated nanoparticles at different initial protein theoretical protein loading (mean ± S.D., *n*=3).

3.5. Release profiles and stability of chitosan coated lysozyme loaded PLGA/PSS nanoparticles

In vitro release studies of lysozyme from chitosan coated nanoparticles indicated that the amount of protein released from this nanocarrier was negligible after incubation in PBS up to 24h (Figure not shown). In contrast, the uncoated

nanoparticles showed complete release after incubation with release medium 1h. This slow release could be attributed to the outer chitosan layer around the nanoparticles, which hinder the diffusion of protein molecules. Further more, since the in vitro release was performed in PBS (pH 7.4), it is possible to deduce that chitosan formed a dense crust on the surface of nanoparticles due to the poor solubility of chitosan in this pH. Moreover, due to this layer-by-layer nanostructure, protein was supposed to be covered by chitosan layer not on the surface of nanoparticles. Thus, both the location of protein in the nanostructure and the covered layer of chitosan led to this negligible release. Additionally, Prego et al also reported that chitosan oligomer coated nanocapsules showed negligible release for up 6h [19]. However, it has also reported that chitosan coated lipid nanoparticles showed lower burst release, as well as a slow release profiles [18]. This discrepancy maybe is due to the different release medium. In the previous work, in vitro release was performed in pH 4 acetate buffer, and chitosan has better solubility in lower pH which favors the release of protein [18,19]. Based on these results, this study gives a better understanding of this nanocarrier system for protein delivery and it is also reasonable to expect this polymer coating together with layer-by-layer structure might protect protein to the most extent.

It has been clear demonstrated that size and surface properties are crucial factors for the destiny of nanoparticulate system in vivo. On the other hand, it is also well known that protein-loaded colloidal systems may suffer a destabilization process mediated by interparticlulate protein interaction [29]. Therefore, during release studies, the stability of chitosan coated nanoparticles was also monitored by measuring the size and zeta-potential. At predetermined intervals, sample of nanoparticles in PBS was taken; subsequently, size and zeta-potential were measured directly at 37°C. As displayed in Fig. 9, the particles size remained unaltered relative to the initial values, and no changes in ζ-potential was observed following the incubation in PBS. This improved stability could be attributed to the higher electrostatic repulsive force between the particles and non-released lysozyme.

This study indicates the layer-by-layer nanocarrier as a protein carrier is feasible

to protect the protein by the outer layer of polymer coating and to improve the stability of colloidal systems through electrostatic repulsive force or steric hindrance effect.

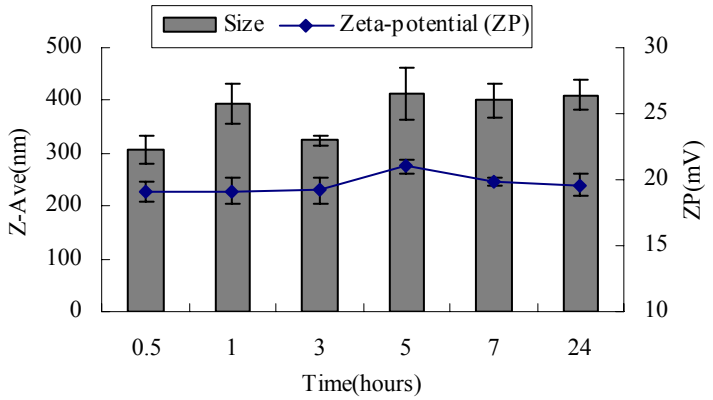

Figure 9 Size (Z-Ave) and zeta-potential (ZP) of chitosan coated nanoaparticles during release in PBS at 37°C (mean ± S.D., n=3).

4. Conclusions

In this work, we describe the feasibility of using chitoan and its derivatives as coating materials to develop a layer-by-layer nanostructure for protein delivery. PLGA/PSS nanoparticles were prepared by solvent displacement method; the subsequent protein loading and polymer coating process were performed by simple incubation of the nanoparticles in an aqueous solution. Negatively charged PLGA/PSS nanoparticles showed a considerable loading capacity of model electropositive protein lysoyzme. Chitosan coating resulted in the increased size and the inversion of the surface charge. In addition, it was observed that detachment of lysozyme due to the chitosan or its derivatives coating was greatly influenced by polymer composition irrespective of the initial protein loading. Finally, more stable particles with chitosan coating were evidenced in PBS, without initial release within 24 hours. These studies demonstrated that it is feasible to design a novel layer-by-layer polymer coated nanoparticles as protein nanocarrier using facile method without shear force and contact with organic solvent to preserve the bioactivity to the most extent. Meanwhile, due to this novel nanostructure enhanced properties was achieved, i.e. protection of

protein, inhabitation of burst release, and improved stability of nanoparticles. This work can be considered as the first step in this direction, and further investigations will be performed with new class negatively charged polymer, sulfobutylated poly(vinyl-alcohol)-graft-poly(lactide-co-glycolide) and poly(vinylsulfonate-co-vinyl alcohol)-g-PLGA , synthesized recently in our research group.

Acknowledgement

Cuifang Cai would like to thank the German Academic Exchange Service (Deutsche Akademische Austauschdienst, DAAD) for the financial support. In addition, we are grateful to Michael Hellwig for his kind help with TEM and SEM experiments.

References

[1] A. Vila, A. Sanchez, M. Tobio, P. Calvo, M.J. Alonso, Design of biodegradable particles for protein delivery, J. Control. Release 78 (2002) 15-24.

[2] V.R. Sinha, A. Trehan, Biodegradable microspheres for protein delivery, J. Control. Release 90 (2003) 261-280.

[3] D.K. Malik, S. Baboota, A. Ahuja, S. Hasan, J. Ali, Recent advances in protein and peptide drug delivery systems, Curr. Drug Deliv. 4 (2007) 141-151.

[4] I. Bravo-Osuna, G. Ponchel, C. Vauthier, Tuning of shell and core characteristics of chitosan-decorated acrylic nanoparticles, Eur. J. Pharm. Sci. 30 (2007) 143-154.

[5] K.S. Soppimath, T.M. Aminabhavi, A.R. Kulkarni, W.E. Rudzinski, Biodegradable polymeric nanoparticles as drug delivery devices, J. Control. Release 70 (2001) 1-20.

[6] C. Prego, M. Garcia, D. Torres, M.J. Alonso, Transmucosal macromolecular drug delivery, J. Control. Release 101 (2005) 151-162.

[7] P. He, S.S. Davis, L. Illum, In vitro evaluation of the mucoadhesive properties of chitosan microspheres, Int. J. Pharm. 166 (1998) 75-88.

[8] S. Mao, X. Shuai, F. Unger, M. Wittmar, X. Xie, T. Kissel, Synthesis,

characterization and cytotoxicity of poly(ethylene glycol)-graft-trimethyl chitosan block copolymers, Biomaterials 26 (2005) 6343-6356.

[9] I. Bravo-Osuna, C. Vauthier, A. Farabollini, G.F. Palmieri, G. Ponchel, Mucoadhesion mechanism of chitosan and thiolated chitosan-poly(isobutyl cyanoacrylate) core-shell nanoparticles, Biomaterials 28 (2007) 2233-2243.

[10] L. Illum, Chitosan and its use as a pharmaceutical excipient, Pharm. Res. 15 (1998) 1326-1331.

[11] I. Bertholon, C. Vauthier, D. Labarre, Complement Activation by Core-Shell Poly(isobutylcyanoacrylate)-Polysaccharide Nanoparticles: Influences of Surface Morphology, Length, and Type of Polysaccharide, Pharm. Res. 23 (2006) 1313-1323.

[12] I. Bravo-Osuna, G. Millotti, C. Vauthier, G. Ponchel, In vitro evaluation of calcium binding capacity of chitosan and thiolated chitosan poly(isobutyl cyanoacrylate) core-shell nanoparticles, Int. J. Pharm. (2007).

[13] I. Bertholon, G. Ponchel, D. Labarre, P. Couvreur, C. Vauthier, Bioadhesive properties of poly(alkylcyanoacrylate) nanoparticles coated with polysaccharide, J. Nanosci. Nanotechnol. 6 (2006) 3102-3109.

[14] I. Bravo-Osuna, T. Schmitz, A. Bernkop-Schnuerch, C. Vauthier, G. Ponchel, Elaboration and characterization of thiolated chitosan-coated acrylic nanoparticles, Int. J. Pharm. 316 (2006) 170-175.

[15] F. Cui, F. Qian, C. Yin, Preparation and characterization of mucoadhesive polymer-coated nanoparticles, Int. J. Pharm. 316 (2006) 154-161.

[16] A.M. De Campos, A. Sanchez, R. Gref, P. Calvo, M.J. Alonso, The effect of a PEG versus a chitosan coating on the interaction of drug colloidal carriers with the ocular mucosa, Eur. J. Pharm. Sci. 20 (2003) 73-81.

[17] M. Garcia-Fuentes, C. Prego, D. Torres, M.J. Alonso, A comparative study of the potential of solid triglyceride nanostructures coated with chitosan or poly(ethylene glycol) as carriers for oral calcitonin delivery, Eur. J. Pharm. Sci. 25 (2005) 133-143.

[18] M. Garcia-Fuentes, D. Torres, M.J. Alonso, New surface-modified lipid nanoparticles as delivery vehicles for salmon calcitonin, Int. J. Pharm. 296 (2005) 122-132.

[19] C. Prego, M. Fabre, D. Torres, M.J. Alonso, Efficacy and mechanism of action of chitosan nanocapsules for oral peptide delivery, Pharm. Res. 23 (2006) 549-556.

[20] H. Yamamoto, Y. Kuno, S. Sugimoto, H. Takeuchi, Y. Kawashima, Surface-modified PLGA nanosphere with chitosan improved pulmonary delivery of calcitonin by mucoadhesion and opening of the intercellular tight junctions, J. Control. Release 102 (2005) 373-381.

[21] L. Zhang, M. Sun, R. Guo, Z. Jiang, Y. Liu, X. Jiang, C. Yang, Chitosan surface-modified hydroxycamptothecin loaded nanoparticles with enhanced transport across Caco-2 cell monolayer, J. Nanosci. Nanotechnol. 6 (2006) 2912-2920.

[22] K.M. Varum, M.M. Myhr, R.J. Hjerde, O. Smidsrod, In vitro degradation rates of partially N-acetylated chitosans in human serum, Carbohydr. Res. 299 (1997) 99-101.

[23] A. Polnok, G. Borchard, J.C. Verhoef, N. Sarisuta, H.E. Junginger, Influence of methylation process on the degree of quaternization of N-trimethyl chitosan chloride, Eur. J. Pharm. Biopharm. 57 (2004) 77-83.

[24] T. Jung, A. Breitenbach, T. Kissel, Sulfobutylated poly(vinyl alcohol)-graft-poly(lactide-co-glycolide)s facilitate the preparation of small negatively charged biodegradable nanospheres, J. Control. Release 67 (2000) 157-169.

[25] T. Jung, W. Kamm, A. Breitenbach, G. Klebe, T. Kissel, Loading of tetanus toxoid to biodegradable nanoparticles from branched poly(sulfobutyl-polyvinyl alcohol)-g-(lactide-co-glycolide) nanoparticles by protein adsorption: a mechanistic study, Pharm. Res. 19 (2002) 1105-1113.

[26] Y. Kawashima, H. Yamamoto, H. Takeuchi, Y. Kuno, Mucoadhesive

DL-lactide/glycolide copolymer nanospheres coated with chitosan to improve oral delivery of elcatonin, Pharm. Dev. Technol. 5 (2000) 77-85.

[27] Y. Aktas, M. Yemisci, K. Andrieux, R.N. Gursoy, M.J. Alonso, E. Fernandez-Megia, R. Novoa-Carballal, E. Quinoa, R. Riguera, M.F. Sargon, H.H. Celik, A.S. Demir, A.A. Hincal, T. Dalkara, Y. Capan, P. Couvreur, Development and brain delivery of chitosan-PEG nanoparticles functionalized with the monoclonal antibody OX26, Bioconjug. Chem. 16 (2005) 1503-1511.

[28] M. Tobio, R. Gref, A. Sanchez, R. Langer, M.J. Alonso, Stealth PLA-PEG nanoparticles as protein carriers for nasal administration, Pharm. Res. 15 (1998) 270-275.

[29] P. Calvo, J.L. Vila-Jato, M.J. Alonso, Effect of lysozyme on the stability of polyester nanocapsules and nanoparticles: stabilization approaches, Biomaterials 18 (1997) 1305-1310.

Chapter 5

Preliminary study of nanoparticles preparation and loading capacity of model protein lysozyme using new class negatively charged polymer SB-PVA-PLGA and P(VS-VA)-PLGA

Manuscript in preparation

Abstract

The aim of this study is to evaluate the properties of nanoparticles prepared with negatively charged polymer P(VS-VA)-PLGA and SB-PVA-PLGA with solvent displacement technique in terms of size, zeta-potential, and loading capacity of model positively charged protein lysoyzme through a gentle adsorption procedure. Stable nanoparticles suspension with narrow size distribution, and high reproducibility was obtained with polymer SB-PVA-PLGA. Longer PLGA chain length of P(VS-VA)-PLGA (6-15) demonstrated better nanoparticles properties as narrow size and single peak zeta-potential distribution than shorter PLGA chain length polymer P(VS-VA)-PLGA(6-5) and (6-10). Increased sulfonic substitution degree of P(VS-VA)-PLGA decreased the size linearly, however, no significant difference in zeta-potntial was observed. SB-PVA-PLGA showed higher loading capacity as 77 μg/mg relative to this new class polymer P(VS-VA)-PLGA. Additionally, higher sulfonic substitution degree resulted in higher loading capacity. Whereas, lower loading capacity of lysozyme was observed for polymer with longer PLGA chain length, indicating that the balance of charge density and hydrophilic property is necessary for this protein adsorption process. Based on this preliminary study, these new class of negatively charged polymers can be suggested as effective nanocarrier for protein delivery.

1. Introduction

In recent years, designing appropriate carrier for hydrophilic macromolecules such as proteins, vaccines and polynucleotides has been the major challenge because of the extreme sensitivity of these molecules. Many efforts have been dedicated in this direction; among them polymeric nanoparticles show some advantages with respect to other drug delivery systems, such as protection of bioactive agent, controlled release, active or passive targeting *in vivo*. Moreover, nanoparticles can be administered through intravenous injection, ocular, nasal, and peroral route. Additionally, it has clearly demonstrated that size distribution and surface properties of the particles have been recognized as crucial characteristics. More specifically, it is well known that in vivo biodistribution or efficacy of drug substance of nanoparticles can be modified taking advantage of size effect or surface properties [1-10]. More importantly, for protein delivery, during the nanoparticles preparation, storage and even under physiological condition, the bioactivity of drug substance should be preserved. Furthermore, for nanoparticles effective drug loading also should be taken into account during formulation and preparation designing. Therefore, to prepare nanoparticles with certain properties like size, surface charge, as well as preservation of bioactivity and high protein loading appears as a big challenge.

The existing preparation methods for nanoparticles include emulsification solvent evaporation, solvent displacement, and interfacial phase deposition induced by salting out or emulsification diffusion processes [11]. Especially, due to the narrow size distribution and facile preparation condition without shear force, the technique of solvent displacement has been extensively employed to prepare protein loaded nanoparticles [11-15]. This method is based on the precipitation of a dissolved polymer in solution by addition to a miscible, surfactant-containing solution, which is a non-solvent for the polymer [15]. However, lower drug loading for hydrophilic drug substance and exposure to organic solvent during preparation still remain challenge as

a protein loaded nanoparticles preparation technique.

With regard to drug loading of nanoparticles, three major strategies can be employed: (1) covalent attachment of the drug to the particle surface or to the polymer prior to preparation, (2) adsorption of the drug to a preformed carrier system, and (3) incorporation of the drug into the particle matrix during particle preparation [16]. Comparatively, absorption process is performed in aqueous solution and at a lower temperature which favor the bioactivity preservation of protein to the highst extent. Hence, we hypothesizd that this loading method probably can makeup the drawback of exposure to the organic solvent for solvent displacement technique. With this idea in mind, adsorption process is adopted to perform the protein loading process for preformed nanoparticles prepared with solvent displacement technique. Thus, the second step is to improve the protein loading. For adsorption processes it is known that the governing factors are hydrophobic and electrostatic interaction between protein and nanoparticles. Due to the negative effect of hydrobobic interaction on the bioactivity of protein, electrostactic interaction should be emphasized. To do this, polymers modified with different functional charged group have been of great interest to prepare particles and suggested to be protein carrier.

Among them, a new type of branched biodegradable polyester, poly(2-sulfobutyl-vinyl alcohol)-g-poly(lactide-co-glycolide) (SB-PVA-g-PLGA) recently has been described [11]. These polymers consists of biodegradable PLGA chains, grafted onto a negatively charged poly(vinyl alcohol) (PVA) backbone shown in Fig. 1. PVA provided a hydrophilic backbone for the copolymer, while the degree of the copolymer hydrophobicity could be varied according to the length of the PLGA side chains grafted onto the PVA. A special feature of this polymer is that the varying amounts of sulfobutyl groups attached to the hydrophilic backbone create polymers with an increasingly negative charge density. This negatively charged polymer facilitates adsorption of oppositely charged hydrophilic macomolecules due to

electrostatic interaction [17]. Moreover, the amphiphilic molecular structure allows the preparation of nanoparticles with defined negatively charged surfaces and narrow size distributions without the use of additional surfactants. The core-corona structure of the nanoparticles provided an optimal surface for the adsorption of a cationic antigen through electrostatic interaction. The application of this polymer as protein carrier has been recently reviewed by Dailey, L. A. et al [18]. It has been also observed that a high degree of sulfobutyl substitution resulted in an increased affinity to the intestinal cells with lower toxicity [19].

Although it has been shown that sulfobutylate substitution is a crucial factor for loading efficiency of protein and in vivo performance of nanoparticle, PVA sulfobutylation has been restricted to get higher degree of substitution for the efficiency of PVA activation. To solve this problem, polymer with higher charge density has been conceived through grafting the sulfonic group directly onto the hydrophilic backbone during first radical polymerization of vinyl sulfonate and vinyl acetate, allowing a easier adjustment of the sulfonic group substitution degree in the P(VS-VA) backbone as depicted in Fig. 2. With this new structure of polymer, higher negative charge density was expected to further improve the drug loading and performance in vivo.

As a preliminary study, the aim of this work was firstly to prepare nanoparticles with solvent displacement technique without surfactant using new polymer P(VS-VA)-PLGA. Additionally, the influence of sulfonic group substitution and chain length of PLGA on the properties of nanoparticles and protein loading was evaluated using lysozyme as a model positively charged protein through adsorption loading process. As a control, nanoparticles prepared with SB-PVA-PLGA were also evaluated with regard to size, ζ-potential, and protein loading based on the same protocol.

2. Materials and methods

2.1. *Chemicals*

The Micro BCA protein assay kit was purchased from Pierce Chemical (Bonn, Germany). Hen egg white lysozyme was obtained from Sigma-Aldrich Chemie GmbH (Germany). All other chemicals were purchased from Sigma, of analytical grade, and used without further purification.

2.1.1. *Poly(2-sulfobutyl-vinyl alcohol)-g-poly(lactide-co-glycolide) (SB-PVA-PLGA)*

Chemical structures and properties of the charged biodegradable polyesters are given in Table 1. Synthesis and characterization are described in detail elsewhere [11,18]. Briefly, polyelectrolyte backbones were obtained by the reaction of activated PVA with 1,4-butane sultone under anhydrous conditions. Biodegradable brush-like grafted PLGAs were synthesized by ring opening melt polymerization of the lactones, lactide and glycolide (1:1), in the presence of 10% (m/ m) modified or unmodified polyols with stannous octoate as catalyst, thus increased hydrophilicity of PLGA was combined with charged groups in the backbone and a modified three-dimensional architecture. The following nomenclature will be used to characterize the polymers: SB(XX)-PVA- g-PLGA10. The numbers in parenthesis designates the degree of substitution of total hydroxyl groups by sulfobutyl groups (SB) in the PVA backbone. Following letters specify the type of branched polymer chains (PLGA) which is grafted (g) onto the back-bone. The last two digits are describing the weight ratio of backbone to grafted polyester chains (10% backbone:90% PLGA chains) [11].

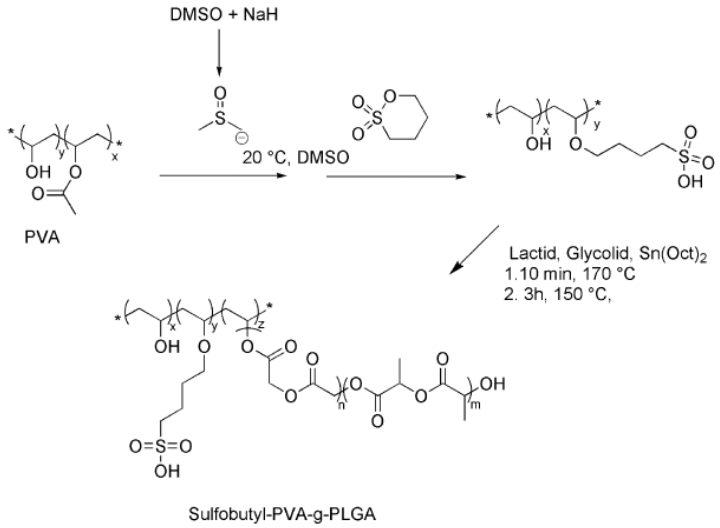

Figure 1. Synthesis of the negatively charged, sulfobutylated branched polyesters, SB-PVA-g-PLGA

Polymer: P(SB-VA):PLGA (x-10)	Polymer properties				Particle properties		
	Degree of substitution[b] (%)	PLGA Units per Chain [c]	Polymer M_n [d] (kg/mol)	LA:GA [e] (mol%)	Particle size (nm)	Polydispersity Index	ζ-potential (mV)
(44-10)	44.3	16.8	346.3	51.3:48.7	85.47 ± 2.29	0.111 ± 0.013	-38.04 ± 1.20
(41-10)	41.3	17.6	453.4	51.7:48.3	86.77 ± 1.11	0.134 ± 0.015	-38.04 ± 1.31

Table 1 Physicochemical properties of the SB-PVA-g-PLGA systems[a]

a. backbone PVA M_w=15 000g/mol

b. calculated from the sulphur element analysis

c. from ^{1}H NMR analysis by intensity comparison of PLGA chain and end groups

d. calculated from ^{1}H NMR analysis assuming complete conversion of PVA hydroxyl groups

e. from 1H NMR analysis

2.1.2. Poly(vinyl sulfonate-co-vinyl alcohol)-g-PLGA (P(VS-VA)-g- PLGA)

Sulfonate modified polyesters were synthesized in a three-step process (Fig.2) as follows: A: Radical copolymerization of vinyl sulfonate(VS) and vinyl acetate(VA); B: alcoholysis of poly(vinylsulfonate-co-vinylacetate)/(poly(VS-VA)) C: grafting of PLGA(50:50). The following nomenclature will be used to characterize the polymers: P(VS-VA)-g- PLGA(X-Y). The first numbers(X) in parenthesis designates the ratio of VS:VA in the first step of copolymerization. The second numbers(Y) in parenthesis denotes the weight ratio of backbone to grafted polyester chains (the weight ratio of P(VS-VA):PLGA in feed = 1:5 or 1:10).

A. Radical copolymerization of vinyl sulfonate and vinyl acetate

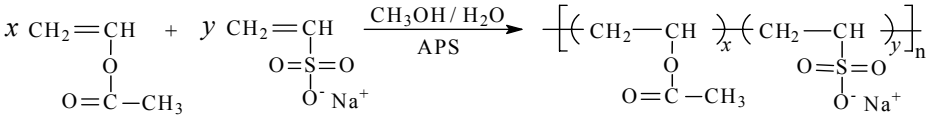

B. Alcoholysis of poly(vinylsulfonate-co-vinylacetate)

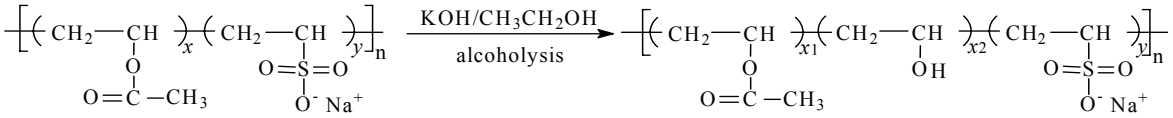

C: grafting PLGA(50:50)

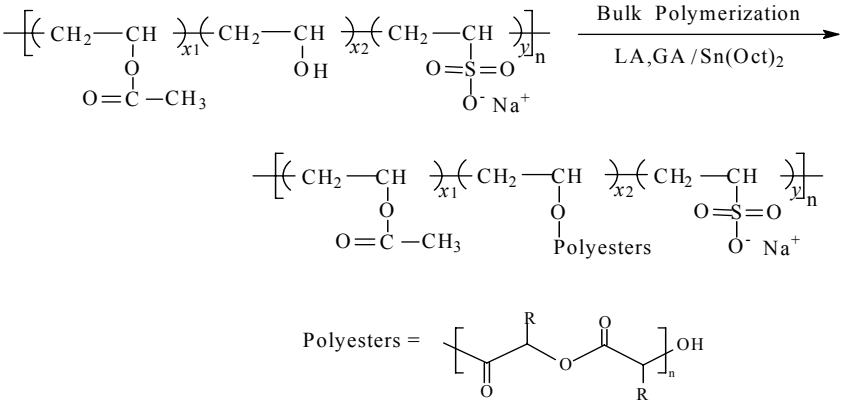

Figure 2. Synthesis of the negatively charged polyesters, poly(vinyl sulfonate-*co*-vinyl alcohol)-g-PLGA

P(VS-VA)-g-PLGA	Polymer properties			Particles properties		
	Copolymer P(VS-VA) (%VS) [a]	PLGA Units per Chain [b]	LA:GA [c] (mol%)	Particle size (nm)	Polydispersity Index	ζ-potential (mV)
2-15	37.8	32.3	51.3:48.7	99.10 ± 1.83	0.122 ± 0.024	-41.47 ± 3.8
4-15	51.8	20.4	51.3:48.7	92.19 ± 4.54	0.13 ± 0.016	-40.84 ± 1.24
6-15	71.8	51.2	51.3:48.7	81.89 ± 1.58	0.098 ± 0.012	-35.19 ± 2.44
6-5	71.8	14.1	50.5: 49.5	83.2 ± 0.84	0.109 ± 0.016	-37.36 ± 3.9
6-10	71.8	30.1	51.6:48.4	80.66 ± 2.31	0.119 ± 0.013	-36.12 ± 8.22
8-15	85.9	54.4	51.4: 48.6	67.46 ± 0.88	0.130 ± 0.022	-39.87 ± 1.26

Table 2 Physicochemical properties of the P(VS-VA)-g-PLGA systems

a. from elemental analyis

b. from ^{1}H NMR analysis by intensity comparison of PLGA chain and end groups

c. from ^{1}H NMR analysis

2.2. Nanoparticles preparation

Nanoparticles were prepared by a solvent displacement technique, described in detail elsewhere [11,17]. Briefly, 10.0 mg of polymer used was dissolved in 1 ml of acetone at 25°C. The resulting solution was subsequently injected to a magnetic stirred (500rpm) 5 ml aqueous phase of filtrated and double distilled water (pH 7.0, conductance 0.055 μS/cm, 25°C) using a special apparatus. The apparatus consists of an electronically adjustable single-suction pump which was used to inject the organic solution into the aqueous phase through an injection needle (Sterican 0.55×25mm) at constant flow rates (10.0 ml/ min). The pump rate was regulated and constantly monitored by an electric power control. After the injection of the organic phase the resulting colloidal suspension was stirred for 8 h under reduced pressure to remove the organic solvents. Particles were characterized and used directly after the preparation.

2.3. Loading of model protein lysozyme

Nanoparticle suspensions of defined concentrations were incubated with defined amounts of lysozyme for 5 h at 4°C. The amount of absorbed protein on the nanoparticles was calculated by measuring the difference between the amount of protein added to the nanoparticles solution and the measured non-entrapped protien remaining in the aqueous phase. After incubation, samples were centrifuged for 30 min at 13 000 rpm (25°C), and the supernatant was checked for the non-bound protein by bicinchonic acid assay (BCA). In this study, the protein concentration was defined at the therectical drug loading 20%. Protein loading efficiency was calculated as follows:

$$\text{Protein loading efficiency} = \frac{\text{Total amount of protein} - \text{Free protein}}{\text{Total amount of protein}} \times 100\%$$

2.4. Particle size and size distribution

The average particle size and zeta potential of the NPs were measured using a Zetasizer Nano ZS/ZEN3600 (Malvern Instruments, Malvern, UK). Particle size and polydispersity were determined using non-invasive back scatter (NIBS) technology, which allows sample measurement in the range of 0.6nm-6μm. Freshly prepared particles suspension (800 μl) was placed in a green disposable zeta cell (folded capillary cell DTS 1060) without dilution. The measurement was carried out using a 4mW He-Ne laser (633nm) as light source at a fixed angle 173°. The following parameters were used for experiments: medium refractive index 1.330, medium viscosity 0.88 mPa s, a dielectric constant of 78.54, temperature 25°C. Each size measurement was performed at least 10 runs. All measurements were carried out in triplicate directly after NP preparation, and the results were expressed as mean size ± S.D.

2.5. Zeta potential measurements

After the size measurement, zeta potential was measured with the M3-PALS Technique (a combination of laser Doppler velocimetry and phase analysis light scattering (PALS). A Smoluchowsky constant *F* (K_a) of 1.5 was used to achieve zeta potential values from electrophoretic mobility. Each zeta-potential measurement was performed automatically at 25°C. All measurements were carried out in triplicate directly after NP preparation, and the results were expressed as mean size ± S.D.

3. Results and discussion

3.1. Characteristics of nanoparticles (NPs) prepared with negatively charged polymer SB-PVA-PLGA and P(VS-VA)-PLGA

3.1.1 Characteristics of NPs prepared with negatively charged polymer SB-PVA-PLGA

Following the protocol, NPs were prepared and the properties are shown in Table 1. Size and zeta-potential of NP prepared with both polymers were comparable about 85nm and -38mV. A narrow size distribution with PdI<0.15, single peak zeta-potential distribution, and good reproducibility were observed as seen in Fig.3. Both polymers showed good quality to preparation NPs. These results are consistent with the previous report of T. Jung et al [11], in which SB-PVA-PLGA could be prepared nanoparticles without surfactant in the aqueous phase.

With respect to these comparable properties of nanoparticles, it is mostly due to both polymers have comparable sulfobutyl substitution (44.3%, 41.3%), PLGA units per chain (16.8, 17.6), and molecular weight (346.3 kg/mol, 453.4 kg/mol).

A

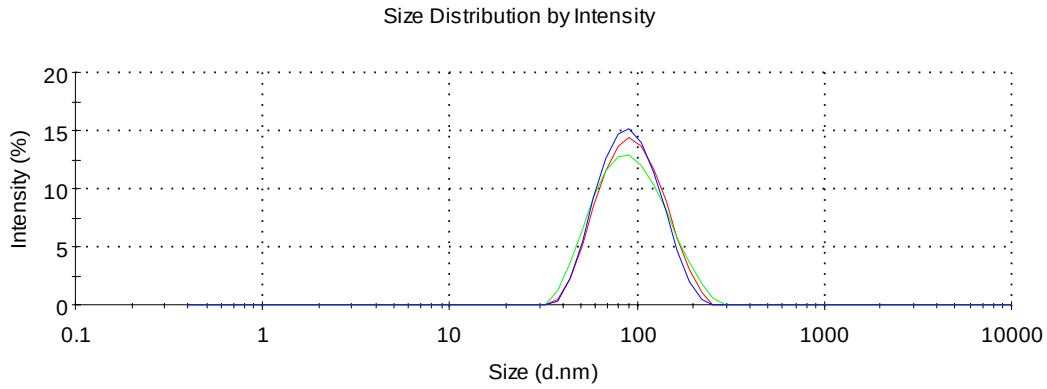

B

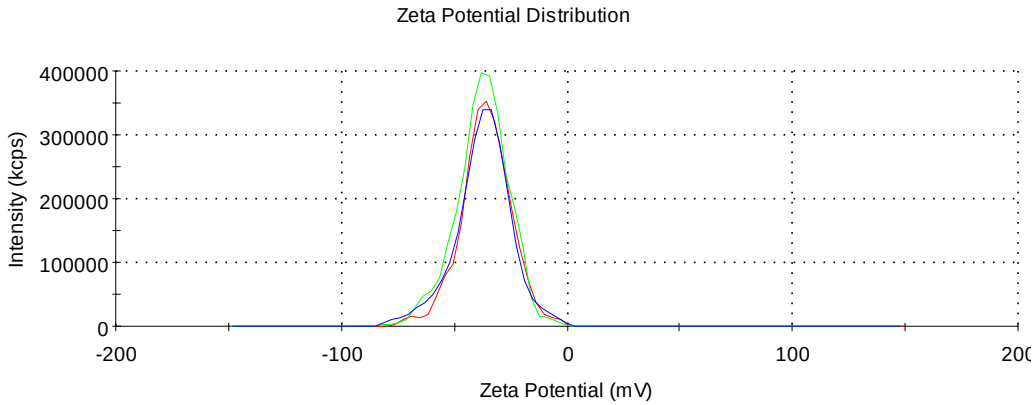

Figure 3. Size and zeta-potential distribution of nanoparticles prepared with SB-PVA-PLGA. A: size distribution; B: zeta-potential distribution.

3.1.2 Characteristics of nanoparticles prepared with negatively charged polymer P(VS-VA)-PLGA (6-X) with different PLGA chain length

In this experiment a new class polymers P(VS-VA)-PLGA with different PLGA chain length were selected to prepare nanoparticles according to the standard protocol. The properties of nanoparticles prepared with this series polymer were listed in Table 2. Interestingly, the results showed that there is no significant difference in the size and zeta-potential for all nanoparticles prepared. All particles showed monodomal distribution with low PdI. However, the zeta-potential of nanoparticles prepared with short chains of PLGA as P(VS-VA)-PLGA(6-10) and P(VS-VA)-PLGA (6-5) was characterized with multi-peak and poor reproducibility as shown in Fig.4. Maybe this is attributed to the impurity of the polymers. The acetone solution of P(6-5) is opaque, and obvious flecks did not dissolve in acetone for P(6-10). Additionally, this result probably suggests that this new polymer with long chain length is preferable for

preparation of nanoparticles considering the size, zeta-potential and reproducibility.

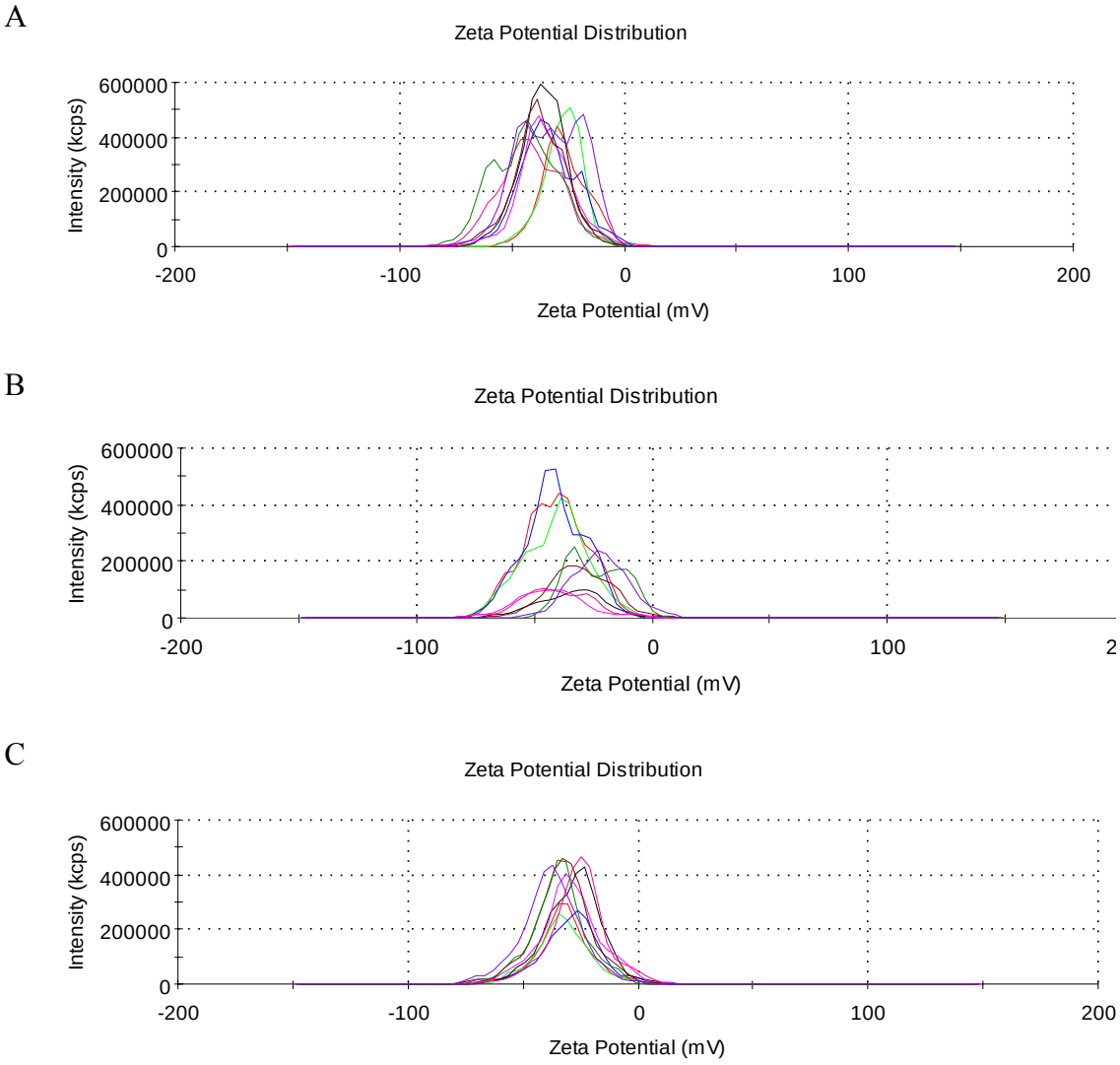

Figure 4. Zeta-potential distribution of NPs prepared with A: P(VS-VA)(6-5); B: P(VS-VA) (6-10); C: P(VS-VA) (6-15). Each experiment has been done in triplicate and each measurement was performed three times.

3.1.3 Characteristics of nanoparticles prepared with negatively charged polymer P(VS-VA)-PLGA (X-15) with different sulfonate substitution degree

In this experiment a series of polymers P(VS-VA)-PLGA with different substitution degree of sulfonic group were selected to prepare nanoparticles and the properties of nanoparticles were listed in Table 2. All formulations showed monodomal size distribution and a steep peak of zeta-potential, indicating a well-defined colloidal system formed with these series polymers. Using single-factor ANOVA statistics,

significant difference was observed in size for all formulations ($P<0.01$). Decreased sulfobutyl substitution degree resulted in a linearly increased size. This result can be well explained by the increased hydrophilicity of polymer due to higher sulfonate substitution based on same PLGA chain length. Higher sulfonbutyl substitution led to low viscosity of copolymer P(VS-VA) which has been measured. It is well known that the size of nanoparticles is closely related to the viscosity of polymer organic solution. Therefore, the sulfobutyl substitution can significantly influence the size of nanoparticles.

However, significant difference in the zeta-potential of nanoparticles was not observed surprisingly, even these experiments were repeated 3 times. These unexpected results give information that the zeta-potential of nanoparticles is also possibly influenced by the particle size.

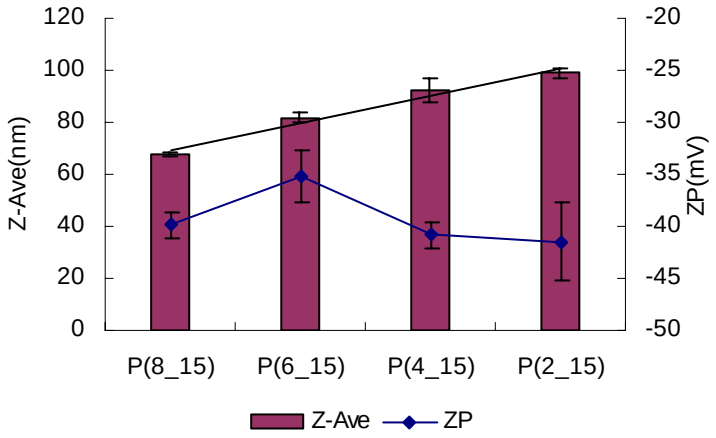

Figure 5. Size (Z-Ave) and zeta-potential (ZP) of nanoparticles prepared with P(VS-VA)(X-15)

3.2. Evaluation of loading capacity of nanoparticles prepared with negatively charged polymer

Using this negatively charged polymer, it is expected to obtain nanoparticles carrying high negative charge, intending to improve the adsorption efficiency of protein. Herein, modified polymers were synthesized and nanoparticles were prepared. In this part, the loading capacity of model oppositely charged protein lysozyme to

nanoparticles was evaluated. Based on the previous experiment, the followed experiments were performed at the theoretical protein loading of 20%.

3.2.1. loading capacity of nanoparticles (NPs) prepared with SB-PVA-PLGA

Because of the similar composition of polymers were selected for SB(41)-PVA-PLGA(10) and SB(41)-PVA-PLGA(10). Based on the nanoparticles with comparable size and zeta-potential, after incubation with lysozyme, size increased and zeta-potential reversed from negative to positive for both formulations. Obvious aggregation and precipitation was observed which was characterized with increased size and broader size distribution for nanoparticles prepared with SB(41)-PVA-PLGA(10). Although for SB(44)-PVA-PLGA(10), the size was also increased from 80 nm to 196 nm, aggregation and precipitation was less pronounce than the first one. Zeta-potential of NPs from both polymer changed from about –38 mV to about 30 mV. Adsorption efficiency showed the comparable loading amount of protein 77 μg/mg and 78 μg/mg. Interestingly, this results are consistent with the previously report of T. Jung et al [17] about the adsorption of tetanus toxoid to SB-PVA-PLGA nanoparticles, in which the maximum adsorption amount of tetanus toxoid was achieved as 57μg/mg with high sulfobutyl substitution degree of 43%. In our experiment, a higher loading amount is possibly due to the positively charged protein resulting in stronger electrostatic interaction between protein and particles. Additionally, in this preliminary study, aggregation was observed which also possible leads to a pseudo-high loading of protein.

Based on these results, both polymers SB(41)-PVA-PLGA(10) and SB(41)-PVA-PLGA(10) are good candidates for NPs preparation and protein loading. However, the loading procedure should be optimized to avoid aggregation.

Polymer type	Particle size (nm)	Polydispersity Index	Zeta-potential (mV)	Γ(μg lysozyme /mg NP)
SB-PVA-PLGA (44-10)	224 ± 10	0.370 ± 0.017	30.7 ± 0.6	77 ± 2
SB-PVA-PLGA (41-10)	196 ± 3	0.194 ± 0.018	34.1 ± 0.2	78 ± 5

Table 3. Size, zeta-potential of NPs after incubation with lysozyme and adsorption amount of lysozyme.

3.2.2. The effect of different PLGA chain length of poly(vinyl sulfonate-co-vinyl alcohol)-g-PLGA(6-X)

After incubation with lysozyme, the size of NPs prepared with P(VS-VA)-g-PLGA(6-5) and (6-15) increased dramatically from about 80nm to about 180nm , along with zeta-potential as about 30mV shown in table 4. By contrast, Obvious aggregation was observed For NPs suspension prepared from P(VS-VA)-g-PLGA (6-10) together with zeta-potential 23mV.

Loading amount of lysozyme is 66μg/mg and 44μg/mg for P(VS-VA)-g-PLGA (6-5) and (6-15), indicating a reduced adsorption due to increased PLGA chain length. This might be explained by reduction in charge density induced by longer PLGA chain length base on the same P(VS-VA) backbone. For the adsorption procedure, electrostatic interaction is supposed to be the main driving force; hence, decreased adsorption was observed polymers with lower charge density. In addition, adsorption efficiency of NPs prepared with P(VS-VA)-g-PLGA (6-10) was much higher than that with other two formulations. This abnormal behavior maybe due to the obvious aggregates formed during adsorption. Based on these data, it can be deduced that for these polymers adsorption process is primarily governed by charge density of polymer not the hydrophobicity induced by PLGA chain.

Polymer type	Size (nm)	Polydispersity Index	Zeta-potential (mV)	Γ(μg lysozyme /mg NP)
P(VS-VA)(6-5)	177 ± 11	0.201 ± 0.022	30.2 ± 0.7	66 ± 15
P(VS-VA)(6-10)	333 ± 88	0.471 ± 0.123	23.7 ± 0.8	113 ± 21
P(VS-VA)(6-15)	178 ± 37	0.254 ± 0.091	33.6 ± 0.5	44 ± 14

Table 4. Size and zeta-potential of NP after incubation with lysozyme and adsorption amount of lysozyme

3.2.3. The effect of different sulfobutyl substitution degree of poly(vinyl sulfonate-co-vinyl alcohol)-g-PLGA(X-15) (P(X-15))

After incubation with lysozyme, the size increased dramatically from about 80nm to about 200 nm for all formulations as shown in Table 5. PdI increased remarkably and obvious aggregation was observed for nanoparticles suspension prepared with P(8-15) and P(4-15). Based on similar zeta-potential about -40mV, zeta-potential of nanoparticles reversed to about 30 mV for all formulations after incubation with lysozyme.

Adsorption amount of lysozyme for nanoparticles prepared with P(8-15) and P(4-15) are 78 μg/mg and 76 μg/mg, respectively. These are much higher than other two polymers, which are 44 μg/mg and 55 μg/mg for P(6-15) and P(2-15), respectively. This maybe attributed to the obvious aggregation of P(8-15) and P(4-15) two formulations during adsorption. Influence of sulfobutyl substitution degree on the adsorption is not a straightforward question to answer. Taking P(6-15) and P(2-15) for example, as shown above increased substitution degree led to decreased size and increased hydrophilic property of polymer. Based on the polymer structure of P(6-15) and P(2-15), it is supposed that higher charge density of P(6-15) should result in a high loading efficiency than that of P(2-15). However, this unexpected result showed the adsorption process is quite complicated and it maybe also related to the size, or the balance of hydrophilic or hydrophobic property and charge density of nanoparticles.

Therefore, the loading process of nanoparticles prepared with this new class polymer should be investigated in detail with clear properties of nanoparticles like

exact charge density, hydrophilic or hydrophobic and size.

Polymer type	Particle size (nm)	Polydispersity Index	Zeta-potential (mV)	Γ(μg lysozyme /mg NP)
P(VS-VA)(8-15)	224 ± 10	0.348 ± 0.062	30.4 ± 0.8	78 ± 14
P(VS-VA)(6-15)	178 ± 37	0.246 ± 0.088	33.6 ± 0.5	44 ± 14
P(VS-VA)(4-15)	236 ± 4	0.268 ± 0.016	33.8 ± 0	76 ± 2
P(VS-VA)(2-15)	234 ± 63	0.310 ± 0.069	32.3 ± 0.7	55 ± 1

Table 5 Size, zeta-potential NPs after incubation of lysozyme and adsorption amount of lysozyme

4. Conclusions

Nanoparticles were prepared with solvent displacement technique without surfactant using new negatively charged polymer P(VS-VA)-PLGA. SB-PVA-PLGA nanoparticles showed narrow size distribution, with monodomal distribution of zeta-potential and high reproducibility. Higher PLGA chain length of P(VS-VA)-PLGA demonstrated better properties as narrow size and single peak zeta-potential distribution. Sulfonbutyl substitution degree of P(VS-VA)-PLGA has pronounced influence on particles size. Increased substitution degree decreased the size linearly, however, no significant different in zeta-potential was observed.

With regard to the loading capacity of lysozyme, SB-PVA-PLGA showed higher loading capacity relative to this new class polymer P(VS-VA)-PLGA. The introduce of sulfonate group to backbone may lead to higher charge density, meanwhile, it may decrease the affinity of protein due to increased hydrophilic property. Higher sulfonic substitution degree resulted in higher loading capacity. However, lower loading capacity of lysozyme was observed for polymer with longer PLGA chain length, indicating that the balance of charge density and hydrophilic property is necessary for this protein adsorption process.

For this new class polymer, further investigated is required to clarify the property of NPs prepared with different polymer composition and the underlined protein adsorption mechanism also should be studied in more detail.

References

[1] Y. Hu, J. Xie, Y.W. Tong, C.H. Wang, Effect of PEG conformation and particle size on the cellular uptake efficiency of nanoparticles with the HepG2 cells. J. Control. Release 118 (2007) 7-17.

[2] K.E. Carr, R.A. Hazzard, S. Reid, G.M. Hodges, The effect of size on uptake of orally administered latex microparticles in the small intestine and transport to mesenteric lymph nodes. Pharm. Res. 13 (1996) 1205-1209.

[3] I. Bala, S. Hariharan, M.N. Kumar, PLGA nanoparticles in drug delivery: the state of the art. Crit Rev Ther Drug Carrier Syst 21 (2004) 387-422.

[4] M. Cegnar, J. Kristl, J. Kos, Design of protein-loaded nanoparticles. Farmacevtski Vestnik (Ljubljana, Slovenia) 54 (2003) 37-46.

[5] J. Cheng, B.A. Teply, I. Sherifi, J. Sung, G. Luther, F.X. Gu, E. Levy-Nissenbaum, A.F. Radovic-Moreno, R. Langer, O.C. Farokhzad, Formulation of functionalized PLGA-PEG nanoparticles for in vivo targeted drug delivery. Biomaterials (2006).

[6] C. Fang, B. Shi, Y.Y. Pei, M.H. Hong, J. Wu, H.Z. Chen, In vivo tumor targeting of tumor necrosis factor-alpha-loaded stealth nanoparticles: effect of MePEG molecular weight and particle size. Eur. J. Pharm. Sci. 27 (2006) 27-36.

[7] A.S. Zahr, C.A. Davis, M.V. Pishko, Macrophage uptake of core-shell nanoparticles surface modified with poly(ethylene glycol). Langmuir 22 (2006) 8178-8185.

[8] K.Y. Win, S.S. Feng, Effects of particle size and surface coating on cellular uptake of polymeric nanoparticles for oral delivery of anticancer drugs. Biomaterials 26 (2005) 2713-2722.

[9] A. Weissenbock, M. Wirth, F. Gabor, WGA-grafted PLGA-nanospheres: preparation and association with Caco-2 single cells. J. Control. Release 99 (2004) 383-392.

[10] M. Tobio, A. Sanchez, A. Vila, I. Soriano, C. Evora, J.L. Vila-Jato, M.J. Alonso,

The role of PEG on the stability in digestive fluids and in vivo fate of PEG-PLA nanoparticles following oral administration. Colloids Surf. B Biointerfaces 18 (2000) 315-323.

[11] T. Jung, A. Breitenbach, T. Kissel, Sulfobutylated poly(vinyl alcohol)-graft-poly(lactide-co-glycolide)s facilitate the preparation of small negatively charged biodegradable nanospheres. J. Control. Release 67 (2000) 157-169.

[12] U. Bilati, E. Allemann, E. Doelker, Nanoprecipitation versus emulsion-based techniques for the encapsulation of proteins into biodegradable nanoparticles and process-related stability issues. AAPS PharmSciech 6 (2005) E594-604.

[13] U. Bilati, E. Allemann, E. Doelker, Development of a nanoprecipitation method intended for the entrapment of hydrophilic drugs into nanoparticles. Eur. J. Pharm. Sci. 24 (2005) 67-75.

[14] T. Jung, W. Kamm, A. Breitenbach, K.D. Hungerer, E. Hundt, T. Kissel, Tetanus toxoid loaded nanoparticles from sulfobutylated poly(vinyl alcohol)-graft-poly(lactide-co-glycolide): evaluation of antibody response after oral and nasal application in mice. Pharm. Res. 18 (2001) 352-360.

[15] G. Francois, J.L. Katz, Nanoparticles and nanocapsules created using the Ouzo effect: spontaneous emulisification as an alternative to ultrasonic and high-shear devices. Chemphyschem 6 (2005) 209-216.

[16] S. Dreis, F. Rothweiler, M. Michaelis, J. Cinatl, Jr., J. Kreuter, K. Langer, Preparation, characterisation and maintenance of drug efficacy of doxorubicin-loaded human serum albumin (HSA) nanoparticles. Int. J. Pharm. (2007).

[17] T. Jung, W. Kamm, A. Breitenbach, G. Klebe, T. Kissel, Loading of tetanus toxoid to biodegradable nanoparticles from branched poly(sulfobutyl-polyvinyl alcohol)-g-(lactide-co-glycolide) nanoparticles by protein adsorption: a mechanistic study. Pharm. Res. 19 (2002) 1105-1113.

[18] L.A. Dailey, M. Wittmar, T. Kissel, The role of branched polyesters and their

modifications in the development of modern drug delivery vehicles. J. Control. Release 101 (2005) 137-149.

[19] T. Jung, W. Kamm, A. Breitenbach, E. Kaiserling, J.X. Xiao, T. Kissel, Biodegradable nanoparticles for oral delivery of peptides: is there a role for polymers to affect mucosal uptake? Eur. J. Pharm. Biopharm. 50 (2000) 147-160.

Chapter 6

Summary and outlook

1. Summary

In this work, microparticles and nanoparticles were investigated as protein delivery system, with the aim to achieve desired protein release profiles for microparticles and to achieve high protein loading with fully preserved bioactivity of protein for nanoparticles.

Chapter 1 firstly describes development and current status of degradable polymer microspheres as protein delivery systems. Based on PLGA polymer, basic knowledge about protein loaded microspheres are imparted and crucial problems related to the release profiles of protein were highlighted.

Separately, polymeric nanoparticles as protein delivery system were discussed with regard to the preparation method, drug loading, protein stability and release profiles. Concerning the preparation process, main problems are the instability of protein due to high shear force and exposure to the organic solvent, and reproducibility of well defined nanoparticles. Solvent displacement with its narrow size distribution and without use of shear force was extensively employed for protein loaded nanoparticles preparation. However, a new strategy is still badly needed because of the low encapsulation efficiency and exposure to organic solvent especially for protein loaded nanoparticles.

Taking all information into account, it was postulated that charged nanoparticles can be oppositely charged protein nanocarrier, and adsorption process can effectively load protein onto nanoparticles through electrostatic interaction. This whole process doesn’t use high shear force, surfactant and avoid exposure to the organic solvent; hence, the bioactivity of protein is expected to be preserved. In order to further improve the release profiles and stability of this protein loaded colloidal system, we assumed that chitosan and its derivatives as polycationic polymer with potential functional application can be deposited on the surface of protein loaded nanoparticles taking advantage of the surface negative charge surplus of nanoparticles.

In Chapter 2 with the aim to establish the relationship of particles morphology, drug distribution and release profiles based on different polymer properties, relatively hydrophobic and hydrophilic PLGAs with different end functional groups were

selected to prepare microspheres using W/O/W method with different porosity, pore size and drug loading. The results showed that morphology of particles play a different role in the release process depending on the property of polymer. For relative hydrophilic polymer, as RG503H, morphology influenced the burst release to the less extent relative to hydrophobic polymer RG502. Vice verse, at the slow release stage, morphology showed much less pronounced influence for hydrophobic polymer RG502. This study suggests that morphology and drug distributin modification intended to achieve desired release profiles should be based on polymer properties.

In Chapter 3 with the purpose to achieve high protein loading and to improve the release profiles, we supposed that protein can be effectively absorbed onto charged nanoparticles and can be released in the controlled manner. PLGA and PSS polymer blend were used to mimic negatively charged polymer and to prepare charged nanoparticles with variable surface charge density through adjusting the ratio of PSS to PLGA. Increased PSS led to the increment of size and high charge density of nanoparticles. Adsorption isotherm showed higher affinity of protein to the nanoparticles with increased PSS. Loading capacity of lysozyme closely related to charge density of nanoparticles. Adsorption process of protein and loading capacity investigations suggest that the electrostatic forces dominate the interaction between proteins and nanoparticles. Bioactivity determination showed protein remains intact during whole process and the release profiles were dependent on protein loading. This study proves our hypothesis that it is a feasible and mild method using charged nanoparticles to effectively load oppositely charged protein with full bioactivity.

In Chapter 4 due to the fast release and location of protein on the surface of nanoparticles prepared in chapter 3, a layer-by-layer nanostructure was assumed to fulfill these requirements. Using chitosan and its derivatives as coating materials with potential functional application like mucoadhesivity, penetration enhancement, layer-by-layer nanocarriers through deposition of polymer on the surface of protein loaded nanoparticles were investigated. Increased size and inversion of zeta-potential of particles, as well as TEM observations evidenced the coating of chitosan on the

surface. Due to the stronger electrostatic interaction between chitosan and nanoparticles, dissociation of lysozyme was observed. Dissociation of lysozyme was dependent on polymer composite, irrespective of initial protein loading. Moreover, with this polymer coating more stable particles were detected in PBS, without initial release within 24 hours. This study showed the feasibility of designing a layer-by-layer protein nanocarrier with polymer coating on the surface of protein loaded nanoparticles to further improve the stability and release profiles of protein.

In Chapter 5 based on the promising results of chapter 3, same strategies including nanoparticles preparation and protein loading method were employed using negatively charged polymer SB-PVA-PLGA and P(VS-VA)-PLGA. Stable nanoparticles suspension with narrow size distribution, and high reproducibility was obtained with polymer SB-PVA-PLGA. Based on equal sulfonic substitution, longer PLGA chain length of P(VS-VA)-PLGA demonstrated better nanoparticles properties as narrow size and single peak zeta-potential distribution than shorter PLGA chain length polymer. Increased sulfonic substitution degree of P(VS-VA)-PLGA decreased the size linearly, however, no significant difference in zeta-potential was observed. SB-PVA-PLGA showed higher loading capacity as 77 μg/mg relative to this new class polymer P(VS-VA)-PLGA. Additionally, higher sulfonic substitution degree resulted in higher loading capacity. Whereas, lower loading capacity of lysozyme was observed for polymer with longer PLGA chain length, indicating that the balance of charge density and hydrophilic property is necessary for this protein adsorption process.

2. Outlook

Investigation of the comprehensive effects of polymer nature, morphology, drug distribution on release behavior for PLGA microspheres prepared by the double emulsion method has given valuable knowledge for further optimize of this effective drug delivery formulation. Previous studies have shown the importance of different process parameters on morphology and drug release, but in this work it is clear that polymer nature is a determining factor. In this study, the emphasis was attached on the pore diffusion process. However, the results showed that it was difficult to modify the slow release phase for microparticles prepared from hydrophobic polymer.

Feasibility study of protein loaded nanoparticles open a new perspective for the nanocarrier with high drug loading, fully preserved bioactivity using a facile method. With layer-by-layer nanostructure, protein was sandwiched in multilayers with higher stability. Chitosan and its derivatives coating suggest a promising mucosal nanoparticles delivery system. Thus, based on this feasibility study, nanoparticles prepared with new class of negatively charged polymer is possible to be evaluated using same strategies to load protein like human recombinant nerve growth factor (rh-NGF), also a basic protein with an isoelectric point of 9.3. Possible potential application of this chitosan coated NGF loaded nanoparticles targeted to brain through nasal rout or local catheter infusion is suggested for further investigation. In addition, through different polymer coating at the outmost layer, like Poly(l-lysine)-PEG, biotin-functionalized Poly(l-lysine)-PEG, et al, nanoparticles are possible to achieve different objectives like long circulation in vivo, cellular uptake or targeting.

Appendices

ABBREVIATIONS

TEM	Transmission electron microscopy
AFM	Atomic force microscopy
CLSM	Confocal laser scanning microscopy
SEM	Scanning electron microscopy
DSC	Differential scanning calorimetry
PEG	Poly(ethylene glycol)
SD	Standard deviation
PVA	Poly(vinyl alcohol)
PLGA	Poly(lactide-co-glycolide)
DMSO	Dimethylsulfoxide
ANOVA	Analysis of variance
DCM	Dichloromethane
Mw	Weight average molecular weight
PBS	Phosphate buffered saline
Tg	Glass transition temperature
SB-PVA-PLGA	Poly(2-sulfobutyl-vinyl alcohol)-g-poly(lactide-co-glycolide)
P(VS-VA)-g- PLGA	Poly(vinyl sulfonate-co-vinyl alcohol)-g-PLGA
PdI	Polydispersity index
CS	Chitosan
TMC	Trimethyl chitosan
PEG-g-TMC	PEG-graft-Trimethyl chitosan
NP	Nanoparticles
W/O/W	Water in oil in water
FD	Fluorescein Isothiocyanate labeled Dextran or FITC-dextran

PUBLICATIONS

Research Articles

C. Cai, S. Mao, O. Germershaus, A. Schaper, E. Rytting, and T. Kissel. Influence of morphology and drug distribution on the release process of FITC-dextran loaded microspheres prepared with different types of PLGA. Submitted to: J. Microencapsulation

C. Cai, U. Bakowsky, E. Rytting, A. Schaper, and T. Kissel. Charged nanoparticles as protein delivery systems: A feasibility study using lysozyme as model protein. European Journal of Pharmaceutics and Biopharmacy: in preparation

C. Cai, J. Sitterberg, S. Mao, A. Schaper, and T. Kissel. Layer-by-layer nanostructure of protein loaded nanoparticles: A feasibility study using lysozyme as model protein and chitosan as coating materials. European Journal of Pharmaceutics and Biopharmacy: in preparation

S. Mao, J. Xu, **C. Cai,** O. Germershaus, A. Schaper, and T. Kissel. Effect of WOW process parameters on morphology and burst release of FITC-dextran loaded PLGA microspheres. Int. J. Pharm. 2007, 334 (1-2):137-48.

Posters

C. Cai, O. Germershaus, S. Mao, A. Schaper, and T. Kissel. Influence of porosity and PLGA polymer nature on the release behavior of FITC-dextran loaded PLGA microspheres. Controlled Release Society German Chapter Annual Meeting in Freiburg, March 2007, Germany.

C. Cai, M. Hellwig, U. Bakowsky, E. Rytting, and T. Kissel. A facile method to prepare protein loaded nanoparticles. Controlled Release Society German Chapter Annual Meeting in Freiburg, March 2007, Germany.

C. Cai, J. Sitterberg, E. Rytting, A. Schaper, and T. Kissel. A facile method to prepare protein loaded nanocarrier with a layer-by-layer nanostructure. The 3th Materialforschungstag Mittelhessen, July 2007, Germany

S. Mao, J. Xu, **C. Cai,** O. Germershaus, A. Schaper, and T. Kissel. Influence of process parameters on the internal porosity and burst release of FITC-dextran loaded PLGA microspheres. 33th International Symposium on Controlled Release of Bioactive Materials, Vienna, 2006

S. Mao, J. Xu, **C. Cai,** O. Germershaus, A. Schaper, and T. Kissel. Influence of process parameters on the internal morphology of FITC-dextran loaded PLGA microspheres. Controlled Release Society German Chapter Annual Meeting in Jena, February 2006, Germany.

CURRICULUM VITAE

Name: Cuifang Cai

Date and place of birth: May 5, 1974 Shandong/Qingyun

Nationality: Chinese

Marital status: Married

Fundamental Education

1980.9-1985.7 Shandong Yaoqian elementary school

1985.9-1988.7 Shandong Donglangwu junior high school

1988.9-1991.7 Shandong Qingyun No.1 senior high school

Higher Education:

1991.9-1995.7 The East China University of Science and Technology, Bachelor Degree, Major: Chemical Pharmaceutics

1998.9-2001.7 Shenyang Pharmaceutical University, Master Degree, Major: Pharamceutics

2005.10-present Department of Pharmaceutis and Biopharmacy, Philipps Universität Marburg, Ph. D Candidate

Other Education:

2004.9-2005.6 Tongji University learn German

2005.8-2005.9 Speak & Write Marburg learn German

Working Experience:

1995.7-1998.9 Assistant engineer, Northeast Pharmaceutical General Factory

2001.8-2004.8 Lecturer, Pharmaceutics and Pharmaceutics experiments in Shenyang Pharmaceutical University